KTH Engineering Sciences

Doctoral Thesis

Theoretical and Phenomenological Studies of Neutrino Physics

Mattias Blennow

Theoretical Particle Physics, Department of Theoretical Physics
Royal Institute of Technology, SE-106 91 Stockholm, Sweden

Stockholm, Sweden 2007

Typeset in LaTeX

Akademisk avhandling för teknologie doktorsexamen (TeknD) inom ämnesområdet teoretisk fysik.

Scientific thesis for the degree of Doctor of Philosophy (PhD) in the subject area of Theoretical Physics.

Cover illustration: A neutrino oscillogram of the Earth describing the neutrino oscillation probability P_{ee} with the neutrino oscillation parameters $\theta_{12} = 33.2°$, $\theta_{13} = 11.4°$, $\theta_{23} = 45°$, $\Delta m^2_{21} = 8 \cdot 10^{-5}$ eV^2, and $\Delta m^2_{31} = 2 \cdot 10^{-3}$ eV^2.

ISBN 978-91-7178-646-3

TRITA-FYS 2007:31
ISSN 0280-316X
ISRN KTH/FYS/--07:31--SE

Printed in Sweden by Universitetsservice US AB, Stockholm 2007

Abstract

This thesis is devoted to the theory and phenomenology of neutrino physics. While the standard model of particle physics has been extremely successful, it fails to account for massive neutrinos, which are necessary to describe the observations of neutrino oscillations made by several different experiments. Thus, neutrino physics is a possible window for exploring the physics beyond the standard model, making it both interesting and important for our fundamental understanding of Nature.

Throughout this thesis, we will discuss different aspects of neutrino physics, ranging from taking all three types of neutrinos into account in neutrino oscillation experiments to exploring the possibilities of neutrino mass models to produce a viable source of the baryon asymmetry of the Universe. The emphasis of the thesis is on neutrino oscillations which, given their implication of neutrino masses, is a phenomenon where other results that are not describable in the standard model could be found, such as new interactions between neutrinos and fermions.

Key words: Neutrino mass, neutrino mixing, neutrino oscillations, matter effects, non-standard effects, the day-night effect, solar neutrinos, accelerator neutrinos, exact solutions, three-flavor effects, large density, neutrino decay, neutrino decoherence, neutrino absorption, non-standard neutrino interactions, seesaw mechanism, stability criteria, leptogenesis.

Preface

This thesis is a compilation of seven scientific papers which are the result of my research at the Department of Physics and the Department of Theoretical Physics during the period June 2003 to May 2007. The thesis is divided into two separate parts. The first part is an introduction to the subject of neutrino physics in general and contains the basic concepts needed to understand the scientific papers and put them into context. It includes a short review of the history of neutrino physics as well as a review of the standard model of particle physics and how it can be altered in order to allow for massive neutrinos. The second part of this thesis consists of the seven scientific papers listed below.

List of papers

My research has resulted in the following scientific papers:

[1] *Mattias Blennow*, Tommy Ohlsson, and Håkan Snellman
Day-night effect in solar neutrino oscillations with three flavors
Phys. Rev. D **69**, 073006 (2004).
`hep-ph/0311098`

[2] *Mattias Blennow* and Tommy Ohlsson
Exact series solution to the two flavor neutrino oscillation problem in matter
J. Math. Phys. **45**, 4053 (2004).
`hep-ph/0405033`

[3] *Mattias Blennow* and Tommy Ohlsson
Effective neutrino mixing and oscillations in dense matter
Phys. Lett. B **609**, 330 (2005).
`hep-ph/0409061`

[4] *Mattias Blennow*, Tommy Ohlsson, and Walter Winter
Damping signatures in future reactor and accelerator neutrino oscillation experiments
JHEP **06**, 049 (2005).
`hep-ph/0502147`

[5] *Mattias Blennow*, Tommy Ohlsson, and Walter Winter
Non-standard Hamiltonian effects on neutrino oscillations
Eur. Phys. J. C **49**, 1023 (2007).
`hep-ph/0508175`

[6] *Mattias Blennow*, Tommy Ohlsson, and Julian Skrotzki
Effects of non-standard interactions in the MINOS experiment
`hep-ph/0702059`

[7] Evgeny Akhmedov, *Mattias Blennow*, Tomas Hällgren, Thomas Konstandin, and Tommy Ohlsson
Stability and leptogenesis in the left-right symmetric seesaw mechanism
JHEP **04**, 022 (2007).
`hep-ph/0612194`

The thesis author's contribution to the papers

In all papers, I was involved in the scientific work as well as in the actual writing. I am also the corresponding author of all papers except Paper [7].

[1] The paper was based on my M.Sc. thesis with some improvements. I performed the analytic and numeric calculations. I also constructed the figures and did most of the writing.

[2] I had the idea of setting up a real non-linear differential equation for the neutrino oscillation probabilities rather than a linear differential equation for the neutrino oscillation amplitudes. I performed the expansion of the solution and implemented the result numerically to test the convergence of the solution. I also did most of the writing and constructed the figures.

[3] The idea to use degenerate perturbation theory for large matter potentials was mine. I performed the analytic and numeric calculations and constructed the figures. I did most of the work on the discussion of effective two-flavor cases and I also did most of the writing.

[4] The work was divided equally among the authors. In Sec. 3, I did all the calculations and wrote most of the discussion. I also did much of the writing in Sec. 2 and constructed Fig. 1.

[5] The work was divided equally among the authors. I did most of the analytic discussion in Secs. 2, 3, and 4 as well as Apps. A and C. I also wrote parts of Secs. 5 and 6 and constructed Figs. 2 and 6.

[6] The paper is a continuation of the work done in Paper [5] and the numeric simulations were mainly performed by Julian Skrotzki. I performed additional numeric simulations, did the analytic considerations, constructed the figures, and wrote the text.

[7] I was involved in the construction of the programs for the numerical calculations and performed some of the analytic considerations. I also constructed all of the figures.

Acknowledgments

First of all, I wish to thank my supervisor, Tommy Ohlsson, who has been involved in the scientific work of all the papers included in the Part II of this thesis. In addition, we have had some nice discussions on physics in general, teaching, and other things which are unrelated to physics, making the years throughout my graduate studies very enjoyable.

I would also like to give special thanks to Håkan Snellman, who was my M.Sc. thesis supervisor and introduced me to the field of neutrino physics as a co-author of my first paper. His enthusiasm for physics and philosophy really is contagious and he has been a great source of inspiration.

Special thanks are also due to Evgeny Akhmedov. It was an honor to collaborate with him during his time as a guest professor at the Royal Institute of Technology and I learned a lot from him which I believe I will find very useful in the future.

Furthermore, I would like to give special thanks to Walter Winter for our collaboration, which resulted in Papers [4, 5] of this thesis.

Tomas Hällgren, Thomas Konstandin, and Sofia Sivertsson, all of whom I share office with, should also receive thanks for all of our interesting discussions regarding both physics, everyday life, and totally unrelated stuff. In addition, Tomas and Thomas are co-authors of Paper [7] and should also be thanked for their collaboration.

I am also grateful to the Royal Institute of Technology (KTH) for providing the financial means necessary for my graduate studies, and thus, allowing me to be involved in the research of elementary particle physics.

All of the lecturers with whom I have worked as a teaching assistant (Håkan Snellman, Jouko Mickelsson, Edwin Langmann, and Patrik Henelius) also deserve thanks for letting me be a part of the efforts in teaching undergraduate courses. I have really enjoyed every minute of teaching and my students should also receive thanks for coming to my sessions with the will to learn.

In addition, I would also like to thank my other fellow Ph.D. students, including (but not restricted to) Martin Hallnäs and Pedram Hekmati, for great company both on and off working hours. Such thanks (off working hours) are also due to all of my friends, including (but not restricted to) Mattias Andersson and Martin Blom.

Finally, I want to thank all the members of my family for their great support. My grandparents, Märta, Gunvor, and Bertil, have always been very important to me and I have a hard time believing someone could even wish for better ones as they have always taken good care of all of their grandchildren.[1] My sister Malin, who has always been my friend and a source of support, and my brother-in-law (by the time of my dissertation) Max Winerdahl for being such a great company. My brother Victor whose company I really enjoy. My girlfriend Katarina Olsson for

[1] Mina far- och morföräldrar, Märta, Gunvor, och Bertil, har alltid varit viktiga för mig och jag har svårt att föreställa mig att någon ens kan önska sig bättre eftersom de alltid tagit väl hand om alla sina barnbarn.

loving me and accepting me for who I am. Leia, Trixie, Otis, and Rex for being the greatest dogs in the world as they always make me feel appreciated.

Last, but not least, I wish to thank my parents, Mats and Elisabeth, for raising me to become who I am and for always being a great support. This thesis is dedicated to them as it would not have been possible to complete it without them.

Mattias Blennow, April 8, 2007

Contents

To My Parents

Part I

Background material

Chapter 1

Introduction

What I try to do in the book is to trace the chain of relationships running from elementary particles, fundamental building blocks of matter everywhere in the Universe, such as quarks, all the way to complex entities, and in particular complex adaptive system like jaguars.
– Murray Gell-Mann

Describing the clock-work of Nature has always been one of the greatest challenges of humanity, although the methods have changed. Modern science was essentially born with Newton's publication of *Principia Mathematica* [8] and has developed ever since.

The aim of physics is to describe quantified observations of Nature using well-defined theories written with a mathematical language. Ideally, a good physical theory accurately describes the results of experiments that have already been performed and makes solid predictions that can be tested in future experiments. As the predictions are confirmed, the theory becomes more and more accepted, until there are experimental observations that contradict it, in which case it has to be revised or even abandoned in favor of some other theory, which gives a better description. A very important part of the scientific process is that a theory can never be regarded as true, it can never be anything more than a good (or bad) description of Nature. Even if all the predictions of a theory are verified, it is only a verification of the predictions, not the theory itself. However, a theory can definitely be invalidated or proven inadequate if any of its predictions are found to be wrong.

One of the most successful physical theories of the last century is the Standard Model of particle physics, which describes the elementary particles and their interactions. The Standard Model has made extremely accurate predictions for the properties of particles and the cross-sections in particle interactions. However, even though the Standard Model has had such a great success, we know that it is not a complete description of the inner workings of Nature. In fact, it was known to be

inadequate even before any of its predictions were verified, since it does not include the interaction that is most apparent to us on a macroscopic level, *i.e.*, gravity.

In the later part of the last century, further observations that do not fit into the Standard Model were made. One of these observations was the evidence for neutrino oscillations presented in 1998 by the Super-Kamiokande collaboration [9]. As will be described in this thesis, neutrinos are necessarily massless in the Standard Model and neutrino oscillations require massive neutrinos, and thus, the Standard Model needs to be revised and extended in order to provide a description of Nature. Because of this fact, the study of neutrino masses and oscillations provide what could be a very important window for examining the physics beyond the Standard Model. This thesis consists of two parts, where the first part contains an introduction to the Standard Model and how it can be extended in order to accommodate neutrino masses. The second part consists of the papers that have resulted from my own work during my PhD studies.

1.1 Outline of the thesis

The introductory part of this thesis is structured as follows. In Ch. 2, the history of neutrino physics is briefly presented before we go into details about the physical theory in Ch. 3, where the Standard Model of particle physics is introduced. After going through the Standard Model, we review its possible extensions to include neutrino masses in Ch. 4 and the theory of neutrino oscillations in Ch. 5. In Ch. 6, we go through the current experimental evidence for neutrino oscillations. Chapter 7 contains a short introduction to the subject of leptogenesis, which is a mechanism for generating the baryon asymmetry of the Universe. Finally, in Ch. 8, the introductory part is summarized and we present some of the more important conclusions of the papers included in the second part of the thesis.

Chapter 2

A brief history of neutrinos

No great discovery was ever made without a bold guess.
– Sir Isaac Newton

The history of neutrino physics starts in 1930 and is quite intriguing as the neutrino itself remained undetected for 26 years. The early 20th century had been a time of great progress in physics with the birth of both quantum mechanics and the theory of relativity. The electron had been discovered by Thompson already in 1897 [10] and the proton by Rutherford in 1918 [11], these were believed to be the elementary particles. According to the Rutherford model, the nucleus consisted of a number of protons to make up for its mass and a smaller number of electrons in order to balance its electric charge properly. Experiments by Meitner and Hahn [12] as well as Chadwick [13] had shown that the beta-decay process had a continuous energy spectra rather than the discrete spectra predicted by a two-body decay. In addition, the Rutherford model was unable to properly describe the total spin of nuclei and it had even been suggested that energy and spin were only conserved on a statistical level. Neutrino physics were then born on December 4, 1930, as Pauli proposed the existence of the "neutron", a new spin 1/2 particle with small mass and no electric charge, in a letter to a physicist meeting in Tübingen[1]. As Pauli himself stated in the letter, this was a "desperate remedy" in order to save the conservation of energy and angular momentum as only two elementary particles, the proton and the electron, were believed to exist at this time. The fact that the "neutron" had not yet been discovered was implied by its weak interaction with matter due to the lack of electric charge.

Two years later, in 1932, Chadwick made the experimental discovery of the neutron [14]. However, it was clear that this particle could not be the same as Pauli's "neutron", since it was far too heavy. Thus, Fermi renamed Pauli's neutron to "neutrino", meaning neutral and small, in 1933 as it was certainly a bad idea to

[1] Pauli himself was unable to attend the meeting as he was "indespensible" due to a ball in Zürich.

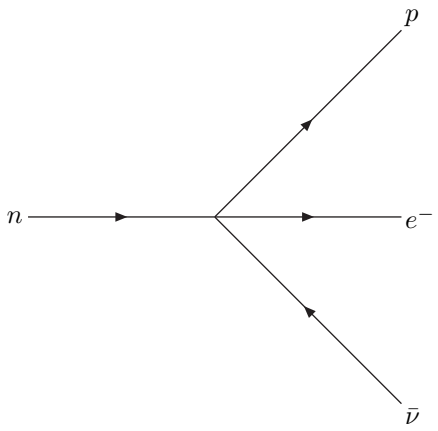

Figure 2.1. The Fermi theory of beta-decay involves an interaction term which allows a neutron to decay into a proton, an electron, and an anti-neutrino.

use the same name for two different particles. The following year, the neutrino was a fundamental part in the theory of beta-decay [15,16] presented by Fermi. The Fermi theory of beta-decay, which is an effective low-energy theory involving an interaction with one neutron decaying into a proton, an electron, and an anti-neutrino (see Fig. 2.1), later on became the foundation of the Glashow–Weinberg–Salam (GWS) theory of electroweak interactions [17–19] unifying the electromagnetic and weak interactions into one common framework. The model for the nucleus was now that it consisted of protons and neutrons and beta-decay was described as one of the neutrons decaying into a proton which remained inside the nucleus while the electron and the anti-neutrino escaped, thus making the beta-decay a three-body decay with a continuous energy spectrum. Although described in somewhat more detail by the knowledge of the existence of quarks in the nucleons, this description of beta-decay is still valid.

The first calculations of neutrino interaction rates were made by Bethe and Peierls in 1934 [20] using the Fermi theory of beta-decay and the beta-decay rates. The resulting cross-sections were so small that many physicists doubted that neutrinos could ever be discovered by experiments. In fact, Pauli himself is known to have proclaimed that he had made a "terrible mistake" by "inventing a particle that cannot be detected".

Despite the small interaction cross-sections of neutrinos, it was suggested by Pontecorvo in 1946 [21] that they could be detected by using the process

$$\nu_e + {}^{37}\mathrm{Cl} \longrightarrow {}^{37}\mathrm{Ar} + e^-$$

of a neutrino hitting a Chlorine nucleus turning it into an Argon nucleus by transforming a neutron into a proton while emitting an electron. On June 14, 1956,

almost 26 years after the proposal by Pauli, Cowan and Reines telegraphed Pauli to inform him of their successful attempt to use the inverse beta-decay process

$$\bar{\nu} + p \longrightarrow n + e^+$$

to detect the anti-neutrinos resulting from beta-decays in a nuclear reactor at Savannah River [22, 23]. About 30 years later, an old student of Pauli sent Reines a letter which Pauli had written in response in 1956, but which had never arrived [24]:

> *Thanks for the message. Everything comes to him who knows how to wait.*
> – Pauli

The existence of a second type of neutrino, the muon neutrino ν_μ, was confirmed by the Brookhaven National Laboratory in 1962 [25]. When the third charged lepton, the tau τ^-, was discovered in 1975 [26], it was natural to assume that it would also have a neutrino associated to it. However, it was not until 2000 that the tau neutrino ν_τ was actually detected by the DONUT collaboration [27], completing the third generation of fermions in the Standard Model of particle physics (see Ch. 3).

2.1 The history of neutrino oscillations

Oscillations of neutrinos were first discussed by Pontecorvo in 1957 [28, 29]. However, since only one neutrino flavor was known at the time, Pontecorvo's discussion was treating oscillations between neutrinos and anti-neutrinos. The oscillations of neutrinos into anti-neutrinos were introduced in analogy to the oscillations between the neutral kaons K^0 and $\bar{K}^0$ [30].

After the discovery of the muon neutrino, the mixing of two massive neutrinos was discussed by Maki, Nakagawa, and Sakata in 1962 [31] as well as by Nakagawa *et al.* in 1963 [32], while neutrino oscillations between two different neutrino flavors were first discussed by Pontecorvo in 1967 [33]. Two years later, Pontecorvo and Gribov published a study [34] in which they presented a phenomenological theory for the oscillations between ν_e and ν_μ. However, this study failed to provide the correct oscillation length as the value presented differed by a factor of two from the correct one. The correct oscillation length was first presented by Fritzsch and Minkowski in 1976 [35]. The first study of three-flavor neutrino oscillations was done by Bilenky in 1987 [36].

An important ingredient in the theory of neutrino oscillations is how they are influenced by the presence of matter. The matter effect was first studied by Wolfenstein [37] and further elaborated on by Mikheyev and Smirnov [38, 39]. It plays a significant role in the analysis of solar neutrino experiments, where the adiabatic approximation is used to describe how electron neutrinos oscillate into a linear combination of muon and tau neutrinos.

Experimentally, neutrino oscillations were indicated already by early attempts to measure the flux of solar neutrinos in radiochemical experiments [40–46] and in

the Kamiokande experiment (Kamioka Nucleon Decay Experiment) [47–49], which was initially designed to measure proton decay. While the Kamiokande experiment was able to actually measure that the solar neutrinos came from the Sun [48, 49], and thus, giving proof that the Sun is indeed a source of neutrinos, all of these experiments measured a deficit in the neutrino flux compared to what is expected from solar models [50, 51].

The first evidence for neutrino oscillations was presented by the Super-Kamiokande experiment in 1998 [9]. The Super-Kamiokande experiment is the successor of the Kamiokande experiment and consists of a 50 kton water tank surrounded by photo multiplier tubes. The evidence was in the form of a directional analysis of the fluxes of atmospheric neutrinos coming from different directions, and thus, having traveled different distances since their production in the atmosphere. While the electron neutrino flux was in agreement with what could be expected without oscillations, there was a deficit in the muon neutrino flux when the neutrinos had traveled a significant distance through the Earth. This is interpreted as oscillations of muon neutrinos into tau neutrinos.

Since this first discovery, further evidence for neutrino oscillations have been observed in experiments with neutrinos coming from the Sun [52–57], the atmosphere [9,58,59], reactors [60,61], and accelerators [62–64]. The most compelling evidence are the observations from the Sudbury Neutrino Observatory (SNO) [56, 57], which has been able to measure both the electron neutrino flux and the total neutrino flux from the Sun. As the total neutrino flux is larger by a factor of three and only electron neutrinos can be produced in the Sun, it follows that the electron neutrinos must have changed their flavor as they have propagated from the Sun to the detector. In addition, the actual oscillatory pattern in the neutrino flavor transitions (generally, one could think of other mechanisms than oscillations for the change in neutrino flavor) have been observed in atmospheric [58] as well as reactor [61] experiments. For further discussion on the experimental evidence for neutrino oscillations, see Ch. 6.

Chapter 3

The Standard Model of particle physics

Every word or concept, clear as it may seem to be, has only a limited range of applicability.
– Werner Heisenberg

3.1 An overview of the Standard Model

The Standard Model (SM) of particle physics is one of the most successful models in modern physics. It is a model which describes what is believed to be the fundamental building blocks of Nature and their interactions, from the quarks and their interactions within nucleons to the weak interactions coupling neutrinos to other particles. In this chapter, we will introduce the SM and discuss its implications. In particular, we will discuss the electroweak interaction part of the SM [which is nothing else than the Glashow–Weinberg–Salam (GWS) model [17–19] for unifying electromagnetic and weak interactions], since it will be the part of the SM which is relevant to neutrino physics. Although the SM is very successful, we know that it cannot be the final description of Nature. Despite its very accurate predictions, there are a number of observations that do not fall within the scope of what the SM can describe. These observations will be discussed toward the end of the chapter.

The SM is a description of three out of the four fundamental interactions (the SM does not include gravity). These interactions are modeled by the exchange of particles; the electromagnetic interaction is described by the exchange of photons, the strong interaction by the exchange of gluons, and the weak interaction by the exchange of massive vector bosons. In addition, the SM contains three generations of fermions, each including two quarks and two leptons. By construction, the bosons and fermions in the SM are massless. However, from observations we know that many of the particles in the SM do have masses. Thus, the SM also includes

	Related symmetry	Fields
Electroweak bosons	$U(1)_Y$	B_μ
	$SU(2)_L$	W_μ^i $(i = 1, 2, 3)$
Gluons	$SU(3)_C$	V_μ^j $(j = 1, \ldots, 8)$

Table 3.1. The gauge field content of the SM. Each generator has a corresponding gauge field associated to it.

a mechanism for generating these masses through a process known as the Higgs mechanism, where the masses arise due to interactions with a Higgs field which has a non-zero vacuum expectation value (vev).

3.2 Gauge structure

In technical terms, the interactions of the SM are described by a quantized Yang–Mills theory [65] based on the non-Abelian gauge symmetry group $G_{\text{SM}} = U(1)_Y \times SU(2)_L \times SU(3)_C$. Since G_{SM} is a twelve dimensional Lie group, it has twelve different generators, each corresponding to a particle mediating a SM interaction. The generators of $SU(3)_C$ are the eight gluons responsible for the strong interaction, while the generators of $U(1)_Y \times SU(2)_L$ are responsible for mediating the electroweak interaction as will be described below. The Yang–Mills Lagrangian density is given by

$$\mathcal{L}_{\text{YM}} = -\frac{1}{4}\left[F_{\mu\nu}F^{\mu\nu} + G^i_{\mu\nu}G^{i\mu\nu} + H^j_{\mu\nu}H^{j\mu\nu}\right], \tag{3.1a}$$

where $F_{\mu\nu}$, $G^i_{\mu\nu}$ $(i \in \{1, 2, 3\})$ and $H^j_{\mu\nu}$ $(j \in \{1, \ldots, 8\})$ are the field strength tensors for the symmetry groups $U(1)_Y$, $SU(2)_L$ and $SU(3)_C$, respectively, *i.e.*,

$$F_{\mu\nu} = \partial_\mu B_\nu - \partial_\nu B_\mu, \tag{3.1b}$$
$$G^i_{\mu\nu} = \partial_\mu W^i_\nu - \partial_\nu W^i_\mu + g\varepsilon^{ijk}W^j_\mu W^k_\nu, \tag{3.1c}$$
$$H^j_{\mu\nu} = \partial_\mu V^j_\nu - \partial_\nu V^j_\mu + g'' f^{jk\ell}V^k_\mu V^\ell_\nu. \tag{3.1d}$$

Here, B_μ, W^i_μ, and V^j_μ are the Yang–Mills potentials, ε^{ijk} and $f^{jk\ell}$ are the structure constants and g and g'' the gauge couplings of $SU(2)_L$ and $SU(3)_C$, respectively. Note that, unlike quantum electrodynamics (QED), the Yang–Mills Lagrangian density contains self-interaction terms because of the non-Abelian gauge structure, leading to the interaction vertices shown in Fig. 3.1. The gauge field content of the SM is summarized in Tab. 3.1.

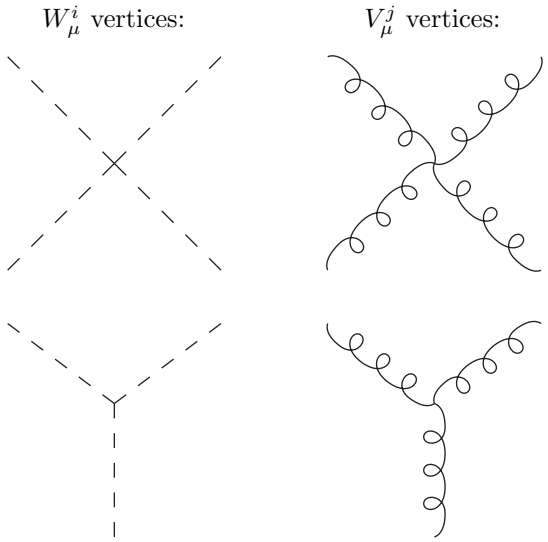

Figure 3.1. The self-interaction vertices in the SM due to the non-Abelian structure of the gauge groups. The B_μ field does not interact with itself, since the $U(1)_Y$ gauge group is Abelian.

3.3 Particle content

The second ingredient of the SM is the particle content in terms of fermions, *i.e.*, the quarks and the leptons. The kinetic term in the Lagrangian density for a free massless fermion ψ is given by

$$\mathcal{L}_\psi = i\overline{\psi}\partial\!\!\!/\psi. \tag{3.2a}$$

If we now assume that ψ is a collection of fermions which transforms as a multiplet under the SM gauge group, then this Lagrange density is not invariant under gauge transformations. In order to ensure this gauge invariance, we employ the minimal coupling scheme, where the differential operator $\partial\!\!\!/$ is replaced by the covariant derivative $D\!\!\!/$ according to $\partial\!\!\!/ \to D\!\!\!/ = \partial\!\!\!/ - ig'B\!\!\!/(Y/2) - igW\!\!\!/^i\tau^i - ig''V\!\!\!/^j\rho^j$, *i.e.*,

$$\mathcal{L}_\psi = i\overline{\psi}D\!\!\!/\psi, \tag{3.2b}$$

where g' is the $U(1)_Y$ gauge coupling, $Y/2$ is the representation of the hypercharge operator (generator of the $U(1)_Y$ symmetry), the τ^i are the representations of the $SU(2)_L$ generators, and ρ^j are the representations of the $SU(3)_C$ generators acting on the multiplet ψ.[1] The interactions introduced by this prescription correspond to Feynman vertices with one gauge boson connecting to a fermion line, see Fig. 3.2.

[1]Note that $\tau^i\psi = 0$ if ψ is an $SU(2)_L$ singlet and $\rho^j\psi = 0$ if ψ is an $SU(3)_C$ singlet as ψ then transforms in the trivial representations of $SU(2)_L$ and $SU(3)_C$, respectively.

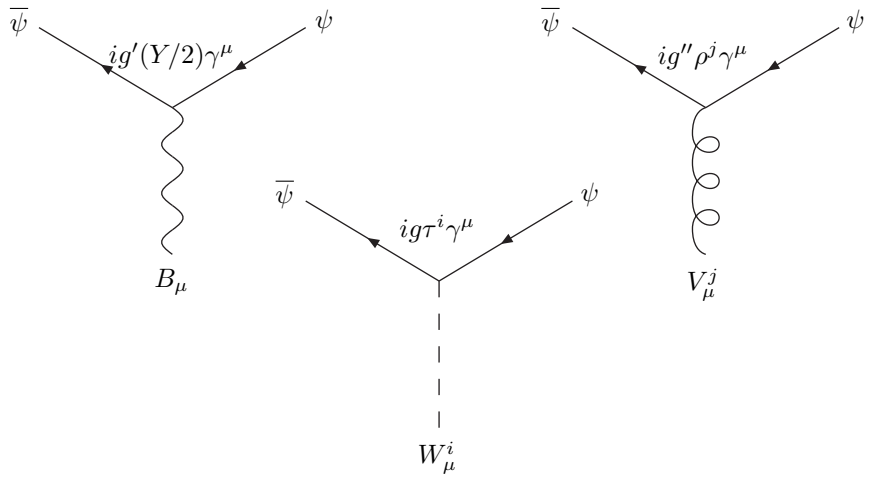

Figure 3.2. The Feynman vertices for the fermion-gauge boson interactions introduced by the minimal coupling prescription.

We introduce a generation of quarks by having one $SU(2)_L$ doublet and two $SU(2)_L$ singlets of fermions that transform under the **3** and $\bar{\mathbf{3}}$ representations of $SU(3)_C$, respectively. The quark content of a generation can be written as

$$Q_L = \begin{pmatrix} u_L \\ d_L \end{pmatrix}, \quad u_R, \quad \text{and} \quad d_R.$$

In a similar manner, a generation of leptons is introduced by adding one $SU(2)_L$ doublet and one $SU(2)_L$ singlet, which are both $SU(3)_C$ singlets, and thus, the lepton content of a single generation is

$$L_L = \begin{pmatrix} \nu_L \\ \ell_L \end{pmatrix}, \quad \text{and} \quad \ell_R.$$

Note that the right-handed neutrino field ν_R is not introduced in the SM. The number of generations in the SM is three and the full fermionic content is displayed in Tab. 3.2.

3.4 The Higgs mechanism

In the above introduction of the SM gauge and fermion content, we have not included any mass term. Thus, all particles introduced have been massless. This is obviously in violation of experimental results. For example, we know that the electron has a mass of about 511 keV and that the weak interactions are mediated by

	$SU(2)_L$ doublets	$SU(2)_L$ singlets
Quarks	$\begin{pmatrix} u_L \\ d_L \end{pmatrix}, \begin{pmatrix} c_L \\ s_L \end{pmatrix}, \begin{pmatrix} t_L \\ b_L \end{pmatrix}$	u_R, d_R, c_R, s_R, t_R, b_R
Leptons	$\begin{pmatrix} \nu_{eL} \\ e_L \end{pmatrix}, \begin{pmatrix} \nu_{\mu L} \\ \mu_L \end{pmatrix}, \begin{pmatrix} \nu_{\tau L} \\ \tau_L \end{pmatrix}$	e_R, μ_R, τ_R

Table 3.2. The fermionic content of the SM.

vector bosons with masses of the order of 100 GeV [66]. Let us start by considering the masses of the vector bosons.

The description of the vector boson masses in the SM is the introduction of spontaneous symmetry breaking of the electroweak $SU(2)_L \times U(1)_Y$ gauge symmetry down to the electromagnetic gauge symmetry $U(1)_{\text{EM}}$. To break this symmetry, we introduce an $SU(2)_L$ doublet of scalar[2] fields

$$\Phi = \begin{pmatrix} \phi^+ \\ \phi^0 \end{pmatrix} \tag{3.3}$$

with hypercharge $Y = 1$. These scalar fields are known as Higgs fields [67–70] and the corresponding Lagrangian density is given by

$$\mathcal{L}_{\text{Higgs}} = (D_\mu \Phi)^\dagger (D^\mu \Phi) - V(|\Phi|) \tag{3.4}$$

and includes the potential term $V(|\Phi|)$. This Lagrangian density is obviously symmetric under gauge transformations and the symmetry breaking comes from the potential $V(|\Phi|)$ not having its minimum at $|\Phi| = 0$, making the vacuum of the theory break the $SU(2)_L \times U(1)_Y$ symmetry (thus, the naming "spontaneous" symmetry breaking, signifying that the symmetry is not broken by the Lagrangian density but rather by the choice of vacuum state).

In the simplest model, the Higgs potential includes only a quartic and a quadratic term, *i.e.*,

$$V(|\Phi|) = -\mu^2 |\Phi|^2 + \lambda |\Phi|^4. \tag{3.5}$$

The shape of this potential is shown in Fig. 3.3. The minimum of the potential is obtained for $|\Phi| = \mu/\sqrt{2\lambda} \equiv v/\sqrt{2}$ and we obviously have some freedom in the particular choice of vacuum (since all the states with $|\Phi| = v/\sqrt{2}$ are equivalent). We choose the vev of the Higgs field to be

$$\Phi_0 = \begin{pmatrix} 0 \\ \frac{v}{\sqrt{2}} \end{pmatrix}. \tag{3.6}$$

This particular choice does not affect any physics as we can always make an $SU(2)$ transformation to put Φ_0 on the above form and redefine the gauge and fermion

[2] With respect to space-time transformations.

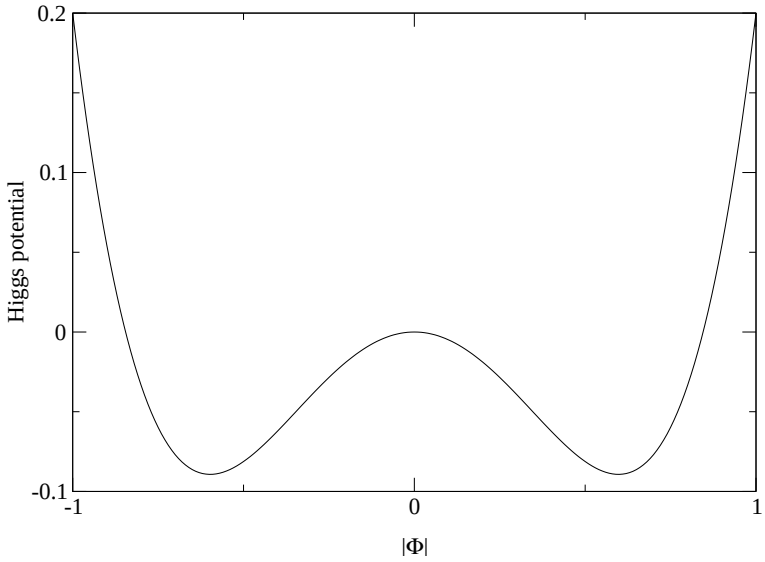

Figure 3.3. The shape of the Higgs potential given in Eq. (3.5). The parameter values have been chosen to $\mu^2 = 1/2$ and $\lambda = 0.7$ (arbitrary units).

fields accordingly. Writing the Higgs field as $\Phi = \Psi + \Phi_0$, the Higgs Lagrangian density will include the terms

$$\mathcal{L}_{m,\text{gauge}} = \frac{1}{4}\frac{v^2}{2}\left[(g'B_\mu - gW_\mu^3)^2 + 2g^2 W_\mu^+ W^{-\mu}\right], \tag{3.7}$$

where $W_\mu^\pm = (W_\mu^1 \mp i W_\mu^2)/\sqrt{2}$. These terms are the mass terms of the massive vector bosons. With $Z_\mu = \cos(\theta_W)W_\mu^3 - \sin(\theta_W)B_\mu$, $A_\mu = \sin(\theta_W)W_\mu^3 + \cos(\theta_W)B_\mu$, and the Weinberg angle θ_W given by

$$\tan(\theta_W) = \frac{g'}{g}, \tag{3.8}$$

this mass term becomes

$$\mathcal{L}_{m,\text{gauge}} = \frac{1}{2}\frac{g^2 v^2}{4}\left[\frac{1}{\cos^2(\theta_W)} Z_\mu Z^\mu + 2W_\mu^+ W^{-\mu}\right], \tag{3.9}$$

corresponding to the masses

$$m_W = \frac{gv}{2}, \quad m_Z = \frac{gv}{2\cos(\theta_W)}, \quad \text{and} \quad m_A = 0.$$

The remaining $U(1)$ symmetry corresponding to A_μ is nothing else than the electromagnetic gauge symmetry and A_μ itself is nothing else than the photon field.

Multiplet	Hypercharge (Y)
Q_L	$1/3$
u_R	$4/3$
d_R	$-2/3$
L_L	-1
ℓ_R	-2

Table 3.3. The hypercharges of the fermion multiplets in one fermion generation.

Let us examine the coupling of the gauge fields A_μ, Z_μ, and W_μ to fermions. From the minimal coupling prescription, the electroweak interactions between gauge and fermion fields are given by

$$\mathcal{L}_{\text{EWint}} = g' B_\mu \overline{\psi} \frac{Y}{2} \gamma^\mu \psi + g W_\mu^i \overline{\psi} \tau^i \gamma^\mu \psi \equiv g' B_\mu j'^\mu + g W_\mu^i j^{i\mu}. \tag{3.10a}$$

Rewriting this Lagrangian density in terms of the fields A_μ, Z_μ, and $W_\mu^\pm$, we obtain

$$\mathcal{L}_{\text{EWint}} = e A_\mu j_{\text{EM}}^\mu + g Z_\mu j_Z^\mu + g(W_\mu^+ j^{+\mu} + W_\mu^- j^{-\mu}), \tag{3.10b}$$

where we have defined the currents

$$j_{\text{EM}}^\mu = \overline{\psi} \gamma^\mu \left(\tau^3 + \frac{Y}{2} \right) \psi, \tag{3.10c}$$

$$j_Z^\mu = \frac{1}{\cos(\theta_W)} \overline{\psi} \gamma^\mu \left[\cos^2(\theta_W) \tau^3 - \sin^2(\theta_W) \frac{Y}{2} \right] \psi, \tag{3.10d}$$

$$j^{\pm\mu} = \frac{1}{\sqrt{2}} \overline{\psi} \gamma^\mu \tau^\pm \psi, \tag{3.10e}$$

and $\tau^\pm = \tau^1 \pm i\tau^2$. Note that the generator $\tau^3 + Y/2$ in the electromagnetic current j_{EM}^μ exactly corresponds to the weak analogue of the Gell-Mann–Nishijima relation [71, 72], since we know that the electromagnetic interaction couples to fermions as

$$\mathcal{L}_{\text{EMint}} = e A_\mu \overline{\psi} \gamma^\mu Q \psi, \tag{3.11}$$

where Q is the electromagnetic charge, and thus, we have $Q = \tau^3 + Y/2$. From this relation and observations, we can deduce the hypercharges of the fermions in the SM. With the appropriate choice of hypercharges (see Tab. 3.3), the electromagnetic current is

$$j_{\text{EM}}^\mu = \overline{\ell} \gamma^\mu (-1) \ell + \overline{u} \gamma^\mu \left(+\frac{2}{3} \right) u + \overline{d} \gamma^\mu \left(-\frac{1}{3} \right) d, \tag{3.12a}$$

where we have introduced the Dirac spinors[3]

$$\ell = \begin{pmatrix} \ell_L \\ \ell_R \end{pmatrix}, \quad u = \begin{pmatrix} u_L \\ u_R \end{pmatrix}, \quad \text{and} \quad d = \begin{pmatrix} d_L \\ d_R \end{pmatrix}.$$

[3]Note that these are four-component Dirac spinors under space-time transformations, not $SU(2)_L$ doublets.

The weak interaction currents are then given by

$$j^{+\mu} = \frac{1}{\sqrt{2}}\left(\overline{\nu_L}\gamma^\mu \ell_L + \overline{u_L}\gamma^\mu d_L\right), \tag{3.12b}$$

$$j^{-\mu} = \frac{1}{\sqrt{2}}\left(\overline{\ell_L}\gamma^\mu \nu_L + \overline{d_L}\gamma^\mu u_L\right), \tag{3.12c}$$

$$\begin{aligned} j_Z^\mu = \frac{1}{\cos(\theta_W)}\Big[&\overline{\nu_L}\gamma^\mu \frac{1}{2}\nu_L - \overline{\ell_L}\gamma^\mu \frac{1}{2}\ell_L + \overline{\ell}\gamma^\mu \sin^2(\theta_W)\ell \\ &+ \overline{u_L}\gamma^\mu \frac{1}{2}u_L - \overline{u}\gamma^\mu \frac{2}{3}\sin^2(\theta_W)u \\ &- \overline{d_L}\gamma^\mu \frac{1}{2}d_L + \overline{d}\gamma^\mu \frac{1}{3}\sin^2(\theta_W)d\Big]. \end{aligned} \tag{3.12d}$$

3.5 Masses of quarks and charged leptons

While the above introduction of the Higgs mechanism is perfectly successful in breaking the electroweak $SU(2)_L \times U(1)_Y$ symmetry down to the electromagnetic $U(1)_{\rm EM}$ symmetry and providing masses for the $W^\pm$ and Z fields, we have so far not seen how the fermion masses can be introduced into this theory. However, if we want to allow for the most general form of the Lagrangian density, there should also be terms of the type

$$\mathcal{L}_{\rm Yuk} = -y^d \overline{Q_L}\Phi d_R - y^u \overline{Q_L}\Phi^c u_R - y^\ell \overline{L_L}\Phi \ell_R + \text{h.c.}, \tag{3.13}$$

where y^d, y^u, and y^ℓ are dimensionless Yukawa coupling constants. In the case of one fermion generation, they can always be made real by a rephasing of the fermion fields. In the above expression, $\Phi^c = i\tau^2\Phi^*$ is the charge conjugate of Φ and transforms as an $SU(2)_L$ doublet with hypercharge -1 (because of the complex conjugation). Note that all the terms in the expression above are invariant under all SM gauge transformations. Since quarks and leptons have different hypercharges, we cannot introduce terms like $\overline{Q_L}\Phi\ell_R$ into the Lagrangian density. When the Higgs field Φ acquires its vev, the Lagrangian density has the form

$$\begin{aligned} \mathcal{L}_{\rm Yuk} &= \frac{v}{\sqrt{2}}\left[-y^d\overline{d_L}d_R - y^u\overline{u_L}u_R - y^\ell\overline{\ell_L}\ell_R\right] + \text{h.c.} + \ldots \\ &= \frac{v}{\sqrt{2}}\left[-y^d\overline{d}d - y^u\overline{u}u - y^\ell\overline{\ell}\ell\right] + \ldots. \end{aligned} \tag{3.14}$$

Comparing this with the mass term $-m\overline{\psi}\psi$ for a Dirac fermion, we conclude that the Higgs field gives rise to the effective masses

$$m_d = \frac{vy^d}{\sqrt{2}}, \quad m_u = \frac{vy^u}{\sqrt{2}}, \quad \text{and} \quad m_\ell = \frac{vy^\ell}{\sqrt{2}}$$

as it acquires its vev.

3.5.1 Quark mixing

When there are several fermion generations, as is the case in the SM, the most general form of the Yukawa interaction with quarks is given by

$$\mathcal{L}_{\text{Yuk}} = -y^d_{ij}\overline{Q^i_L}\Phi d^j_R - y^u_{ij}\overline{Q^i_L}\Phi^c u^j_R + \text{h.c.}, \tag{3.15a}$$

where y^d_{ij} and y^u_{ij} are now the components of general complex matrices and the indices i and j denote the different fermion generations. The mass terms following from the spontaneous symmetry breaking then become

$$\mathcal{L}_{\text{mass}} = -m^d_{ij}\overline{d^i_L}d^j_R - m^u_{ij}\overline{u^i_L}u^j_R + \text{h.c.}, \tag{3.15b}$$

where $m^d = y^d v/\sqrt{2}$ and $m^u = y^u v/\sqrt{2}$. Since any complex matrix can be diagonalized by a bi-unitary transformation, we can write

$$m^d = U^\dagger_L \tilde{m}^d U_R \quad \text{and} \quad m^u = V^\dagger_L \tilde{m}^u V_R, \tag{3.16a}$$

where U_R, U_L, V_R, and V_L are unitary matrices and $\tilde{m}^d$ and $\tilde{m}^u$ are real and diagonal matrices. If we also introduce the rotated fermion fields

$$d'^i_R = U_{R,ij}d^j_R, \quad d'^i_L = U_{L,ij}d^j_L, \quad u'^i_R = V_{R,ij}u^j_R, \quad \text{and} \quad u'^i_L = V_{L,ij}u^j_L, \tag{3.16b}$$

then the mass terms are of the form

$$\mathcal{L}_{\text{mass}} = -\tilde{m}^d_{ij}\overline{d'^i_L}d'^j_R - \tilde{m}^u_{ij}\overline{u'^i_L}u'^j_R + \text{h.c.}, \tag{3.17}$$

and thus, the fields d' and u' are the quark fields with definite masses. However, in terms of these new states, the interaction terms involving the W fields and the quarks are given by

$$\begin{aligned}
\mathcal{L}_{W\text{int}} &= \frac{g}{\sqrt{2}}W^+_\mu \overline{u^i_L}\gamma^\mu d^i_L + \text{h.c.} \\
&= \frac{g}{\sqrt{2}}W^+_\mu (V_L U^\dagger_L)_{ij}\overline{u'^i_L}\gamma^\mu d'^j_L + \text{h.c.} \\
&\equiv \frac{g}{\sqrt{2}}W^+_\mu U^{\text{CKM}}_{ij}\overline{u'^i_L}\gamma^\mu d'^j_L + \text{h.c.},
\end{aligned} \tag{3.18}$$

where $U^{\text{CKM}} = V_L U^\dagger_L$ is the Cabibbo–Kobayashi–Maskawa (CKM) matrix [73, 74] (or quark mixing matrix), relating the quark mass eigenstates to the quark weak interaction eigenstates.

A general unitary $n \times n$ matrix has n^2 real parameters of which $n(n-1)/2$ are mixing angles and $n(n+1)/2$ are complex phases. However, by rephasing the quark fields as $u'^i_L \to \exp(i\phi_i)u'^i_L$ and $d'^j_L \to \exp(i\psi_j)d'^j_L$, we can remove $2n-1$ of the complex phases of the CKM matrix.[4] By making the same rephasing of

[4] Redefining the up- or down-type quark fields would remove n phases. However, in both cases, one of the removed phases is an overall phase which can be removed by either the up- or down-type redefinitions. Thus, the total number of removed phases is $n + n - 1 = 2n - 1$.

Generations (n)	Mixing angles	Complex phases	Total
1	0	0 [0]	0 [0]
2	1	0 [1]	1 [2]
3	3	1 [3]	4 [6]
4	6	3 [6]	9 [12]
$\vdots$	$\vdots$	$\vdots$	$\vdots$
n	$\frac{n(n-1)}{2}$	$\frac{(n-1)(n-2)}{2}$ $\left[\frac{n(n-1)}{2}\right]$	$(n-1)^2$ $[n(n-1)]$

Table 3.4. The number of mixing parameters for different number of generations. The numbers within the square brackets indicate the number of parameters if either the up- or down-type fields cannot be rephased. This will be important when we discuss neutrino mixing in the case of Majorana mass terms.

Mixing parameter	Experimental value
θ_{12}^q	$13.1^\circ \pm 0.1^\circ$
θ_{23}^q	$2.42^{\circ\,+0.05^\circ}_{\;\;-0.08^\circ}$
θ_{13}^q	$0.22^\circ \pm 0.04^\circ$
δ^q	$57^{\circ\,+5^\circ}_{\;\;-11^\circ}$

Table 3.5. The quark mixing parameters with corresponding errors [66].

the right-handed fields, the mass terms are left invariant and we conclude that the phases we have removed are not physically observable. It follows that we are left with $n(n-1)/2$ mixing angles and $(n-1)(n-2)/2$ physical complex phases in the general n-flavor quark mixing matrix. In Tab. 3.4, we show the number of mixing parameters for different n.

In the case of three generations of quarks, as in the SM, the standard parametrization of the CKM matrix is [66]

$$U^{\rm CKM} = \begin{pmatrix} c_{12}c_{13} & s_{12}c_{13} & s_{13}e^{-i\delta^q} \\ -s_{12}c_{23} - c_{12}s_{23}s_{13}e^{i\delta^q} & c_{12}c_{23} - s_{12}s_{23}s_{13}e^{i\delta^q} & s_{23}c_{13} \\ s_{12}s_{23} - c_{12}c_{23}s_{13}e^{i\delta^q} & -c_{12}s_{23} - s_{12}c_{23}s_{13}e^{i\delta^q} & c_{23}c_{13} \end{pmatrix}, \tag{3.19}$$

where $c_{ij} = \cos(\theta_{ij}^q)$, $s_{ij} = \sin(\theta_{ij}^q)$. Here, the parameters θ_{12}^q, θ_{23}^q, and θ_{13}^q are the three quark mixing angles and δ^q is the complex phase. The mixing in the quark sector is small (*i.e.*, the quark mixing angles are close to zero, see Tab. 3.5), which, as we will discuss in the following chapters, will not be the case in the lepton sector.

3.5.2 Charged lepton masses

In contrast to the quarks, if there are n generations of leptons, then the most general lepton mass term arises from the Yukawa coupling

$$\mathcal{L}_{\text{Yuk}} = -y^{\ell}_{ij}\overline{L^i_L}\Phi\ell^j_R + \text{h.c.}, \tag{3.20a}$$

with the corresponding effective mass term

$$\mathcal{L}_{\text{mass}} = -m^{\ell}_{ij}\overline{\ell^i_L}\ell^j_R + \text{h.c.}, \tag{3.20b}$$

where $m^{\ell} = y^{\ell}v/\sqrt{2}$, after the electroweak symmetry breaking. Again, since m^{ℓ} is a general complex matrix, it can be diagonalized by a bi-unitary transformation

$$m^{\ell} = U^{\dagger}_L \tilde{m}^{\ell} U_R, \tag{3.21a}$$

where U_L and U_R are unitary matrices and $\tilde{m}^{\ell}$ is a diagonal matrix with real and positive entries. However, since there is no neutrino mass term in this case, we can define

$$L'^i_L = U_{L,ij}L^j \quad \text{and} \quad \ell'^i_R = U_{R,ij}\ell^j, \tag{3.21b}$$

which will diagonalize the lepton mass term. However, since we have used the same unitary transformation for the both entries of the $SU(2)_L$ doublets L^i_L, L'^i_L will also be $SU(2)_L$ doublets and no mixing matrix will appear in the weak interaction term for the leptons. For convenience, we simply define the charged leptons with definite masses as the electron, muon, and tau, respectively, and the corresponding neutrinos are defined as the neutrinos which are produced in charged-current weak interactions with these eigenstates.

3.6 Shortcomings of the Standard Model

Even though the SM is one of the most successful modern theories in physics and has been able to describe all particle interactions observed to this date with very high precision, some of its shortcomings are gradually revealing themselves just as we believe its final ingredient (the Higgs particle) is about to be detected at the Large Hadron Collider (LHC). While the present chapter has been a quick review of the construction of the SM, the remaining chapters will deal with situations where it fails.

The most obvious drawback of the SM is the fact that it does not contain gravity. In addition, there are no neutrino masses in the model. The introduction of a right-handed neutrino field could give rise to neutrino masses in an analogous manner to the introduction of the other fermion masses, *i.e.*, by Yukawa couplings to the Higgs field. However, there is then a problem of naturalness in the fact that the neutrino masses are so much smaller than the other fermion masses. The issue of introducing neutrino mass terms in the SM will be dealt with in the next chapter.

The introduction of neutrino masses is necessary to describe neutrino oscillations, a phenomenon that will be treated extensively in Ch. 5. For neutrino oscillations to occur, it is necessary that neutrinos are massive and that there is mixing in the lepton sector similar to that in the quark sector described above. Furthermore, the SM is unable to provide a viable dark matter candidate, and as the astronomical and cosmological evidence for dark matter is now overwhelming, the need of being able to describe it by a fundamental theory is ever increasing. In addition, the SM by itself is not capable of describing the baryon asymmetry of the Universe in a satisfactory way. As the experimental evidence for this asymmetry is also quite overwhelming, a final theory of particle physics should be able to describe it. The conclusion from these facts must be that, although its extreme success in describing particle interactions, the SM must be extended in order to be a theoretical model consistent with observations.

Chapter 4

Models of neutrino masses

Necessity is the mother of invention.
– Plato

4.1 Why neutrinos are different

In the simplest version of the SM, neutrinos are massless. In fact, this has been a very good description of Nature for a very long time, since the neutrino masses are so much smaller than the masses of the other fermions. However, from neutrino oscillation experiments, we know that neutrinos are massive (see Ch. 5), and thus, we must find a way of introducing neutrino masses into the SM. At first glance, the most appealing way would seem to be adding neutrino masses by coupling the neutrinos to the Higgs field, which would give rise to neutrino masses in the same way as the other fermion masses. The problem with this approach is to explain why the neutrino masses would be so much smaller than the masses of the other fermions, see Fig. 4.1.

Unlike the other fermions, neutrinos do not carry color or electric charge. This implies that neutrinos can be fundamentally different from the other fermions; it can actually be its own anti-particle. Such a fermion is known as a Majorana fermion (the fermion which is not its own anti-particle is known as a Dirac fermion) [75]. At the present time, there are no observations that have been able to probe if neutrinos are Dirac or Majorana fermions and this is one of the most intriguing prospects for future neutrino experiments.[1] However, in the case of Majorana neutrinos, there are problems in describing the neutrino masses in a natural way.

One of the most appealing ways of introducing neutrino masses is known as the seesaw mechanism. It can describe the existence of the small neutrino masses by the

[1] There have been claims of measurements of neutrinoless double beta-decay [76], which would indicate that neutrinos are Majorana fermions. However, the validity of these results are disputed [77–79].

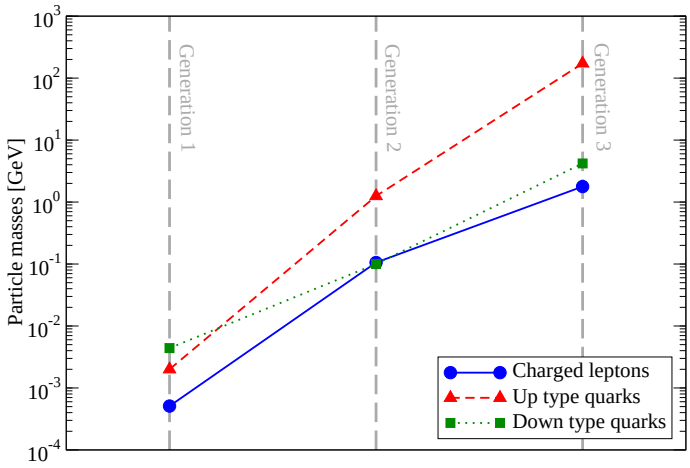

Figure 4.1. While the masses of the charged fermions span five orders of magnitude, the masses of the charged fermions within a given generation are still within two orders of magnitude. However, this is not true if we try to include the neutrino masses. The data for this figure has been adapted from Ref. [66].

introduction of very heavy Majorana neutrinos, which would typically have masses of the order of some higher energy scale (for example the scale of grand unification). If such heavy neutrinos exist and neutrinos are affected by the Higgs mechanism in a way similar to the other fermions, then this will give rise to neutrino masses which are suppressed by the ratio of the mass scale of the other fermions and the mass scale of the very heavy Majorana neutrinos. Thus, this model would naturally describe the small neutrino masses that we observe in Nature, see Fig. 4.2.

4.2 Dirac masses

The most obvious way of introducing neutrino masses into the SM is to introduce right-handed neutrino fields ν_R, which are $SU(2)_L$ and $SU(3)_C$ singlets with hypercharge zero. Obviously, such fields cannot be detected directly, since they do not couple to any of the gauge bosons. The only term in which it appears in the Lagrangian density except for its kinetic term is the Yukawa coupling term

$$\mathcal{L}_{\text{Yuk},\nu} = -y^{\nu}\overline{L_L}\Phi^c\nu_R + \text{h.c.}, \tag{4.1a}$$

which becomes

$$\mathcal{L}_{\text{Yuk},\nu} = -\frac{y^{\nu}v}{\sqrt{2}}\overline{\nu_L}\nu_R + \text{h.c.} + \ldots \tag{4.1b}$$

after the spontaneous breaking of the $SU(2)_L \times U(1)_Y$ symmetry. Thus, in analogy with the masses of the other fermions, we would have a neutrino mass of $m_\nu =$

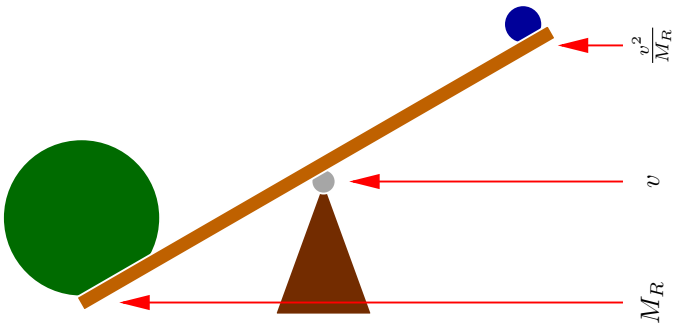

Figure 4.2. The seesaw mechanism makes the left-handed neutrinos very light as some other particle becomes very heavy. The neutrino masses decrease as the mass scale of the heavy particles increases.

$y^\nu v/\sqrt{2}$. If there are several fermion generations, then we introduce the same number of right-handed neutrinos, labeled by a generation index. The introduction of the Yukawa couplings for the neutrinos will then imply that there can also be mixing in the lepton sector. By the same construction as in the quark sector, we will have a unitary lepton mixing matrix $U_{\rm PMNS}$, which is the product of the left-handed unitary matrices diagonalizing the neutrino and the charged lepton Yukawa couplings, respectively.[2] Just as in the quark case, the neutrino and charged lepton fields can be rephased, leading to the removal of $n(n-1)$ unphysical complex phases from the lepton mixing matrix (in the case of n fermion generations), leaving $(n-1)^2$ physical parameters. It is customary to use the same type of parametrization for the lepton mixing matrix as for the quark mixing matrix, *i.e.*, in the case of three fermion generations, [66]

$$U_{\rm PMNS} = \begin{pmatrix} c_{12}c_{13} & s_{12}c_{13} & s_{13}e^{-i\delta^\ell} \\ -s_{12}c_{23} - c_{12}s_{23}s_{13}e^{i\delta^\ell} & c_{12}c_{23} - s_{12}s_{23}s_{13}e^{i\delta^\ell} & s_{23}c_{13} \\ s_{12}s_{23} - c_{12}c_{23}s_{13}e^{i\delta^\ell} & -c_{12}s_{23} - s_{12}c_{23}s_{13}e^{i\delta^\ell} & c_{23}c_{13} \end{pmatrix}, \tag{4.2}$$

where now $c_{ij} = \cos(\theta^\ell_{ij})$, $s_{ij} = \sin(\theta^\ell_{ij})$. The four mixing parameters in the lepton mixing matrix are the mixing angles θ^ℓ_{12}, θ^ℓ_{23}, and θ^ℓ_{13} as well as the *CP*-violating phase δ^ℓ. In the remainder of this thesis, we will drop the superscript ℓ, since we will only be concerned with the lepton mixing parameters and we will also adopt the short-hand notation $U = U_{\rm PMNS}$ unless explicitly stated otherwise.

The neutrino mass term introduced above is known as a Dirac mass term, it is in complete analogy with the mass term introduced for all other fermions and of

[2] The lepton mixing matrix is also known as the Pontecorvo–Maki–Nakagawa–Sakata (PMNS) matrix. It is usually defined as the mixing between $\overline{\ell'^\alpha_L}$ and ν'^i_L in the interaction with the W^- field rather than the mixing between $\overline{\nu'^i_L}$ and ℓ'^β_L in the interaction with the W^+ field (these definitions differ by Hermitian conjugation).

the form $-m\overline{\psi}\psi$, where ψ is a four-component Dirac spinor. At first glance, this scheme looks very appealing and it would seem like there is little reason to search for any other way of introducing neutrino masses. However, the Yukawa couplings needed in order to accommodate neutrino masses of the correct size are orders of magnitude smaller than the Yukawa couplings for the quarks and charged leptons.[3]

4.3 Majorana masses

As a matter of fact, there may not even be the need to extend the SM with extra right-handed neutrinos. As it turns out, the Dirac mass term is not the only possible fermion mass term. To be more specific, if we have a left-handed neutrino ν_L, then we can construct a Majorana mass term

$$\mathcal{L}_{\text{Maj}} = i\frac{m}{2}\nu_L^T\sigma^2\nu_L + \text{h.c.} \tag{4.3a}$$

or, in the case of several fermion generations,

$$\mathcal{L}_{\text{Maj}} = i\frac{M_{M,ij}}{2}\nu_L^{iT}\sigma^2\nu_L^j + \text{h.c.}, \tag{4.3b}$$

where M_M is the Majorana mass matrix. By the anti-commutativity of the components of the Weyl fermion, it follows that $\nu_L^{iT}\sigma^2\nu_L^j = \nu_L^{jT}\sigma^2\nu_L^i$, and thus, M_M can be taken to be complex symmetric, since only the symmetric part is physically significant.

Any complex symmetric matrix M_M can be diagonalized by a unitary transformation U_M such that

$$\tilde{M}_M = U_M^T M_M U_M, \tag{4.4a}$$

where $\tilde{M}_M$ is real and diagonal. By defining the new left-handed neutrino states

$$\nu_L'^i = U_{M,ij}\nu_L^j, \tag{4.4b}$$

the Majorana mass term takes the form

$$\mathcal{L}_{\text{Maj}} = i\frac{\tilde{M}_{M,ij}}{2}\nu_L'^{iT}\sigma^2\nu_L'^j + \text{h.c.}, \tag{4.5a}$$

while the weak interaction terms involving W and lepton fields are given by[4]

$$\mathcal{L}_{W\text{lep}} = \frac{g}{\sqrt{2}}W_\mu^+(U_M U_L^\dagger)_{i\alpha}\overline{\nu_L'^i}\gamma^\mu\ell_L'^\alpha + \text{h.c.}, \tag{4.5b}$$

[3] Although the Yukawa couplings for quarks and charged leptons also vary by orders of magnitude, the couplings within the same generation are roughly of the same order.

[4] It is common to denote the indices in the basis where the charged lepton mass matrix is diagonal by Greek indices (α, β, γ, ...) and the indices in the basis where the neutrino mass matrix is diagonal by Latin indices (i, j, k, ...). This convention will be adopted throughout the remainder of this thesis. The basis where the charged lepton mass matrix is diagonal will be referred to as the "flavor" basis, while the basis where the neutrino mass matrix is diagonal will be referred to as the "mass" basis. The flavor basis indices will run over the charged lepton flavors (e, μ, ...), while the mass basis indices will run from 1 to n.

where U_L is the left-handed unitary matrix involved in diagonalizing the Dirac mass term for the charged leptons. Thus, in the case of Majorana neutrinos, we also have a unitary lepton mixing matrix given by $U = U_L U_M^\dagger$. The difference to the case of Dirac neutrinos is that we cannot rephase the Majorana neutrino fields $\nu_L'^i$ without violating Eq. (4.4a) (*i.e.*, $\tilde{M}_M$ will no longer be kept real). Thus, the phases of the Majorana neutrino fields are physical and cannot be removed from the lepton mixing matrix. It follows that there are $n-1$ extra physical phases in the case of Majorana neutrinos (see Tab. 3.4). The lepton mixing matrix for Majorana neutrinos can be written as $U = U_D K$, where $K = \mathrm{diag}(1, e^{i\alpha_1}, e^{i\alpha_2}, \ldots)$, α_i are the extra physical Majorana phases, and U_D is parametrized as the lepton mixing matrix in the case of Dirac neutrinos.

As will be shown in Ch. 5, the Majorana phases do not affect any observables in neutrino oscillations [80, 81]. However, they can be observed in experiments which are sensitive to different effective neutrino masses. For example, experiments searching for neutrinoless double-beta decay are sensitive to the effective electron neutrino mass [82]

$$|m_{\nu_e}| = \left| \sum_i U_{ei}^2 m_i \right| , \tag{4.6}$$

where m_i is the mass of $\nu_L'^i$.

Even though the Majorana mass terms are appealing in the sense that we do not have to introduce any additional neutrino fields, there is still a number of issues that are not so satisfying. For example, the Majorana mass terms explicitly break the $SU(2)_L$ symmetry of the SM. In addition, the mass m was put in by hand and there is no argument why it should be small. It is possible to partially solve these problems by introducing a heavy $SU(2)$ triplet which couples to both the Higgs field and to the lepton $SU(2)_L$ doublets L_L^i. This is known as type II seesaw and will be treated in more detail in Sec. 4.4.2.

4.4 The seesaw mechanism

One very attractive way of introducing small neutrino masses into the SM is the seesaw mechanism [35, 83–91]. By this mechanism, the left-handed neutrinos of the SM are very light due to some other particles being very heavy (*e.g.*, at the scale of some grand unified theory). Furthermore, the addition of the very heavy particles naturally provides a way of generating the baryon asymmetry of the Universe, this mechanism will be treated in Ch. 7.

4.4.1 Type I seesaw

As we introduced right-handed neutrinos into the SM in order to write down a Dirac mass term, we did not consider the fact that since the right-handed neutrinos are

SM singlets, the Majorana mass term

$$\mathcal{L}_{\mathrm{RH,Maj}} = -i\frac{M_R}{2}\nu_R^\dagger \sigma^2 \nu_R^* + \mathrm{h.c.} \tag{4.7}$$

is invariant under gauge transformations, and thus, should be included into the Lagrangian density. The mass M_R is generally expected to be of the scale where some unified theory with a larger symmetry is broken, *i.e.*, a scale high above the electroweak scale.

In order to study the implications of such large right-handed Majorana mass terms, it is convenient to introduce the charge-conjugate $n_L^i = -i\sigma^2\nu_R^{i*}$ of the right-handed neutrino fields. The fields n_L^i are left-handed Weyl spinors and the Majorana mass term for the right-handed neutrinos is then

$$\mathcal{L}_{\mathrm{RH,Maj}} = i\frac{M_{R,ij}}{2} n_L^{iT}\sigma^2 n_L^j + \mathrm{h.c.} \tag{4.8}$$

It is now possible to write both the Dirac mass term as well as the right-handed neutrino mass term as one Majorana mass term

$$\mathcal{L}_{\mathrm{MD}} = i\frac{\mathcal{M}_{ij}}{2} N_L^{iT}\sigma^2 N_L^j + \mathrm{h.c.}, \tag{4.9}$$

where $N_L^i = \nu_L^i$ for $i = 1, \ldots, n$ and $N_L^i = n_L^{i-n}$ for $i = n+1, \ldots, 2n$. The full mass matrix $\mathcal{M}$ is given by

$$\mathcal{M} = \begin{pmatrix} 0 & m_D \\ m_D^T & M_R \end{pmatrix}, \tag{4.10}$$

where m_D is the Dirac mass matrix and M_R is the right-handed Majorana mass matrix. Since the right-handed neutrino masses are taken to be much larger than the Dirac masses, the full mass matrix $\mathcal{M}$ is approximately block-diagonalized as

$$\tilde{\mathcal{M}} = \begin{pmatrix} -m_D M_R^{-1} m_D^T & 0 \\ 0 & M_R \end{pmatrix} \simeq U^T \mathcal{M} U, \tag{4.11}$$

where

$$U = \begin{pmatrix} 1 & m_D^* M_R^{*-1} \\ -M_R^{-1} m_D^T & 1 \end{pmatrix} \equiv \begin{pmatrix} 1 & \alpha \\ -\alpha^\dagger & 1 \end{pmatrix}.$$

It follows that what we have just constructed is a Majorana mass term for the fields $N_L'^i \simeq \nu_L^i + \alpha_{ij} n_L^j$. Disregarding the small part of the right-handed neutrinos in these fields, the situation is now equivalent to that of a Majorana mass term for the left-handed neutrinos. The great benefit is that the eigenvalues of this new mass term are suppressed from the scale of the charged fermions by the quotient between the fermion and the right-handed neutrino mass scales, thus providing a natural description for the lightness of the left-handed neutrinos.

The above scheme for describing small left-handed neutrino masses is known as type I seesaw. The effect on the lepton mixing is that the heavy neutrino mass eigenfields, which are mainly composed from the non-interacting right-handed fields, also

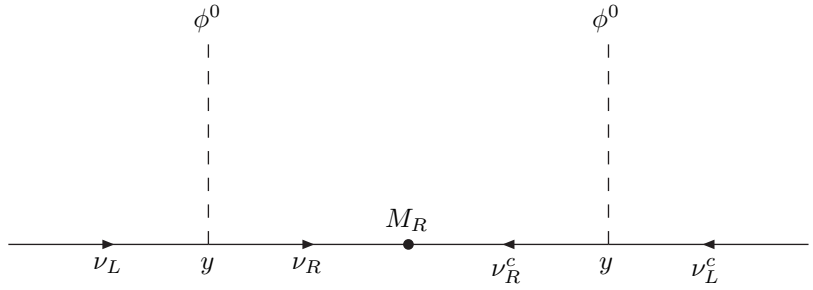

Figure 4.3. The Feynman diagram representing the interaction term giving rise to the type I seesaw mechanism as ϕ^0 acquires a vev. The diagram is suppressed by the Majorana mass term for the right-handed neutrino.

have a small part consisting of left-handed fields. Since the heavy neutrinos are too heavy to be produced in ordinary processes, this will be reflected by a seemingly non-unitary lepton mixing matrix as only a 3×3 block of the full unitary 6×6 matrix will be observed. However, this deviation from unitarity is also suppressed by the ratio between the fermion and the right-handed neutrino mass scales. The generation of the Majorana mass term for the left-handed neutrinos can be illustrated in terms of the Feynman diagram shown in Fig. 4.3.

4.4.2 Type II seesaw

Unlike in the type I seesaw, the type II seesaw does not introduce any additional right-handed neutrinos, and thus, there are no Yukawa couplings. Instead, the left-handed neutrinos receive their effective mass term from a coupling to a heavy $SU(2)_L$ triplet

$$\Delta = \begin{pmatrix} \Delta^+/\sqrt{2} & \Delta^{++} \\ \Delta^0 & -\Delta^+/\sqrt{2} \end{pmatrix}$$

of Lorentz scalars with hypercharge +2, which also couples to the Higgs field. The Lagrangian density for these interactions and the Δ mass term is

$$\mathcal{L}_\Delta = -m_\Delta^2 \operatorname{tr}(\Delta\Delta^\dagger) + [\mu\Phi^{c\dagger}\Delta^\dagger\Phi + ikL_L^T\sigma^2(i\tau^2)\Delta L_L + \text{h.c.}], \tag{4.12}$$

where m_Δ is the Δ mass, while k and μ are coupling constants (k is dimensionless and μ has dimension one). As the Higgs doublet acquires its vev, the effective potential for the triplet becomes

$$V(v, \Delta) = m_\Delta^2(|\Delta^{++}|^2 + |\Delta^+|^2 + |\Delta^0|^2) - \mu v^2 \operatorname{Re}\Delta^0. \tag{4.13}$$

This potential does not have its minimum at $\Delta = 0$, but will result in a real vev for Δ^0 such that

$$\langle \Delta \rangle = \begin{pmatrix} 0 & 0 \\ \frac{\mu v^2}{2m_\Delta^2} & 0 \end{pmatrix} \equiv \begin{pmatrix} 0 & 0 \\ \frac{v_\Delta}{2} & 0 \end{pmatrix}, \tag{4.14}$$

with the mass of Δ^0 being unchanged, since the interaction term with the Higgs field is linear in Δ.[5] Expanding the interaction term between the triplet and the left-handed neutrino, we have

$$\mathcal{L}_{\rm II} = i\frac{kv_\Delta}{2}\nu_L^T\sigma^2\nu_L + \text{h.c.}, \tag{4.15}$$

which is an effective Majorana mass term with $m_\nu = kv_\Delta$ for the left-handed neutrino. In the case of several fermion generations, the coupling k will be replaced by a coupling matrix k_{ij} leading to a Majorana mass matrix $M_{ij}^{\rm II} = k_{ij}v_\Delta$, with corresponding results for lepton mixing. Assuming that μ and m_Δ are of similar order, the type II seesaw will give rise to neutrino masses of the order v^2/m_Δ, which are again suppressed from the Higgs vev and some large mass.

4.4.3 Left-right symmetric seesaw

In general, there is nothing that prevents the type I and type II seesaw mechanisms to be present at the same time, a setting known as the type I+II seesaw mechanism. In such a case, the full neutrino mass term can be written as

$$\mathcal{L}_{\rm I+II} = i\frac{\mathcal{M}_{ij}^{\rm I+II}}{2}N_L^{iT}\sigma^2 N_L^j + \text{h.c.}, \tag{4.16a}$$

where N_L^i are the same fields as defined in the case of type I seesaw and

$$M^{\rm I+II} = \begin{pmatrix} M^{\rm II} & m_D \\ m_D^T & M_R \end{pmatrix}. \tag{4.16b}$$

As $M^{\rm II}$ is to be considered small compared with m_D and M_R, this mass matrix can be block-diagonalized by the same transformation as the pure type I seesaw mass matrix, resulting in the Majorana mass matrix

$$\mathcal{M} = M^{\rm II} - m_D M_R^{-1} m_D^T \tag{4.17}$$

for the left-handed neutrinos. The implications for the neutrino mixing is the same as in the type I seesaw.

[5] The existence of the interaction term between the triplet and the Higgs field will change the minimum of the Higgs potential, since it is quadratic in Φ. In principle, the theory should be expanded about the minimum of the full potential for both Φ and Δ.

In left-right (LR) symmetric models, the SM is extended to include an explicit symmetry between the left- and right-handed parts. The minimal LR symmetric model [88, 91–93] is based on the gauge symmetry group $SU(3)_C \times SU(2)_L \times SU(2)_R \times U(1)_{B-L}$ and is spontaneously broken down to the SM at some high-energy scale. In LR symmetric models, the right-handed fermion fields are all part of $SU(2)_R$ doublets just as the left-handed fermion fields are $SU(2)_L$ doublets in the SM. In addition, the Higgs content of the minimal LR symmetric model consists of one Higgs bidoublet with a $B - L$ charge of zero

$$\Phi = \begin{pmatrix} \phi_1^0 & \phi_1^+ \\ \phi_2^- & \phi_2^0 \end{pmatrix}, \tag{4.18a}$$

which will turn into two $SU(2)_L$ doublets with hypercharge ± 1, as well as left- and right-handed triplets Δ_L and Δ_R according to

$$\Delta_{L,R} = \begin{pmatrix} \frac{\Delta_{L,R}^+}{\sqrt{2}} & \Delta_{L,R}^{++} \\ \Delta_{L,R}^0 & -\frac{\Delta_{L,R}^+}{\sqrt{2}} \end{pmatrix}, \tag{4.18b}$$

which transform as triplets under $SU(2)_L$ and $SU(2)_R$ with $B - L = 2$, respectively. As the LR and electroweak symmetries are broken, the bidoublets will be responsible for the fermion masses just as the Higgs doublet of the SM provides fermion masses, while the triplets will provide Majorana mass terms for the left- and right-handed neutrinos, respectively. With the most general potential for the Higgs sector of the minimal LR symmetric model, the requirements for the minimum of the full potential will include the relation [94]

$$v^2 \propto v_L v_R, \tag{4.19}$$

where v^2 is an expression of second order in the bidoublet vevs and v_L and v_R are the vevs of the left- and right-handed triplets, respectively. Thus, if the right-handed vev is large, then the vev of the left-handed triplet must be small in comparison to the bidoublet vevs, producing a large Majorana mass term for the right-handed neutrinos and a small Majorana mass term for the left-handed neutrinos. The smallness of v_L is implied by observations of the masses of the left-handed gauge bosons and the Weinberg angle θ_W. The ratio between m_W and m_Z is predicted to be $\cos(\theta_W)$ at tree-level in the SM and a large v_L would give significant corrections to the left-handed gauge boson masses, which could not be accounted for by SM loop-corrections.

For the theory to be LR symmetric, there must be a discrete exchange symmetry between the left- and right-handed sectors, *i.e.*, the Lagrangian density should be invariant under the exchange

$$\Phi \longleftrightarrow \Phi^\dagger, \quad \Delta_L \longleftrightarrow \Delta_R, \quad \text{and} \quad \psi_L \longleftrightarrow \psi_R, \tag{4.20}$$

where $\psi_{L,R}$ are the fermion fields, then the couplings of the left- and right-handed neutrinos to the triplets must be the same, implying that

$$M^{\rm II} = v_L f \quad \text{and} \quad M_R = v_R f \tag{4.21}$$

in the type I+II seesaw relation of Eq. (4.17). Thus, the type I+II seesaw relation in the LR symmetric case is

$$\mathcal{M} = v_L f - \frac{1}{v_R} m_D f^{-1} m_D^T, \tag{4.22}$$

and if we consider $\mathcal{M}$, v_L, v_R, and m_D as known quantities, then this is a non-linear equation for the coupling matrix f. Since the equation is non-linear, we expect that there exist several solutions and it has been shown that the number of solutions is 2^n [95], where n is the number of fermion generations. For $n \leq 3$, there exist analytic expressions for these 2^n solutions [95–97], the most interesting one being the analytic form of the eight solutions in the case where $n = 3$. From low-energy phenomenology, we can only determine $\mathcal{M}$, and thus, we will need other criteria for discriminating among the eight possible solutions. This is the topic of Paper [7], where we have studied leptogenesis and fine-tuning issues for the different solutions.

Chapter 5

Theory of neutrino oscillations

A child of five would understand this. Send someone to fetch a child of five.
– Groucho Marx

5.1 Basic concepts of neutrino oscillations

In general, if neutrinos are massive, then they will oscillate. This means that if a neutrino is produced in a reaction involving a charged lepton of a given generation, it can later be detected in a reaction involving a charged lepton of another generation, *i.e.*, the generation to which the neutrino belongs has changed during its propagation from the point of production to the point of detection. An example of a process involving an oscillating neutrino is given in Fig. 5.1.

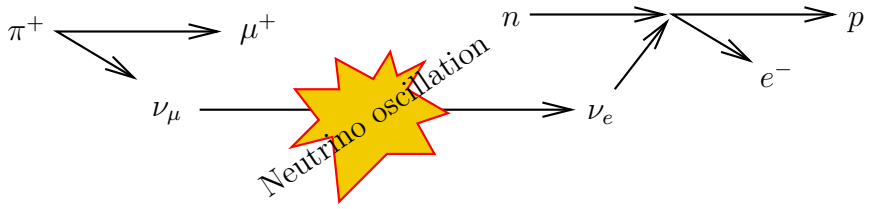

Figure 5.1. An example of a neutrino oscillation process: A muon neutrino ν_μ is produced along with a charged muon μ^+ in the decay of a charged pion π^+. As it propagates from the point of production to the point of detection, it turns into an electron neutrino ν_e which produces an electron e^- in the detector.

The probability for the oscillation of a neutrino of a given generation into a neutrino of another given generation can be calculated to be dependent on the difference between the squares of the neutrino masses. Thus, if neutrinos are massless, or if they all have the same mass, then they will not oscillate. It follows that if neutrino oscillations are observed, then neutrinos must be massive with at least two different masses. In addition to this, there must also be mixing in the lepton sector as the amount of mixing will determine the oscillation amplitudes. As will be described in Ch. 6, hints of neutrino oscillations have been around ever since the first experiments involving solar neutrinos [40–46]. However, it was not until 1998 that the Super-Kamiokande collaboration released the results [9] which included the first evidence for neutrino oscillations.

At the present time, there is evidence for neutrino oscillations coming from a vast number of different sources [9, 52–64]. The solar neutrino experiments have been able to prove that the electron neutrinos coming from the Sun actually turn into neutrinos of a different generation (many of the neutrino oscillation experiments only measure the disappearance of the initially produced neutrino type) [56,57]. In addition, the actual oscillating pattern has been observed for the neutrinos coming from the interactions of cosmic rays with the atmosphere [58] and for the neutrinos coming from the nuclear processes in reactors [61].

5.2 Heuristic derivation

In this section, we will make a lot of simplifying assumptions. Although these assumptions will not be fulfilled, we will still be able to derive the correct result for ultra-relativistic neutrinos, which is what we will be dealing with. For ultra-relativistic neutrinos, we can define a flavor eigenstate of momentum p as [98]

$$|\nu_\alpha(p)\rangle \equiv \sum_i U^*_{\alpha i} \, |\nu_i(p)\rangle \,, \tag{5.1a}$$

where $|\nu_i(p)\rangle$ is the neutrino in mass eigenstate i with momentum p. According to this, we have defined the flavor eigenstates in terms of mass eigenstates with the same momentum. We could also define the flavor eigenstates as superpositions of states with the same energy. However, for ultra-relativistic neutrinos, the difference is not noticeable and the final neutrino oscillation probabilities will be the same, while for non-relativistic neutrinos, the superposition does not make sense to begin with. The complex conjugation of the lepton mixing matrix in Eq. (5.1a) is due to the states being created from the vacuum by the conjugate fields $\overline{\nu_i}$. In the same manner, the anti-neutrino flavor eigenstate is defined as

$$|\bar{\nu}_\alpha(p)\rangle \equiv \sum_i U_{\alpha i} \, |\bar{\nu}_i(p)\rangle \,. \tag{5.1b}$$

Since the neutrino mass eigenstates $|\nu_i(p)\rangle$ are states with definite energies $E_i^2 = p^2 + m_i^2$, their time evolution will simply be given by the addition of a phase factor

$$|\nu_i(p,t)\rangle = \exp(-iE_i t)\,|\nu_i(p)\rangle\,. \tag{5.2}$$

Furthermore, the ultra-relativistic nature of the neutrinos allows us to make an expansion of E_i as

$$E_i = \sqrt{p^2 + m_i^2} = p + \frac{m_i^2}{2p} + p\mathcal{O}(m_i^4/p^4). \tag{5.3}$$

The momentum p is common for all of the mass eigenstates, since we assumed them to have the same momentum. Thus, the leading order phase difference between the mass eigenstates will arise due to the first correction term $m_i^2/(2p)$.

The probability amplitude of finding a neutrino of initial flavor ν_α in the flavor state $|\nu_\beta\rangle$ at time t is given by

$$A_{\alpha\beta} = \langle\,\nu_\beta(p)|\,\nu_\alpha(p,t)\rangle\,, \tag{5.4a}$$

where $|\nu_\alpha(p,t)\rangle$ is given by propagating the mass eigenstates in $|\nu_\alpha(p)\rangle$ separately according to Eq. (5.2). Thus, we find

$$A_{\alpha\beta} = \sum_{i,j} U_{\beta j} U^*_{\alpha i} e^{-iE_i t}\,\langle\,\nu_j(p)|\,\nu_i(p)\rangle = \sum_i U_{\beta i} U^*_{\alpha i} e^{-iE_i t}. \tag{5.4b}$$

The corresponding neutrino oscillation probability, *i.e.*, the probability of finding the initial ν_α as a ν_β at time t, is then given by

$$\begin{aligned} P_{\alpha\beta} &= \left|\sum_i U_{\beta i} U^*_{\alpha i} e^{-iE_i t}\right|^2 \\ &= \sum_{i,j} U_{\beta i} U^*_{\alpha i} U^*_{\beta j} U_{\alpha j} e^{-i(E_i - E_j)t} \\ &\equiv \sum_{i,j} J^{ij}_{\alpha\beta} e^{-i\Delta_{ij}}, \end{aligned} \tag{5.5a}$$

where we have defined $J^{ij}_{\alpha\beta} = U_{\beta i} U^*_{\alpha i} U^*_{\beta j} U_{\alpha j}$ as well as $\Delta_{ij} = (E_i - E_j)t \simeq \Delta m^2_{ij} t/(2p)$, and $\Delta m^2_{ij} = m_i^2 - m_j^2$ is the mass squared difference between the mass eigenstates ν_i and ν_j. There is a number of different ways of rewriting this expression, for example,

$$P_{\alpha\beta} = \sum_i J^{ii}_{\alpha\beta} + 2\sum_{i<j} \mathrm{Re}(J^{ij}_{\alpha\beta})\cos(\Delta_{ij}) + 2\sum_{i<j} \mathrm{Im}(J^{ij}_{\alpha\beta})\sin(\Delta_{ij}) \tag{5.5b}$$

$$= \delta_{\alpha\beta} - 4\sum_{i<j} \mathrm{Re}(J^{ij}_{\alpha\beta})\sin^2\left(\frac{\Delta_{ij}}{2}\right) + 2\sum_{i<j} \mathrm{Im}(J^{ij}_{\alpha\beta})\sin(\Delta_{ij}) \tag{5.5c}$$

$$= \sum_i J^{ii}_{\alpha\beta} + 2\sum_{i<j} |J^{ij}_{\alpha\beta}|\cos(\Delta_{ij} - \arg J^{ij}_{\alpha\beta}). \tag{5.5d}$$

If we instead study anti-neutrinos, the only difference is in the definition of the anti-neutrino states in Eq. (5.1b), and we can obtain the anti-neutrino oscillation probability by making the substitution $U_{\alpha i} \to U^*_{\alpha i}$, which is equivalent to $J^{ij}_{\alpha\beta} \to J^{ij*}_{\alpha\beta} = J^{ij}_{\beta\alpha} = J^{ji}_{\alpha\beta}$, in the neutrino oscillation probability. As can be readily observed in Eqs. (5.5), this substitution will not affect the oscillation probability if $J^{ij}_{\alpha\beta}$ is real. Thus, in order to have *CP*-violation in neutrino oscillations, $J^{ij}_{\alpha\beta}$ must have an imaginary part. In addition, we note that if we redefine the lepton mixing matrix as $U_{\alpha i} \to U_{\alpha i} e^{i\phi_i}$ or $U_{\alpha i} \to U_{\alpha i} e^{i\psi_\alpha}$, then this rephasing will not affect $J^{ij}_{\alpha\beta}$, since such rephasings will cancel out. Thus, any phases that can be removed in this way will not enter into the neutrino oscillation probabilities. The rephasings of the latter type are the same rephasings that were made to the charged lepton fields, and thus, this does not remove any extra phases as neutrino oscillation parameters. However, the former type of rephasing is the equivalent of changing the phases of the neutrino fields, which could not be made in the case of Majorana neutrinos. The above consideration shows that, in the case of neutrino oscillations in vacuum, Majorana phases are not observable in neutrino oscillations. This is in fact a general result, which also holds in the case of neutrino oscillations in matter. In the three-flavor case, this leaves us with only one *CP*-violating phase among the physically observable neutrino oscillation parameters, regardless of the nature of neutrinos. Furthermore, we note that

$$A_{\beta\alpha} = \sum_{i,j} J^{ij}_{\beta\alpha} e^{-i\Delta_{ij}} = \sum_{i,j} J^{ji}_{\alpha\beta} e^{i\Delta_{ji}} = A^*_{\bar{\alpha}\bar{\beta}}, \tag{5.6}$$

where $A_{\bar{\alpha}\bar{\beta}}$ is the amplitude for $\bar{\nu}_\alpha$ to oscillate into $\bar{\nu}_\beta$. It follows that $P_{\beta\alpha} = P_{\bar{\alpha}\bar{\beta}}$, *i.e.*, time reversal is equivalent to *CP*-conjugation for the neutrino oscillation probabilities and in order to have *T*-violation, there must also be Dirac phases in the lepton mixing matrix.

Since we are dealing with ultra-relativistic neutrinos, it is common to use the approximations $t \simeq L$ and $p \simeq E$ in the oscillation phases Δ_{ij}, *i.e.*,

$$\Delta_{ij} \simeq \frac{\Delta m^2_{ij}}{2E} L, \tag{5.7}$$

where L is the distance traveled by the neutrinos and E is the neutrino energy. This convention will be followed throughout the remainder of this text.

5.3 Hamiltonian formalism

A common way of describing neutrino oscillations among n neutrino flavors is in terms of an n level quantum mechanical system, where the neutrino state $|\nu\rangle$ is represented by the state vector

$$\nu_m = \begin{pmatrix} \langle \nu_1 | \nu \rangle \\ \langle \nu_2 | \nu \rangle \\ \vdots \end{pmatrix} \tag{5.8a}$$

in the mass eigenstate basis and

$$\nu_f = \begin{pmatrix} \langle \nu_e | \, \nu \rangle \\ \langle \nu_\mu | \, \nu \rangle \\ \vdots \end{pmatrix} \tag{5.8b}$$

in the flavor eigenstate basis. In this matrix representation of the neutrino states, the relation between the mass and flavor eigenstate bases is[1]

$$\nu_f = \begin{pmatrix} \langle \nu_e | \, \nu_i \rangle \langle \nu_i | \, \nu \rangle \\ \langle \nu_\mu | \, \nu_i \rangle \langle \nu_i | \, \nu \rangle \\ \vdots \end{pmatrix} = \begin{pmatrix} U_{ei} \langle \nu_i | \, \nu \rangle \\ U_{\mu i} \langle \nu_i | \, \nu \rangle \\ \vdots \end{pmatrix} = U \nu_m. \tag{5.9}$$

The matrix representation of the Hamiltonian of the system is most easily written in the mass eigenstate basis as

$$H_{m,ij} = \langle \nu_i \, | H | \, \nu_j \rangle \simeq \delta_{ij} \left(p + \frac{m_i^2}{2E} \right) \tag{5.10a}$$

or, equivalently,

$$H_m \simeq \left(p + \frac{m_1^2}{2E} \right) \mathbf{1} + \frac{1}{2E} \operatorname{diag}(0, \Delta m_{21}^2, \Delta m_{31}^2, \ldots), \tag{5.10b}$$

where $\mathbf{1}$ is the $n \times n$ unit matrix. Any contribution to the Hamiltonian which is proportional to the unit matrix will only give rise to an overall phase of the evolved state. Thus, subtracting or adding terms proportional to unity will not change the neutrino oscillation probabilities. Therefore, we will make the substitution

$$H_m \longrightarrow \frac{1}{2E} \operatorname{diag}(0, \Delta m_{21}^2, \Delta m_{31}^2, \ldots), \tag{5.10c}$$

where it also becomes apparent that only the mass squared differences (and not the absolute mass) of the neutrinos enter as neutrino oscillation parameters. The Hamiltonian in flavor basis is expressed as

$$H_f = U H_m U^\dagger. \tag{5.11}$$

The time evolution of the neutrino state is given by the Schrödinger equation in either mass or flavor basis as

$$i \frac{d\nu_m}{dL} = H_m \nu_m \quad \text{and} \quad i \frac{d\nu_f}{dL} = H_f \nu_f, \tag{5.12}$$

respectively. This Schrödinger equation has the solution

$$\nu_{f,m}(L) = S_{f,m}(L) \nu_{f,m}(0), \tag{5.13}$$

[1] Note that $|\nu_i\rangle \langle \nu_i|$ is just the identity operator, since $|\nu_i\rangle$ forms a complete set of states.

where the time evolution operator $S_{f,m}(L)$ is a unitary matrix given by

$$S_{f,m}(L) = \exp\left(-iH_{f,m}L\right).$$

The amplitude for transition from the neutrino state ν to ν' is now given by

$$\begin{aligned} A_{\nu\to\nu'} &= \langle\nu'\left|S(L)\right|\nu\rangle \\ &= \langle\nu'|\,\nu_i\rangle\,\langle\nu_i\left|S(L)\right|\nu_j\rangle\,\langle\nu_j|\,\nu\rangle \\ &= \nu_m'^{\dagger}\exp(-iH_mL)\nu_m, \end{aligned} \tag{5.14}$$

with the corresponding expression in flavor basis. With the convention that ν_α is the vector representing the flavor eigenstate $|\nu_\alpha\rangle$ in flavor basis and that ν_i is the vector representing the mass eigenstate $|\nu_i\rangle$ in mass basis, we have

$$\begin{aligned} A_{\alpha\beta} &= \nu_\beta^\dagger U\exp(-iH_mL)U^\dagger\nu_\alpha \\ &= U_{\beta j}\nu_j^\dagger\exp(-iH_mL)\nu_i U_{\alpha i}^* \\ &= \sum_i U_{\beta i}U_{\alpha i}^*\exp\left(-i\frac{\Delta m_{i1}^2L}{2E}\right), \end{aligned} \tag{5.15}$$

which is the same expression as in Eq. (5.4b) up to an overall phase factor.

5.3.1 Two-flavor oscillations

A very important example of neutrino oscillations is the case where we consider only two neutrino flavors, say ν_e and ν_x. Although we know that there are at least three neutrino flavors, the two-flavor scenario has been remarkably successful in describing many neutrino oscillation experiments. The reason for this is that the neutrino oscillation parameters are such that the neutrino oscillations can be effectively described by only two flavors. This will be discussed more in the next subsection, for now we will focus on the two-flavor oscillations.

As was discussed previously, the n-flavor scenario has $n(n-1)/2$ mixing angles, $(n-1)(n-2)/2$ Dirac phases, and $n-1$ mass squared differences, which affect the neutrino oscillation probabilities. Thus, in the two-flavor scenario, there are no Dirac phases, implying that the lepton mixing matrix is real, and the only parameters are the mixing angle θ and the mass squared difference $\Delta m^2 = m_2^2 - m_1^2$. The lepton mixing matrix is then simply a two-dimensional rotation

$$U = \begin{pmatrix} c & s \\ -s & c \end{pmatrix}, \tag{5.16}$$

where $c = \cos(\theta)$ and $s = \sin(\theta)$, and the neutrino oscillation Hamiltonian is

$$H_f = \frac{\Delta m^2}{4E}U\,\mathrm{diag}(-1,1)U^\dagger = \frac{\Delta m^2}{4E}\begin{pmatrix} -\cos(2\theta) & \sin(2\theta) \\ \sin(2\theta) & \cos(2\theta) \end{pmatrix}, \tag{5.17}$$

where, in order to make the Hamiltonian traceless, we have used the fact that any contribution to the Hamiltonian which is proportional to the unit matrix only will

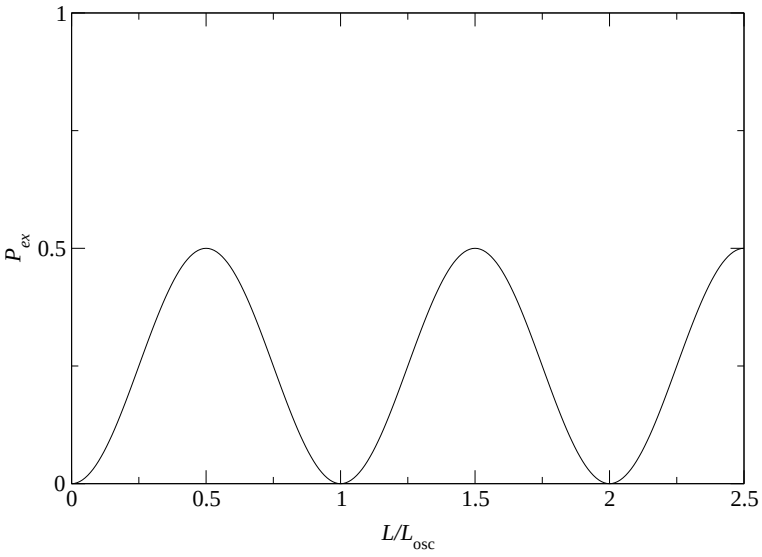

Figure 5.2. The two-flavor neutrino oscillation probability P_{ex} as a function of $L/L_{\rm osc}$ for $\theta = \pi/8$, which corresponds to an oscillation amplitude of $\sin^2(2\theta) = 0.5$.

contribute with an overall phase. The two-flavor neutrino oscillation probabilities are

$$P_{ee} = P_{xx} = 1 - \sin^2(2\theta)\sin^2\left(\frac{\Delta}{2}\right), \tag{5.18a}$$

$$P_{ex} = P_{xe} = \sin^2(2\theta)\sin^2\left(\frac{\Delta}{2}\right), \tag{5.18b}$$

where the oscillation phase is given by $\Delta = \Delta m^2 L/(2E)$. The factor $\sin^2(2\theta)$ does not vary with the baseline L and is therefore the amplitude of the oscillations. The oscillation phase can be written as

$$\frac{\Delta}{2} = \pi\frac{L}{L_{\rm osc}}, \tag{5.19a}$$

where we have defined the neutrino oscillation length

$$L_{\rm osc} = \frac{4\pi E}{\Delta m^2} \tag{5.19b}$$

as the neutrino oscillation period. The two-flavor neutrino oscillation probability P_{ex} for $\theta = \pi/8$ is plotted in Fig. 5.2.

Parameter	Best-fit	3σ region
θ_{12}	33.2°	28.6°-38.1°
θ_{23}	45°	35.6°-55.6°
θ_{13}	0°	$\leq 12.5°$
Δm^2_{21} [10^{-5} eV^2]	8.1	7.2-9.1
$\lvert\Delta m^2_{31}\rvert$ [10^{-3} eV^2]	2.2	1.4-3.3

Table 5.1. The values of the three-flavor neutrino oscillation parameters from the global fit to neutrino oscillation data in Ref. [99]. Other global fits [100,101] provide similar results. Note that the sign of Δm^2_{31} and the *CP*-violating phase δ are not yet determined.

That $P_{ee} = P_{xx}$ and $P_{ex} = P_{xe}$ in the two-flavor scenario is a direct consequence of the unitarity of the evolution operator S, which implies that

$$\sum_\alpha P_{\alpha\beta} = \sum_\alpha P_{\beta\alpha} = 1, \tag{5.20a}$$

i.e.,

$$P_{ee} + P_{ex} = P_{ex} + P_{xx} = P_{xe} + P_{xx} = P_{ee} + P_{xe} = 1. \tag{5.20b}$$

This unitarity condition basically states that no neutrinos are lost during the neutrino evolution (the probability of finding the neutrino in any of the neutrino states is one) and that if a neutrino is detected, then it must have been produced as some type of neutrino (the probability that the neutrino was initially in one of the neutrino states is one). The unitarity condition is present for any number of neutrinos, but does not generally predict $P_{\alpha\beta} = P_{\beta\alpha}$, *c.f.* discussion in next subsection.

5.3.2 Three-flavor oscillations

Even if the two-flavor neutrino oscillation scenario is very intuitive and simple, it is not always a good description. For example, if we wish to measure the neutrino oscillation parameters with high precision, then we have to use the full three-flavor scenario, since this is what defines our parameters. Let us therefore examine the three-flavor scenario and observe in what situations and with which parameter mappings it can be reduced to effective two-flavor scenarios. We will also discuss genuine three-flavor effects such as *CP*-violation.

In the three-flavor scenario, we parametrize the lepton mixing matrix using the standard parametrization of Eq. (4.2). The parametrization of the lepton mixing matrix requires three mixing angles and one *CP*-violating phase. In addition, there will be two independent mass squared differences[2], Δm^2_{21} and Δm^2_{31}. The values of these parameters resulting from global fits to neutrino oscillation data are shown in Tab. 5.1.

[2]By definition, we have $\Delta m^2_{ij} = -\Delta m^2_{ji}$ and $\Delta m^2_{32} = \Delta m^2_{31} - \Delta m^2_{21}$.

Effective two-flavor scenarios

The probability $P_{\alpha\beta}$ of $\nu_\alpha \to \nu_\beta$ is well described by a two-flavor approximation if it is of the form

$$P_{\alpha\beta} = \delta_{\alpha\beta} + (1 - 2\delta_{\alpha\beta}) \sin^2(2\theta) \sin^2\left(\frac{\Delta m^2}{4E} L\right). \tag{5.21}$$

Comparing this with Eq. (5.5c), we observe that there will be oscillation probabilities which are well described by two-flavor formulas if either any of the elements in the lepton mixing matrix or one of the mass squared differences are zero.

In the case when an element of the lepton mixing matrix, say U_{e3},[3] is equal to zero the lepton mixing matrix can be made real by removal of the Majorana phases, which are irrelevant to neutrino oscillations. Thus, the terms involving the imaginary part of $J^{ij}_{\alpha\beta}$ can be dropped in Eqs. (5.5) and we are left with

$$P_{\alpha\beta} = \delta_{\alpha\beta} - 4 \sum_{i<j} \mathrm{Re}(J^{ij}_{\alpha\beta}) \sin^2\left(\frac{\Delta m^2_{ij}}{4E} L\right). \tag{5.22}$$

Furthermore, since $U_{e3} = 0$, it follows that $J^{i3}_{e\alpha} = J^{i3}_{\alpha e} = J^{3i}_{e\alpha} = J^{3i}_{\alpha e} = 0$, and thus, we have the following effective two-flavor expressions

$$\begin{aligned} P_{ee} &= 1 - 4J^{12}_{ee} \sin^2\left(\frac{\Delta m^2_{21}}{4E} L\right) \\ &= 1 - 4|U_{e1}|^2|U_{e2}|^2 \sin^2\left(\frac{\Delta m^2_{21}}{4E} L\right), \end{aligned} \tag{5.23a}$$

$$\begin{aligned} P_{e\alpha} &= -4U_{e1}U_{e2}U_{\alpha1}U_{\alpha2} \sin^2\left(\frac{\Delta m^2_{21}}{4E} L\right) \\ &= P_{\alpha e}, \end{aligned} \tag{5.23b}$$

where we have dropped the complex conjugation of the lepton mixing matrix elements, since they can be made real by removing the Majorana phases. It should be noted that the neutrino oscillation probabilities not involving ν_e are not necessarily of the two-flavor form even if $U_{e3} = 0$. The fact that the above expressions are of the two-flavor form is a direct consequence of ν_e being a superposition of only two different neutrino mass eigenstates when $U_{e3} = 0$. Unless another element in the same row or column as U_{e3} is also equal to zero, the remaining neutrino oscillation probabilities will not be of two-flavor form.

The lepton mixing matrix can also be made real in the case when one of the mass squared differences is zero, in fact, we can then redefine the lepton mixing matrix such that it contains a zero. However, in this situation, all the neutrino oscillation probabilities will be of the two-flavor form for the simple reason that

[3] We choose U_{e3} as an example, since it is known to be small, *c.f.* Tab. 5.1

there will only be one independent mass squared difference left, *i.e.*, if $\Delta m^2_{21} = 0$, then $\Delta m^2_{32} = \Delta m^2_{31}$. The amplitudes and mass squared differences of the above mentioned cases can be found in Tab. 1 of Paper [3].

Even if the above requirements are not exactly fulfilled, but rather $|U_{e3}| \ll 1$ or $\Delta m^2_{21} \ll 2E/L$, these two-flavor formulas can be used as approximations. In addition, there are other scenarios where the final neutrino oscillation probabilities include two-flavor expressions. For example, if $\Delta m^2_{31} \sim \Delta m^2_{32} \gg 2E/L$, then the factors $\cos(\Delta_{3i})$ and $\sin(\Delta_{3i})$ will oscillate so fast that experiments will only be able to observe their averaged effect, which is zero since cosine and sine average to zero. In this limit, the neutrino oscillation probabilities have the form

$$P_{\alpha\beta} = \delta_{\alpha\beta} - 2\,\mathrm{Re}(J^{13}_{\alpha\beta} + J^{23}_{\alpha\beta}) - 4\,\mathrm{Re}(J^{12}_{\alpha\beta})\sin^2\left(\frac{\Delta m^2_{21}}{4E}L\right) - 2\,\mathrm{Im}(J^{12}_{\alpha\beta})\sin\left(\frac{\Delta m^2_{21}}{2E}L\right). \tag{5.24}$$

While the neutrino transition probabilities ($\alpha \neq \beta$) will not only include constants and the characteristic two-flavor modulation $\sin^2[\Delta m^2 L/(4E)]$ due to the *CP*-violating term, the neutrino survival probabilities ($\alpha = \beta$) will be, *e.g.*,

$$P_{ee} = c^4_{13}\left[1 - \sin^2(2\theta_{12})\sin^2\left(\frac{\Delta m^2_{21}}{4E}L\right)\right] + s^4_{13} = c^4_{13}P^{2\mathrm{f}}_{ee} + s^4_{13}, \tag{5.25}$$

where $P^{2\mathrm{f}}_{ee}$ is the two-flavor neutrino survival probability with $\Delta m^2 = \Delta m^2_{21}$ and $\theta = \theta_{12}$. The reason that the two-flavor probability appears in this expression is that one of the neutrino mass eigenstates, in this case ν_3, has a mass which is so different from the masses of the other two states that it effectively decouples from the oscillations.

CP- and *T*-violation

As was discussed earlier, in two-flavor neutrino oscillations, we have T-invariance $P_{\alpha\beta} = P_{\beta\alpha}$ as a direct consequence of unitarity (and thus, also CP-invariance $P_{\bar{\alpha}\bar{\beta}} = P_{\alpha\beta}$ if we assume CPT-invariance, *i.e.*, $P_{\bar{\alpha}\bar{\beta}} = P_{\beta\alpha}$), this is no longer true in the three-flavor scenario. The three-flavor unitarity conditions are given by

$$P_{\alpha e} + P_{\alpha\mu} + P_{\alpha\tau} = P_{e\alpha} + P_{\mu\alpha} + P_{\tau\alpha} = 1, \tag{5.26}$$

where $\alpha \in \{e, \mu, \tau\}$. If we define the T-asymmetries

$$\Delta P_{\alpha\beta} = P_{\alpha\beta} - P_{\beta\alpha}, \tag{5.27}$$

then it is apparent that

$$\sum_\beta \Delta P_{\alpha\beta} = \sum_\beta (P_{\alpha\beta} - P_{\beta\alpha}) = 1 - 1 = 0. \tag{5.28}$$

Since $\Delta P_{\alpha\beta} = -\Delta P_{\beta\alpha}$, there are only three T-asymmetries which could be independent. The number of conditions in Eq. (5.28) would seem to be three, one for

each choice of α. However, because of the anti-symmetry of $\Delta P_{\alpha\beta}$, Eq. (5.28) only constitutes two independent conditions on $\Delta P_{\alpha\beta}$. Since we have three different T-asymmetries on which we impose two conditions, there will only be one independent asymmetry after the conditions have been taken into account [102], *i.e.*,

$$\Delta P_{e\mu} = -\Delta P_{e\tau} = \Delta P_{\mu\tau} = -\Delta P_{\mu e} = \Delta P_{\tau e} = -\Delta P_{\tau\mu}. \tag{5.29}$$

With the standard parametrization of the lepton mixing matrix, we have

$$\Delta P_{e\mu} = 4J \left[\sin\left(\frac{\Delta m^2_{21}}{2E} L\right) + \sin\left(\frac{\Delta m^2_{32}}{2E} L\right) + \sin\left(\frac{\Delta m^2_{13}}{2E} L\right) \right], \tag{5.30}$$

where

$$J = c^2_{13} s_{13} s_{12} c_{12} s_{23} c_{23} \sin(\delta)$$

is the Jarlskog invariant [103]. In the general case of oscillations among n neutrino flavors, it is easy to show that the same argument as above leads to $(n-2)(n-1)/2$ independent CP-asymmetries, *i.e.*, the same number as the number of CP-violating Dirac phases in the lepton mixing matrix.

The violation of the CP- and T-symmetries in neutrino oscillations in vacuum was first discussed by Cabibbo in Ref. [104] and has also been treated in Refs. [80, 81,102], where also the fact that the Majorana phases do not influence the neutrino oscillation probabilities was discussed.

5.4 Neutrino oscillations in matter

As first discussed by Wolfenstein [37] and elaborated on by Mikheyev and Smirnov [38, 39], the presence of matter can greatly affect the propagation of neutrinos. Although the low-energy[4] cross-section for neutrino scattering is proportional to the Fermi constant G_F squared, the neutrino dispersion relation can obtain contributions of first order in the Fermi constant due to coherent forward scattering on the matter constituents. Even though the matter contributions to the neutrino dispersion relation will still be small, their effect should be compared to that of the neutrino masses and, in particular, the mass squared differences as this is what determines the neutrino oscillation frequency. We will start by deriving the effects of coherent forward scattering with the original argumentation and then put this into the context of thermal field theory following the work of Nötzoldt and Raffelt [105].

5.4.1 Origin of the matter potential

We wish to describe how the presence of coherent forward scattering on matter constituents affects the neutrino energy levels. Since neutrinos are only weakly

[4] With low-energy being defined as the center-of-momentum energy, which should be compared to the $W^\pm$ mass.

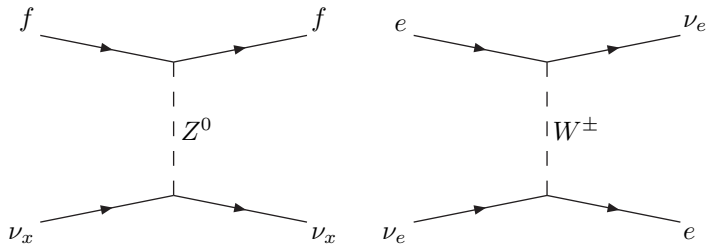

Figure 5.3. Tree-level Feynman diagrams for coherent forward scattering of neutrinos on fermions. While the NC scattering (left) is available for all neutrino flavors, the CC scattering (right) is only possible for electron neutrino scattering on electrons.

interacting, the interaction with matter can occur through either charged-current (CC, $W^\pm$ exchange) or neutral-current (NC, Z^0 exchange) interactions, where the tree-level Feynman diagrams for these processes are shown in Fig. 5.3. The CC process can be described through the effective four-fermion interaction term

$$\mathcal{L}_{\mathrm{CC}} = -\frac{G_F}{\sqrt{2}}[\overline{\nu_e}\gamma^\mu(1-\gamma^5)e][\overline{e}\gamma_\mu(1-\gamma^5)\nu_e], \tag{5.31a}$$

which can be rewritten as

$$\mathcal{L}_{\mathrm{CC}} = -\frac{G_F}{\sqrt{2}}[\overline{\nu_e}\gamma^\mu(1-\gamma^5)\nu_e][\overline{e}\gamma_\mu(1-\gamma^5)e] \tag{5.31b}$$

by a Fierz transformation. By introducing the density matrix

$$\rho_e = \frac{1}{2}\sum_s \int d^3p \frac{|e(\boldsymbol{p},s)\rangle\langle e(\boldsymbol{p},s)|}{2p^0} N_e f(p,T) \tag{5.32}$$

for the electron distribution, where N_e is the electron number density and $f(p,T)$ is the statistical momentum distribution of the electrons at temperature T normalized as

$$\int d^3p f(p,T) = 1, \tag{5.33}$$

the electron degrees of freedom can be integrated out as

$$\begin{aligned}
\mathcal{L}^{\nu}_{\rm CC} &= \mathrm{tr}(\mathcal{L}_{\rm CC}\rho_e) \\
&= -\frac{G_F}{\sqrt{2}}[\overline{\nu_e}\gamma^\mu(1-\gamma^5)\nu_e]\frac{N_e}{2} \\
&\quad \times \sum_s \int \frac{d^3p}{2p^0} \left\langle e(\boldsymbol{p},s)\left|\overline{e}\gamma_\mu(1-\gamma^5)e\right|e(\boldsymbol{p},s)\right\rangle f(p,T) \\
&= -\frac{G_F}{\sqrt{2}}[\overline{\nu_e}\gamma^\mu(1-\gamma^5)\nu_e]\frac{N_e}{2}\int d^3p\,\mathrm{tr}\left[\frac{(\not{p}+m)}{2p^0}\gamma_\mu(1-\gamma^5)\right] \\
&= -\frac{G_F}{\sqrt{2}}[\overline{\nu_e}\gamma^\mu(1-\gamma^5)\nu_e]N_e\int d^3p\frac{p_\mu}{p^0}f(p,T). \qquad (5.34)
\end{aligned}$$

Assuming that we are in the rest-frame of the medium, $f(p,T)$ is an even function and the integral of $p^\mu f(p,T)/p^0$ vanishes unless $\mu = 0$, it follows that

$$\mathcal{L}^{\nu}_{\rm CC} = -\frac{G_F}{\sqrt{2}}[\overline{\nu_e}\gamma^0(1-\gamma^5)\nu_e]N_e\int d^3p f(p,T) = -\frac{G_F N_e}{\sqrt{2}}[\overline{\nu_e}\gamma^0(1-\gamma^5)\nu_e]. \quad (5.35)$$

This interaction term gives a contribution to the electron neutrino self-energy of

$$\Sigma_{\rm CC} = \sqrt{2}G_F N_e \gamma^0 P_L, \qquad (5.36)$$

where $P_L = (1-\gamma^5)/2$ is the projection operator on the left-handed states. Thus, the dispersion relation for the left-handed electron neutrinos is

$$(E - \sqrt{2}G_F N_e)^2 = m^2 + \boldsymbol{p}^2 \quad \Longleftrightarrow \quad E \simeq p + \frac{m^2}{2p} + \sqrt{2}G_F N_e, \qquad (5.37)$$

where m is the electron neutrino mass and we have assumed that the neutrinos are ultra-relativistic ($|\boldsymbol{p}| \gg m$). With several neutrino flavors, we also have to take lepton mixing into account and the corresponding dispersion relation in flavor basis is

$$H = p + \frac{1}{2p}UM^2U^\dagger + H_{\rm CC}, \qquad (5.38)$$

where $M = \mathrm{diag}(m_1, m_2, m_3)$, U is the lepton mixing matrix, H is the Hamiltonian that has to be diagonalized in order to find the propagation eigenstates, and

$$H_{\rm CC} = \sqrt{2}G_F N_e\,\mathrm{diag}(1,0,0,\ldots). \qquad (5.39)$$

We note that when $N_e = 0$, H reduces to the vacuum Hamiltonian of Eq. (5.11) except for a term proportional to unity, which only contributes with an overall phase factor. Since p^0 is negative for anti-neutrinos and the energy E is defined as $E = |p^0|$, the matter potential for anti-neutrinos will differ by a sign from the matter potential for neutrinos, *i.e.*, we have to make the substitution[5] $\sqrt{2}G_F N_e \to -\sqrt{2}G_F N_e$ when treating anti-neutrinos.

[5] In addition to the substitution $\delta \to -\delta$ that was present already in the vacuum case.

The NC interactions can occur between any neutrino flavor and any of the matter constituents and the computations closely follow those of the CC interactions. For an electrically neutral medium, the NC interaction potentials of neutrinos with electrons and protons are of the same magnitude but opposite sign and therefore cancel. Thus, in ordinary matter consisting of protons, electrons, and neutrons, the only remaining NC contribution will come from the interactions with neutrons and be of the form

$$H_{\rm NC} = -\frac{G_F N_n}{\sqrt{2}} \,\mathrm{diag}(\underbrace{1,\ldots,1}_{n \text{ entries}},\underbrace{0,\ldots,0}_{k \text{ entries}}), \tag{5.40}$$

where N_n is the neutron number density, n is the number of active neutrino flavors, and k is the number of sterile neutrino flavors[6]. If there are no sterile neutrinos, then the tree-level NC interactions will not affect the neutrino oscillation probabilities, since the corresponding addition to the effective Hamiltonian is proportional to unity and only amounts to an overall phase in the neutrino oscillation amplitudes.

Thermal field theory approach

A more stringent way of deriving the medium contribution to the neutrino self-energy is to treat it using thermal field theory methods [105]. We are then interested in finding the finite temperature and density (FTD) contributions to the neutrino self-energy from the Feynman diagrams displayed in Fig. 5.4, where the FTD contributions will come from the fermion propagators (the number density of $W^\pm$ and Z^0 in ordinary matter is negligible). With the FTD part of the fermion propagators given by

$$S_{\rm FTD} = -(\not{p} + m)2\pi\delta(p^2 - m^2)[\theta(p^0)n_+(p) + \theta(-p^0)n_-(p)], \tag{5.41}$$

where

$$n_\pm(p) = [e^{(|p\cdot u| \pm \mu)/T} + 1]^{-1} \tag{5.42}$$

are the occupation numbers for particles and anti-particles, respectively, θ is the Heaviside function, μ is the chemical potential, and u is the four-velocity of the medium. Computing the FTD parts of the self-energy diagrams, we obtain the same result as above for Σ.

5.4.2 Formalism of neutrino oscillations in matter

As we have just observed, the presence of matter will alter the effective neutrino oscillation Hamiltonian in flavor basis to

$$H_f = H_0 + V\,\mathrm{diag}(1,0,0,\ldots), \tag{5.43}$$

where $V = \sqrt{2}G_F N_e$ and H_0 is the vacuum Hamiltonian from Eq. (5.11). The eigenstates of the effective Hamiltonian are clearly not the same as the eigenstates

[6] A sterile neutrino is a neutrino which does not participate in the weak interaction. In the standard neutrino oscillation framework, we have three active and zero sterile flavors.

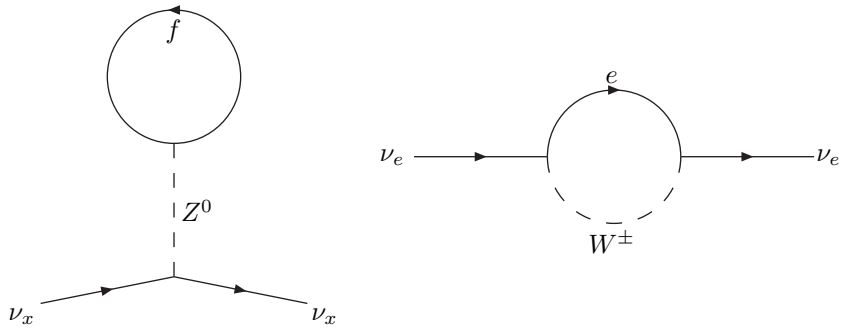

Figure 5.4. The weak interaction contributions to the neutrino self-energy, where the FTD contributions will arise from the fermion propagators. Note that these are exactly the same diagrams as those of Fig. 5.3 with the exception that the fermion lines have been closed.

of H_0. However, we can introduce the basis of matter eigenstates $\tilde{\nu}_i$ as the basis which diagonalizes the effective Hamiltonian. This new basis will be related to the flavor basis as

$$\nu_f = \tilde{U}\tilde{\nu} \quad \Longleftrightarrow \quad \tilde{\nu} = \tilde{U}^\dagger \nu_f, \tag{5.44}$$

where the unitary matrix $\tilde{U}$ is the effective lepton mixing matrix in matter.

For neutrinos propagating in matter of constant electron number density, the effective Hamiltonian is time-independent and the neutrino oscillation probabilities can be computed in the same manner as in the case of neutrino oscillations in vacuum with the substitution $U \to \tilde{U}$ and $E_i \to \tilde{E}_i$, where $\tilde{E}_i$ are the energy eigenvalues of the effective Hamiltonian. However, when neutrinos propagate through matter with varying electron number density, the effective Hamiltonian, and thus also the matter eigenstates, will become time-dependent. The Schrödinger equation in flavor basis can be transformed to the matter eigenstate basis according to

$$\begin{aligned} i\frac{d\nu_f}{dt} = H_f \nu_f \quad &\Longleftrightarrow \quad i\frac{d\tilde{U}\tilde{\nu}}{dt} = \tilde{U}\tilde{H}\tilde{U}^\dagger\tilde{U}\tilde{\nu} \\ &\Longleftrightarrow \quad i\tilde{U}\frac{d\tilde{\nu}}{dt} + i\frac{d\tilde{U}}{dt}\tilde{\nu} = \tilde{U}\tilde{H}\tilde{\nu} \\ &\Longleftrightarrow \quad i\frac{d\tilde{\nu}}{dt} = \left(\tilde{H} - i\tilde{U}^\dagger\frac{d\tilde{U}}{dt}\right)\tilde{\nu}, \end{aligned} \tag{5.45}$$

where $\tilde{H} = \tilde{U}^\dagger H_f \tilde{U}$ is the diagonalized effective Hamiltonian. Even though $\tilde{H}$ is diagonal, there will be transitions from one matter eigenstate to another due to the change in the effective mixing matrix $\tilde{U}$ arising from the varying matter potential.

5.4.3 Two-flavor oscillations in matter

Just as in the case of neutrino oscillations in vacuum, neutrino oscillations in matter are most easily described in the case of two neutrino flavors. As in the vacuum case, many three-flavor problems can be effectively reduced to treating simpler two-flavor problems, and thus, the two-flavor solution is not just a toy model, but can actually be used in the analysis of experiments where the two-flavor approximation is justified. As in the two-flavor treatment of neutrino oscillations in vacuum, the effective lepton mixing matrix will be real and can be parametrized as

$$\tilde{U} = \begin{pmatrix} \tilde{c} & \tilde{s} \\ -\tilde{s} & \tilde{c} \end{pmatrix}, \tag{5.46}$$

where $\tilde{c} = \cos(\tilde{\theta})$, $\tilde{s} = \sin(\tilde{\theta})$, and $\tilde{\theta}$ is the effective mixing angle in matter. The effective Hamiltonian in flavor basis has the form

$$H_f = \frac{\Delta m^2}{4E} \begin{pmatrix} -\cos(2\theta) & \sin(2\theta) \\ \sin(2\theta) & \cos(2\theta) \end{pmatrix} + \frac{V}{2} \begin{pmatrix} 1 & 0 \\ 0 & -1 \end{pmatrix}, \tag{5.47a}$$

where we have subtracted a matrix proportional to unity in order to make H_f traceless. By the relation $H_f = \tilde{U}\tilde{H}\tilde{U}^\dagger$, it must also hold that

$$H_f = \frac{\Delta \tilde{m}^2}{4E} \begin{pmatrix} -\cos(2\tilde{\theta}) & \sin(2\tilde{\theta}) \\ \sin(2\tilde{\theta}) & \cos(2\tilde{\theta}) \end{pmatrix}, \tag{5.47b}$$

where $\Delta\tilde{m}^2 = 2E\Delta E$ and ΔE is the energy difference between the energy eigenvalues in matter. Equating the two expressions for H_f, we obtain

$$\Delta\tilde{m}^2 = \Delta m^2 \sqrt{[\cos(2\theta) - Q]^2 + \sin^2(2\theta)} \tag{5.48a}$$

and

$$\tan(2\tilde{\theta}) = \frac{\sin(2\theta)}{\cos(2\theta) - Q}, \tag{5.48b}$$

where $Q = 2EV/\Delta m^2$. The latter of these relations can be rewritten as

$$\sin^2(2\tilde{\theta}) = \frac{\sin^2(2\theta)}{[\cos(2\theta) - Q]^2 + \sin^2(2\theta)}. \tag{5.48c}$$

Note that Eq. (5.48b) contains more information than Eq. (5.48c), since it is sensitive to whether $\tilde{\theta}$ is larger or smaller than $\pi/4$.

For two-flavor neutrino oscillations in matter of constant density, the neutrino oscillation probabilities are given by

$$P_{ee} = P_{ex} = 1 - \sin^2(2\tilde{\theta}) \sin^2\left(\frac{\Delta\tilde{m}^2}{4E} L\right), \tag{5.49a}$$

$$P_{ex} = P_{xe} = \sin^2(2\tilde{\theta}) \sin^2\left(\frac{\Delta\tilde{m}^2}{4E} L\right), \tag{5.49b}$$

and the derivation is completely analogous to the derivation of the two-flavor neutrino oscillation probabilities in vacuum. From Eq. (5.48c), it is apparent that the neutrino oscillation amplitude $\sin^2(2\tilde{\theta})$ is equal to one if

$$\frac{2EV}{\Delta m^2} = \cos(2\theta). \tag{5.50}$$

This condition is known as the Mikheyev–Smirnov–Wolfenstein (MSW) resonance condition [37–39] and can be fulfilled regardless of the vacuum mixing angle θ. However, the width of the resonance is proportional to $\sin(2\theta)$ [38], and thus, a small mixing angle implies a narrow resonance. In addition, the effective mass squared difference at the resonance is given by

$$\Delta\tilde{m}^2_{\text{res}} = \Delta m^2 \sin(2\theta), \tag{5.51}$$

which implies that the oscillation length at the resonance becomes infinite as $\theta \to 0$. We also note that if θ is chosen such that $0 \leq \theta \leq \pi/4$ (which can always be achieved by permuting the two mass eigenstates), then the MSW resonance condition will be fulfilled either for neutrinos (if $\Delta m^2 > 0$) or for anti-neutrinos (if $\Delta m^2 < 0$), but not for both, since V changes sign for anti-neutrinos.

In matter of varying electron number density, the two-flavor evolution can be expressed as

$$i\frac{d\tilde{\nu}}{dt} = \left[\tilde{H} + \begin{pmatrix} 0 & -i\dot{\tilde{\theta}} \\ i\dot{\tilde{\theta}} & 0 \end{pmatrix}\right] \tilde{\nu}, \tag{5.52}$$

where $\dot{\tilde{\theta}} = d\tilde{\theta}/dt$. In general, there is no simple analytic solution to this problem and one usually relies on approximate solutions. One of the most important approximate solutions is the solution for neutrino oscillations in matter with an electron number density which changes slowly with time, *i.e.*,

$$\gamma \equiv \left|\frac{\Delta\tilde{m}^2}{4E\dot{\tilde{\theta}}}\right| \gg 1, \tag{5.53}$$

where γ is known as the adiabaticity parameter. In this case, we can disregard transitions between the matter eigenstates and the components of $\tilde{\nu}$ just obtain

phase factors from the diagonal entries of $\tilde{H}$, this is known as the adiabatic approximation[7]. As the overall phase does not matter for the neutrino oscillation probabilities, only the phase difference

$$\Phi(t) = \int_0^t \frac{\Delta\tilde{m}^2}{2E} dt \tag{5.54}$$

will be of importance. If the effective mixing angle at time $t = 0$ is $\tilde{\theta}(0) = \theta_i$ and the mixing angle at time $t = T$ is $\tilde{\theta}(T) = \theta_f$, then we have

$$\tilde{\nu}_1(t) = \tilde{c}(t)\nu_e - \tilde{s}(t)\nu_x, \tag{5.55a}$$
$$\tilde{\nu}_2(t) = \tilde{s}(t)\nu_e + \tilde{c}(t)\nu_x, \tag{5.55b}$$

and the neutrino transition probability P_{ex} is given by

$$\begin{aligned} P_{ex}(T) &= \left| \nu_x \tilde{U}^\dagger(T) \begin{pmatrix} 1 & 0 \\ 0 & e^{-i\Phi(T)} \end{pmatrix} \tilde{U}(0)\nu_e \right|^2 \\ &= \left| \begin{pmatrix} -s_f & c_f \end{pmatrix} \begin{pmatrix} 1 & 0 \\ 0 & e^{-i\Phi(T)} \end{pmatrix} \begin{pmatrix} c_i \\ s_i \end{pmatrix} \right|^2 \\ &= \frac{1}{2}\left\{1 - \cos(2\theta_f)\cos(2\theta_i) - \sin(2\theta_f)\sin(2\theta_f)\cos[\Phi(T)]\right\}. \end{aligned} \tag{5.56a}$$

In addition, if the phase Φ can be considered to be rapidly oscillating, then $\cos[\Phi(T)]$ will average out to zero and we are left with

$$P_{ex} = \frac{1}{2}[1 - \cos(2\theta_f)\cos(2\theta_i)]. \tag{5.56b}$$

If we also make the assumption that the neutrinos are produced in a very high-density medium and evolve adiabatically to vacuum, then $\theta_i \to \pi/2$ and $\theta_f = \theta$ and the transition probability is

$$P_{ex} = \cos^2(\theta). \tag{5.56c}$$

Thus, for a small vacuum mixing angle θ, we can obtain an almost complete transition from ν_e to ν_x. However, these computations assume that the adiabaticity condition is fulfilled. From differentiating Eq. (5.48c), we obtain

$$2\dot{\tilde{\theta}} = \frac{\sin(2\theta)}{[\cos(2\theta) - Q]^2 + \sin^2(2\theta)}\dot{Q}. \tag{5.57}$$

If $\dot{Q}$ can be considered to be approximately constant, then

$$\gamma = \left| \frac{\Delta m^2}{2E} \frac{\{[\cos(2\theta) - Q]^2 + \sin^2(2\theta)\}^{3/2}}{\dot{Q}\sin(2\theta)} \right| \tag{5.58a}$$

[7] For discussions on non-adiabatic effects, see Refs. [106–108].

will obtain its smallest value

$$\gamma_{\rm res} = \left| \frac{\Delta m^2}{2E} \frac{\sin^2(2\theta)}{\dot{Q}} \right| \tag{5.58b}$$

at the MSW resonance. Thus, if the adiabaticity condition $\gamma \gg 1$ is violated anywhere, it will be violated at the resonance. Especially, if $\theta \to 0$, then $\gamma_{\rm res} \to 0$ and adiabaticity is violated. Thus, for small enough θ, the conditions in deriving Eq. (5.56c) are not satisfied. The adiabatic approximation is of great importance in, *e.g.*, the treatment of the oscillations of solar neutrinos.

Even though there is no general closed form solution, there exists analytic solutions for some specific forms of the matter density profile, the constant density solution being the most simple. Other examples where the solutions are known are the cases of linear [109] and exponential [110,111] matter density profiles. In addition, there have also been efforts to rewrite the neutrino flavor evolution equations as an ordinary complex non-linear differential equation for the neutrino oscillation amplitude, see *e.g.* Ref. [112]. In Paper [2], we have discussed the exact analytic solution of two-flavor neutrino oscillation in an arbitrary matter density profile as given by a series expansion solution to a real non-linear differential equation for the the neutrino oscillation probability.

5.4.4 Three-flavor oscillations in matter

Just as in the case of neutrino oscillations in vacuum, going from a two-flavor treatment to a full three-flavor treatment when treating neutrino oscillations in matter complicates the analysis rather drastically. Still, some of the three-flavor neutrino oscillation probabilities will again be reduced to two-flavor neutrino oscillation probabilities.

Unlike in the case of two-flavor neutrino oscillations in matter, in the three-flavor treatment, there is no simple analytic form for the effective mixing parameters ($\tilde{\theta}_{ij}$ and $\tilde{\delta}$) and mass squared differences ($\Delta\tilde{m}^2_{ij}$), although there exists approximative expressions [113].

An interesting feature of the three-flavor treatment is the fact that we now have two MSW resonances, which can appear either as two resonances for neutrinos (if $\Delta m^2_{31} > 0$) or as one resonance each for neutrinos and anti-neutrinos (if $\Delta m^2_{31} < 0$).[8] Because of the hierarchy in the mass squared differences (*i.e.*, $\Delta m^2_{21} \ll |\Delta m^2_{31}|$), the two resonances can be treated separately and will often reduce to two-flavor treatments. For example, if $V \sim \Delta m^2_{21}/(2E) \ll |\Delta m^2_{31}/(2E)|$, then the third mass eigenstate will decouple in the same way as described after

[8] Since $\Delta m^2_{21} > 0$ and $\theta_{12} \simeq 33^\circ$, the resonance corresponding to Δm^2_{21} will appear for neutrinos and not anti-neutrinos. In fact, it is the matter effect on the solar neutrinos that has been used to determine the sign of Δm^2_{21}.

Eq. (5.25). The effective Hamiltonian in the remaining two-flavor system will be given by (in the mass eigenstate basis)

$$H_m^{2\mathrm{f}} = \frac{c_{13}^2 V}{2}\begin{pmatrix} \cos(2\theta_{12}) & \sin(2\theta_{12}) \\ \sin(2\theta_{12}) & -\cos(2\theta_{12}) \end{pmatrix} + \frac{\Delta m_{21}^2}{4E}\begin{pmatrix} -1 & 0 \\ 0 & 1 \end{pmatrix}, \tag{5.59}$$

which is nothing else than an ordinary two-flavor Hamiltonian with the two-flavor parameters $V \to c_{13}^2 V$, $\theta \to \theta_{12}$, and $\Delta m^2 \to \Delta m_{21}^2$ [114]. Thus, if the baseline is long enough for the fast oscillations with frequency $\Delta m_{31}^2/(2E)$ to average out, then the $\nu_e \to \nu_e$ oscillation probability will be given by

$$P_{ee} = c_{13}^4 P_{ee}^{2\mathrm{f}} + s_{13}^4, \tag{5.60}$$

where $P_{ee}^{2\mathrm{f}}$ is the two-flavor survival probability calculated from the effective two-flavor framework described above. In particular, this situation is applicable to the oscillation of electron neutrinos produced in the thermonuclear processes in the Sun. In Paper [1], we have computed the three-flavor effects on the day-night asymmetry in the flux of electron neutrinos by exploiting this fact.

On the other hand, if $\Delta m_{21}^2 L/(2E) \ll 1$, then the effects of Δm_{21}^2 are negligible and we can implement this by setting $\Delta m_{21}^2 = 0$. In this case, the mixing angle θ_{12} becomes irrelevant and we have

$$U = U_{23}U_{13} = \begin{pmatrix} 1 & 0 & 0 \\ 0 & c_{23} & s_{23} \\ 0 & -s_{23} & c_{23} \end{pmatrix}\begin{pmatrix} c_{13} & 0 & s_{13}e^{-i\delta} \\ 0 & 1 & 0 \\ -s_{13}e^{i\delta} & 0 & c_{13} \end{pmatrix}. \tag{5.61}$$

By defining a new basis ν' for the neutrino states according to

$$\nu' = U_{23}^\dagger \nu_f, \tag{5.62a}$$

i.e.,

$$\nu_1' = \nu_e, \quad \nu_2' = c_{23}\nu_\mu - s_{23}\nu_\tau, \quad \nu_3' = s_{23}\nu_\mu + c_{23}\nu_\tau, \tag{5.62b}$$

the Hamiltonian takes the form

$$H' = U_{23}^\dagger H_f U_{23} = \begin{pmatrix} V & 0 & 0 \\ 0 & 0 & 0 \\ 0 & 0 & 0 \end{pmatrix} + \frac{\Delta m_{31}^2}{2E}\begin{pmatrix} s_{13}^2 & 0 & s_{13}c_{13} \\ 0 & 0 & 0 \\ s_{13}c_{13} & 0 & c_{13}^2 \end{pmatrix}, \tag{5.63}$$

which shows that this system is now a two-flavor system with ν_2' decoupled from the other two states and with the two-flavor parameters $V \to V$, $\theta \to \theta_{13}$, and $\Delta m^2 \to \Delta m_{31}^2$. In particular, since $\nu_1' = \nu_e$, we have

$$P_{ee} = P_{1'1'}, \tag{5.64}$$

where $P_{1'1'}$ is a two-flavor neutrino survival probability computed with this parameter mapping.

Another interesting two-flavor limit occurs when the matter potential is significantly larger than the vacuum energy splittings, *i.e.*, when $V \gg \Delta m^2_{ij}/(2E)$. In this limit, the electron neutrino decouples and we are left with a vacuum two-flavor oscillation scenario for the oscillations between ν_μ and ν_τ. This scenario was studied in detail in Paper [3].

A more detailed review of the three-flavor effects in neutrino oscillations can be found in Ref. [115]. When the three-flavor effects are relatively small, but not negligible, it is common to make a series expansion in the small parameters s_{13} and $\alpha \equiv \Delta m^2_{21}/\Delta m^2_{31}$, which has been done in Refs. [113, 116–119]. Approximate analytic solutions in the three-flavor regime were presented in Refs. [120, 121] in the case when the two resonances are well separated and can be assumed to be independent. The full three-flavor solution for matter consisting of constant density layers was presented in Ref. [122], where the Cayley–Hamilton formalism was used in order to expand the evolution matrix for each layer. This formalism also provides an easy way of implementing three-flavor neutrino oscillations numerically by approximating the matter density profile with a profile consisting of sufficiently thin constant density layers. The effects of *CP*- and T-violation in matter is also somewhat more involved than the corresponding effects in vacuum, since the matter itself violates *CP*. The effects of *CP*- and T-violation in matter has been studied in Refs. [123–128].

5.5 Non-standard effects

What has been described so far in this chapter is the standard framework for treating neutrino oscillations both in vacuum and in matter. This standard framework has so far been extremely successful in describing all of the neutrino oscillation experiments that have been performed, with the possible exclusion of the LSND result [129–131] (see Ch. 6). In recent years, even the oscillatory behavior of the neutrino flavor transitions have been observed in the Super-Kamiokande [58] and KamLAND [61] experiments, which favors neutrino oscillations as the leading mechanism behind these flavor transitions. However, that other alternatives are not the main cause of the flavor transitions does not imply that they do not contribute. With new generations of neutrino oscillation experiments being planned for measuring the neutrino oscillation parameters with higher accuracy, we may need to invoke secondary contributions from effects not incorporated into the standard neutrino oscillation framework in order to obtain a coherent description of the neutrino flavor transitions. Examples of effects that could give secondary contributions are neutrino decay [132–142], neutrino wave-packet decoherence [143–147], and non-standard interactions [37, 148–175]. The non-standard effects can be subdivided into incoherent and coherent effects, depending on whether they must be implemented on the probability level (incoherent effect) or if they can be implemented in the evolution stage by effectively changing the neutrino evolution Hamiltonian. It

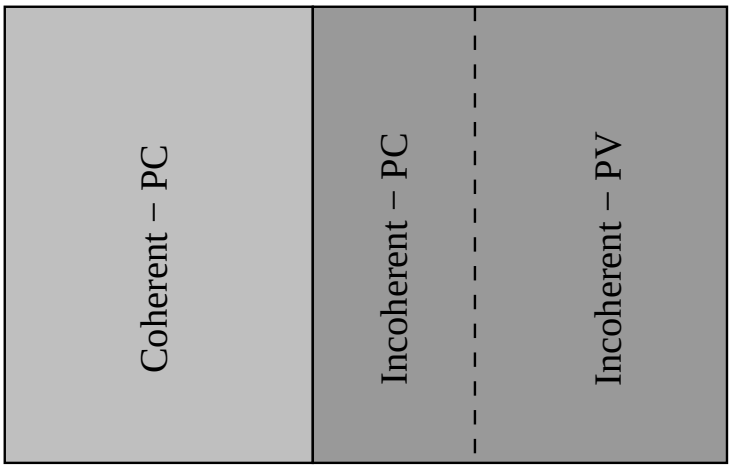

Figure 5.5. An overview of the sets of non-standard effects that could occur in neutrino oscillations. While a coherent effect is necessarily probability conserving (PC), a probability conserving effect is not necessarily coherent, but can also be incoherent. Similarly, a probability violating (PV) effect is necessarily incoherent, but an incoherent effect is not necessarily probability violating.

is also possible to divide the non-standard effects into probability conserving and probability violating effects, depending on whether the condition

$$\sum_{\alpha} P_{\alpha\beta} = \sum_{\beta} P_{\alpha\beta} = 1 \tag{5.65}$$

is fulfilled or not. While coherent effects are probability conserving by construction, incoherent effects can be either probability conserving or probability violating, as shown in Fig. 5.5.

5.5.1 Incoherent effects

By definition, an incoherent (or damping) effect is an effect which introduces a damped interference between two or more of the neutrino mass eigenstates. The neutrino oscillation probabilities are then given by

$$P_{\alpha\beta} = \sum_{i,j} D_{ij} J^{ij}_{\alpha\beta} e^{-i\Delta_{ij}}, \tag{5.66}$$

where $D_{ij} \leq 1$ is the damping factor between mass eigenstate i and mass eigenstate j. Generally, $D_{ij} = D_{ji}$ and can be written on the form

$$D_{ij} = \exp\left(-\alpha_{ij} \frac{|\Delta m^2_{ij}|^{\xi} L^{\beta}}{E^{\gamma}}\right), \tag{5.67}$$

where α_{ij}, ξ, β, and γ are characteristic for the specific type of non-standard effect.

The probability conserving incoherent effects fulfill the condition that $D_{ij} = 1$ if $i = j$, which has the effect that only the oscillating terms in the neutrino oscillation probabilities are damped. Thus, in the limit of $D_{ij} \to 0$ for $i \neq j$, the probability conserving incoherent effects are equivalent to averaging out the oscillatory behavior as the coherence between the mass eigenstates is lost. Examples of probability conserving incoherent effects are wave-packet decoherence (wave-packets of different mass eigenstates evolving at different velocities) [143–147] and neutrino decoherence from interactions with the environment [176–186].

The damping factors of probability violating incoherent effects can usually be factorized to the form

$$D_{ij} = A_i A_j \quad \Longleftrightarrow \quad \alpha_{ij} = \alpha_i + \alpha_j. \tag{5.68}$$

For effects of this type, we generally have $D_{ij} < 1$ even if $i = j$, which means that the sum of the neutrino oscillation probabilities will be less than one. A typical examples of such effect is neutrino decay (where neutrinos are lost due to one or more of the mass eigenstates decaying) [132–142].

In Paper [4], we give an overview of the incoherent effects and their treatment in a three-flavor framework along with an example of how they can affect the results of neutrino oscillation experiments and how one can search for and distinguish them from standard neutrino oscillations as well as from each other.

5.5.2 Coherent effects

While the incoherent non-standard effects were implemented on the probability level, the coherent non-standard effects can be implemented by altering the neutrino evolution Hamiltonian according to

$$H_f \longrightarrow H_f + H_{f,\mathrm{NS}}, \tag{5.69}$$

where $H_{f,\mathrm{NS}}$ is the contribution from the specific non-standard scenario. This replacement is very similar to the replacement of the vacuum Hamiltonian with the effective Hamiltonian in matter when treating neutrino oscillations in a matter background.[9] The structure and energy dependence of $H_{f,\mathrm{NS}}$ is dependent on the specific type of non-standard effect considered. A coherent non-standard effect can be categorized by a characteristic energy dependence or if it takes a simple form in a specific basis for the neutrino states, *e.g.*, if it is diagonal in the neutrino mass eigenstate basis, in which case it does not affect the lepton mixing matrix, but only the effective mass squared differences. Among the examples of coherent non-standard effects are non-standard interactions (NSI) [37, 148–175] of neutrinos with matter and mass-varying neutrinos (MVNs) [187–203].

[9] Note that the standard matter effects are now included in H_f.

In the case of NSI, it is assumed that there are effective four-fermion interactions of the form

$$\mathcal{L}_{\text{NSI}} = -\sqrt{2}G_F \sum_{\alpha,\beta,f,P} \varepsilon^{fP}_{\alpha\beta}[\overline{f}\gamma^\mu Pf][\overline{\nu_\alpha}\gamma_\mu(1-\gamma^5)\nu_\beta], \tag{5.70}$$

where f are the matter constituents and $P = (1 \pm \gamma^5)/2$ are the right- and left-handed projectors. Such terms are expected to arise in the Lagrangian density when going beyond the SM and in order to have a real Lagrangian density, we must have $\varepsilon^{fP}_{\alpha\beta} = \varepsilon^{fP*}_{\beta\alpha}$. In a manner completely analogous to the derivation of the MSW potential V, these effective four-fermion interactions will give a contribution to the effective neutrino evolution Hamiltonian which is of the form

$$H_{f,\text{NSI}} = V \begin{pmatrix} \varepsilon_{ee} & \varepsilon_{e\mu} & \varepsilon_{e\tau} \\ \varepsilon^*_{e\mu} & \varepsilon_{\mu\mu} & \varepsilon_{\mu\tau} \\ \varepsilon^*_{e\tau} & \varepsilon^*_{\mu\tau} & \varepsilon_{\tau\tau} \end{pmatrix}, \tag{5.71}$$

where we have defined

$$\varepsilon_{\alpha\beta} = \sum_{f,P} \varepsilon^{fP}_{\alpha\beta} \frac{N_f}{N_e}$$

and N_f is the number density of fermions of type f.

In Paper [5], we study general coherent non-standard effects, how they affect the neutrino oscillation probabilities and how they can be distinguished from standard oscillations, each other, and incoherent effects in a similar fashion as the study of incoherent effects in Paper [4]. Paper [6] is focused on the implications of including NSI into the analysis of the MINOS experiment.

Chapter 6

Neutrino oscillation experiments

A theory is something nobody believes, except the person who made it. An experiment is something everybody believes, except the person who made it.
– Albert Einstein

No matter how beautiful a physical theory may seem, its predictions must be verified by experiments before it can be accepted as a good description of Nature. Thus, we will now turn toward the experimental verifications of neutrino oscillations in order to examine why they have been accepted as an occurring phenomenon. We will start by discussing some general features of the two-flavor neutrino oscillation probabilities in order to better understand the confidence regions in the parameter space of neutrino oscillations that result from experiments. We will then briefly summarize the different types of experiments that have been performed and see how they contribute to our current view of neutrino oscillations.

6.1 Analyzing two-flavor neutrino oscillation probabilities

If matter effects are not important and a two-flavor framework is sufficient to describe the neutrino oscillations in a given experiment, then the neutrino transition probability is given by

$$P_{\alpha\beta} = \sin^2(2\theta)\sin^2\left(\frac{\Delta m^2}{4E}L\right). \tag{6.1}$$

Since the survival probability only differs from this by a sign and a constant, it is sufficient to study this term in order to examine the isocontours of the neutrino

oscillation probability in the parameter space, which is spanned by the mass squared difference Δm^2 and the lepton mixing angle θ.

Let us suppose that we have an experiment with a fixed baseline $L = L_0$ which measures the oscillation probability for neutrinos with energy $E = E_0$ and is sensitive to values of $P_{\alpha\beta} > p_0$. Thus, in order to determine the sensitivity region of this experiment, we wish to find the isocontour $P_{\alpha\beta} = p_0$ in the neutrino oscillation parameter space. If $\Delta m^2 L_0/(4E_0) \ll 1$, then the oscillatory term in the neutrino oscillation probability can be expanded in order to obtain the relation

$$p_0 = \sin^2(2\theta)\left(\frac{\Delta m^2 L_0}{4E_0}\right)^2 \quad \Longleftrightarrow \quad \sin^2(2\theta) = \alpha\left(\Delta m^2\right)^{-2}, \tag{6.2}$$

where $\alpha = 16 p_0 E_0^2/L_0^2$. Since the largest possible value of $\sin^2(2\theta)$ is one, the smallest value of the mass squared difference which the experiment will be sensitive to is given by $\Delta m^2 = \sqrt{\alpha}$ and the sensitivity limit is then a straight line with slope $-1/2$ when plotted in logarithmic scale in the $\sin^2(2\theta)$–Δm^2 parameter space as long as $\Delta m^2 L_0/(4E_0) \ll 1$ is fulfilled. On the other hand, if $\Delta m^2 L_0/(4E_0) \gg 1$, then the oscillatory behavior in the neutrino oscillation probability will average out due to the finite energy resolution and size of the detector. Thus, in this limit, the sensitivity limit is given by

$$p_0 = \frac{1}{2}\sin^2(2\theta) \tag{6.3}$$

which is independent of Δm^2 and we expect the sensitivity limit to be given by a vertical line in the $\sin^2(2\theta)$–Δm^2 parameter space. In the intermediate region, we expect an oscillatory behavior due to the $\sin^2[\Delta m^2 L/(4E)]$ term in the neutrino oscillation probability, see Fig. 6.1. If an experiment is performed with a range of different neutrino energies, then each energy bin will contribute with its own sensitivity contour, and thus, the final confidence region must not have the exact shape shown in this figure, but will rather be a combination of such contours.

Matter effects are definitely not negligible for the solar neutrinos with the highest energy. In addition, because of the finite energy resolution of detectors, the eccentricity of the Earth's orbit, the size of the production regions inside the Sun, and the intrinsic spread of the wave-packets for neutrinos in different mass eigenstates, the oscillating terms in the solar neutrino oscillation probabilities will all be averaged out. Thus, solar neutrinos are commonly analyzed using the adiabatic approximation of Eq. (5.56b) with $\theta_f = \theta$. The initial effective mixing angle θ_i will depend on where in the Sun the neutrinos are produced and the neutrino energy as well as the neutrino oscillation parameters. For $\Delta m^2/(2EV) \gg 1$ in the production region, the entire evolution is essentially equivalent to vacuum oscillations and the averaged electron neutrino survival probability is

$$P_{ee} = 1 - \frac{1}{2}\sin^2(2\theta). \tag{6.4a}$$

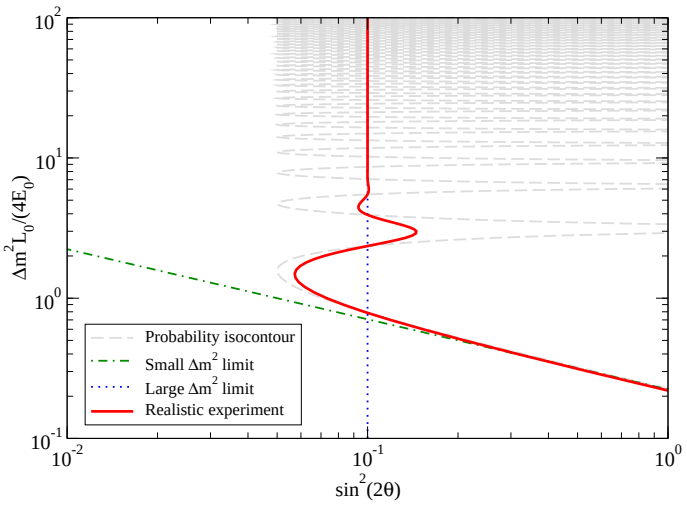

Figure 6.1. The sensitivity contour in the $\sin^2(2\theta)$–Δm^2 parameter space for a realistic neutrino oscillation experiment with $p_0 = 0.05$ is shown by the solid curve. Also shown are the high and low Δm^2 approximations and the isoprobability contour for $P_{\alpha\beta} = p_0$.

However, for $\Delta m^2/(2EV) \ll 1$, the initial effective mixing angle is $\theta_i \simeq \pi/2$ and the electron neutrino survival probability is then instead given by

$$P_{ee} = \cos^2(\theta), \tag{6.4b}$$

assuming that θ is large enough in order for the adiabaticity condition to hold. Thus, the solar neutrino oscillation experiments will be mainly sensitive to the lepton mixing angle θ and the information on Δm^2 will be embedded in how the initial effective mixing angle changes with energy.

6.2 Atmospheric neutrinos

As mentioned in the historical overview, the first evidence of neutrino oscillations were presented by the Super-Kamiokande data for atmospheric neutrinos in 1998 [9]. As the name suggests, atmospheric neutrinos are produced in the Earth's atmosphere when it is hit by cosmic rays [204–207]. A very common product in these collisions are charged pions $\pi^\pm$ which decay as [66]

$$\pi^\pm \longrightarrow \mu^\pm + \overset{(-)}{\nu}_\mu.$$

The resulting $\mu^\pm$ from this decay then subsequently decay according to [66]

$$\mu^\pm \longrightarrow e^\pm + \overset{(-)}{\nu}_\mu + \overset{(-)}{\nu}_e.$$

Figure removed from online version for copyright reasons. See printed version or reference for figure.

Figure 6.2. The result of the Super-Kamiokande experiment from 1998 providing the first evidence for neutrino oscillations. The hatched regions correspond to the expected results without neutrino oscillations and the solid lines to the best-fit expectancy with neutrino oscillations. Apparently, there is a deficit of muon neutrinos for $\cos(\Theta) < 0$, *i.e.*, for neutrinos with longer path-lengths. Reprinted figure with permission from Ref. [9]. ©(1998) by the American Physical Society.

For low energies ($E_\mu \lesssim 5$ GeV), the $\mu^\pm$ will essentially always decay before it hits the ground. Thus, at these energies, the ratio R_{ν_μ/ν_e} between the number of muon neutrinos and the number of electron neutrinos will be two as the above decay chain produces two muon neutrinos and one electron neutrino. At higher energies, the $\mu^\pm$ will hit the Earth's surface and stop before it has had time to decay. As a result, the relative number of electron neutrinos produced at these high energies will decrease, resulting in a higher value of R_{ν_μ/ν_e}.

While atmospheric neutrinos had been studied by several earlier experiments [208–213], Super-Kamiokande was the first one to actually provide evidence of neutrino oscillations [9]. What was done by Super-Kamiokande was to measure the ν_e and ν_μ fluxes at different zenith angles, corresponding to different path lengths from production to detection and the results from their analysis is shown in Fig. 6.2. As there is no significant discrepancy between the expected and measured number of electron neutrino events, the deficit of muon neutrinos in this figure is interpreted as oscillations of muon neutrinos into tau neutrinos.

In 2004, the Super-Kamiokande results were re-analyzed [58] and the neutrino events were categorized according to their L/E values rather than their L values as it is the combination L/E that actually appears in the neutrino oscillation probability. The analysis compared neutrino oscillations to other alternative scenarios to describe the origin of the muon neutrino deficit and found that neutrino oscillations were indeed the favored solution when compared to neutrino decay and neutrino decoherence.[1] The results of this analysis are shown in Fig. 6.3.

Following the Super-Kamiokande results, oscillations of atmospheric neutrinos have also been observed by the Soudan 2 collaboration [214].

6.3 Solar neutrinos

As the Sun produces its energy through thermonuclear reactions, it is in no way a surprise that it is an abundant source of neutrinos. In fact, as the thermonuclear reactions occur in the center of the Sun, it is only the neutrinos from these reactions

[1] This study only considered neutrino decay and neutrino decoherence as the leading mechanism behind the muon neutrino deficit. In Papers [4, 5], we discuss how the effects of such sub-leading effects can influence the neutrino oscillation probabilities.

Figure removed from online version for copyright reasons. See printed version or reference for figure.

Figure 6.3. The results of the Super-Kamiokande L/E analysis [58] which favors neutrino oscillations over neutrino decay and neutrino decoherence as the leading mechanism behind the deficit of muon neutrinos in the atmospheric neutrino flux. The solid curve corresponds to the best-fit prediction of neutrino oscillations, while the other two curves are the best-fit predictions from neutrino decay and neutrino decoherence, respectively. Reprinted figure with permission from Ref. [58]. ©(2004) by the American Physical Society.

Figure removed from online version for copyright reasons. See printed version or reference for figure.

Figure 6.4. The energy spectrum of solar neutrinos coming from different reactions in the center of the Sun. Reprinted with permission from Ref. [217].

that escape the Sun without interacting. Thus, neutrinos, unlike the electromagnetic waves and solar wind, can provide us with information on what is actually going on in the center of the Sun right now (or at least about eight minutes ago, given the travel time). The standard solar model (SSM) [50, 51, 215, 216] has been very successful in describing the composition, energy production, and seismology of our Sun and it also gives a detailed description of what the neutrino flux from the Sun should look like, see Fig. 6.4. The most abundant fusion reaction in the Sun is

$$p + p \longrightarrow {}^2\mathrm{H} + e^+ + \nu_e,$$

which produces the large *pp* flux at $E \lesssim 0.4$ MeV in this figure, but there are also others which play a major role in solar neutrino experiments, since the threshold energy of many experiments is higher.

The first experiment in which the solar neutrino flux was measured was the Homestake experiment [40–42], which used the inverse beta-decay

$$\nu_e + {}^{37}\mathrm{Cl} \longrightarrow {}^{37}\mathrm{Ar} + e^-$$

in a 400 m^3 tank of perchloroethylene, essentially cleaning fluid, where the produced Argon atoms were then counted by radiochemical means. The result of the experiment was that the number of Argon atoms was lower than what was expected from the SSM, this observation became known as the "solar neutrino problem". There were now three possible resolutions to this problem:

1. The SSM could be wrong.
2. The predicted neutrino cross-sections could be wrong.
3. Electron neutrinos were lost somewhere along the propagation from the Sun to the Earth.

Since it was already known that the SSM was in good agreement with other observations of the Sun and there was no reason to doubt the cross-section computations, the main candidate for a resolution was the third option, which would be an indication of neutrino oscillations or some other flavor transition mechanism.

One of the drawbacks of the Homestake experiment was that its threshold energy of about 0.9 MeV was above the energy of the large flux of *pp* neutrinos, and thus, it was sensitive only to neutrino fluxes with larger uncertainties. This drawback was addressed in the Gallium experiments GALLEX [43, 44] and SAGE [45, 46], which both used a method very similar to that of the Homestake experiment. Instead of detecting the inverse beta-decay of Chlorine, these experiments relied on the inverse beta-decay

$$\nu_e + {}^{71}\mathrm{Ga} \longrightarrow {}^{71}\mathrm{Ge} + e^-$$

of Gallium, after which the resulting Germanium can be extracted and counted in the same way that the Argon was counted in the Homestake experiment. The energy threshold of the inverse beta-decay of Gallium is 0.2 MeV, which is low enough to detect a significant fraction of the neutrino flux from the primary *pp* reaction. Still, the results of the Gallium experiments were the same as that of the Homestake experiment, a deficiency in the flux of electron neutrinos from the Sun.

A second drawback of the Homestake experiment, which was shared by the Gallium experiments, was that there was no temporal or directional information for the inverse beta-decays. This drawback is not present in water Cherenkov detectors such as Kamiokande [47–49] and Super-Kamiokande [52–54]. These detectors can detect solar neutrinos by the Cherenkov light in water produced by electrons which have undergone elastic scattering

$$\nu_x + e^- \rightarrow \nu_x + e^-$$

with the neutrinos. Although this process is allowed for all neutrino flavors ν_x, the cross-section for electron neutrinos is about six times higher.[2] Although these detectors have a neutrino energy threshold of about 5 MeV, and thus only measure the high-energy ^{8}B neutrinos, the water Cherenkov technique measures the events in real-time and the direction of the scattered electron gives some information on the direction of the incoming neutrino. In fact, the measurement of the directionality of neutrinos in the Kamiokande was the first proof that the neutrinos were actually originating from the Sun [48]. However, both the Kamiokande and Super-Kamiokande experiments also measured a deficit in the electron neutrino flux, just as the radiochemical experiments had. The measured fluxes of all of the above experiments are compared to the SSM predictions in Fig. 6.5.

The resolution to the solar neutrino problem came with the results of the Sudbury Neutrino Observatory (SNO) [55–57], which uses methods similar to the water

[2] This is due to the fact that the electron neutrino scattering process has an additional diagram involving $W^\pm$ exchange at tree-level.

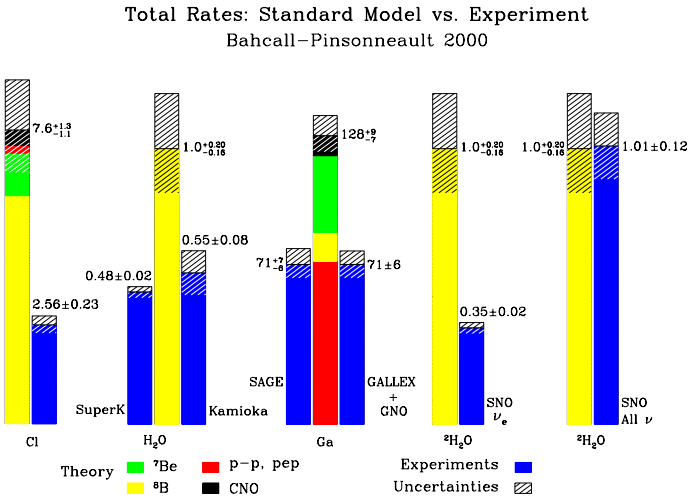

Figure 6.5. The fluxes of solar neutrinos for different neutrino experiments compared to the predictions of the SSM. The figure has been adapted from Ref. [218].

Cherenkov detectors. However, instead of the detector volume being filled with ordinary water, it is filled with heavy water. With the presence of deuterium in the detector, the charged-current (CC)

$$\nu_e + d \longrightarrow p + p + e^-$$

and neutral-current (NC)

$$\nu_x + d \longrightarrow n + p + \nu_x$$

reactions are allowed, making it possible to detect neutrinos also through these reactions. While the CC reaction is only sensitive to electron neutrinos, the cross-section for the NC reaction is independent of the neutrino flavor. Thus, the SNO was able to measure both the flux of electron neutrinos and the total flux of neutrinos independently. As can be observed in Fig. 6.5, the CC measurement shows a deficit of electron neutrinos, while the NC measurement is in full agreement with the SSM prediction. The conclusion from this is that the electron neutrinos produced in the Sun change their flavor during their propagation to the Earth, see Fig. 6.6.

With the data currently available, we know that the solar neutrino oscillations are due to adiabatic transitions with a relatively large mixing angle. Historically, the adiabatic conversion has not been the only neutrino oscillation based solution to the solar neutrino problem. The phenomenology of the solar neutrino oscillation probabilities has been studied in, *e.g.*, Refs. [38, 39, 219–222]. In addition, different

Figure removed from online version for copyright reasons. See printed version or reference for figure.

Figure 6.6. The fluxes of ^{8}B electron neutrinos Φ_e and mu and tau neutrinos $\Phi_{\mu\tau}$ as measured by the SNO experiment in the CC, NC, and elastic scattering (ES) reactions. The SSM prediction for the total neutrino flux is also shown (dashed lines). Reprinted figure with permission from Ref. [56].

oscillation mechanisms, such as the resonant spin-flavor precession [223–229] of neutrinos with a small magnetic moment in a large magnetic field, were discussed as possible solutions.

6.3.1 The day-night effect

Due to the real-time detection of solar neutrinos in Super-Kamiokande and SNO, both of these detectors might be able to tell us if there is any difference in the neutrino flux during day and night. Since the neutrino cross-sections at the energies of solar neutrinos is extremely small, any such effect would be due to the matter effect on the neutrinos traversing the Earth during night and arriving directly to the detector during day. This possibility of having different fluxes during day and night is known as the "day-night effect" and it is quantified by the day-night asymmetry

$$A_{dn} = 2\frac{N - D}{N + D}, \tag{6.5}$$

where D and N are the day- and night-time event rates in the detector and its value generally depends on the neutrino oscillation parameters and on the neutrino energy.

The day-night effect has been thoroughly studied for a long time in the two-flavor framework [230–237]. However, the first full three-flavor treatment was made in Paper [1], in which the Earth was approximated with a sphere of constant matter density. This was generalized to an arbitrary density profile in Refs. [238,239]. With the current knowledge of the neutrino oscillation parameters, we expect the day-night asymmetry to be of the order of a few percent. At the present time, the experimental uncertainties in the value of the day-night asymmetry are still of the same order as the effect itself [240–242]. Thus, the day-night asymmetry can, with the present data, only be used to exclude parameter values which predict a large value of A_{dn}.

6.4 Reactor neutrinos

Through the decays that follow the fission processes in a nuclear reactor, nuclear power plants become an abundant source of artificial low-energy anti-neutrinos

Figure removed from online version for copyright reasons. See printed version or reference for figure.

Figure 6.7. The results of the CHOOZ short-baseline reactor neutrino experiment. Since no oscillations were detected, there is an excluded region with the qualitative shape of Fig. 6.1 [note that the $\sin^2(2\theta)$ scale in this figure is linear rather than logarithmic]. With an external bound on Δm^2_{31}, this exclusion plot can be used to put an upper bound on the lepton mixing angle θ_{13}. Reprinted from Ref. [244], with permission from Elsevier.

with well-known energy spectra. Thus, it becomes natural to try to study the oscillations of these anti-neutrinos. In principle, there are two types of reactor neutrino oscillation experiments. The short-baseline experiments [243–246], where the detectors are placed relatively close[3] to the detector, are trying to find the oscillations associated with the large mass squared difference Δm^2_{31}, where the oscillations governed by Δm^2_{21} have not yet had time to develop. Such experiments are mainly sensitive to the small mixing angle θ_{13} since, for $\Delta m^2_{21} \to 0$,

$$P_{ee} = 1 - \sin^2(2\theta_{13}) \sin^2 \left(\frac{\Delta m^2_{31}}{4E} L \right) \tag{6.6}$$

and the absolute value of Δm^2_{31} is fairly well known from atmospheric neutrino oscillations. In fact, the current upper bound on θ_{13} comes from the CHOOZ experiment [244,245], which was a short-baseline reactor neutrino experiment, along with external bounds on Δm^2_{31}, see Fig. 6.7.

In addition to the short-baseline reactor neutrino experiments, there is also the possibility to detect reactor neutrinos at longer distances, *i.e.*, long-baseline reactor neutrino experiments. In this case, it is not sufficient to study the neutrinos from one single power plant, since the flux will fall off as L^{-2}. Instead, the detector should be placed at about equal distance from a number of nuclear power plants, which will all generate neutrinos that can be detected. The Kamioka site is located at about 180 km away from a large number of nuclear power plants in Japan and Korea and the Kamioka Liquid Scintillator Anti-Neutrino Detector (KamLAND) [60, 61] is detecting the reactor neutrinos coming from these power plants. Because of the longer baseline, the oscillations governed by Δm^2_{31} are effectively averaged out and the oscillations can be described by the neutrino survival probability

$$P_{ee} = c^4_{13} P^{2\text{f}}_{ee} + s^4_{13}, \tag{6.7}$$

where $P^{2\text{f}}_{ee}$ is the two-flavor neutrino survival probability with $\theta = \theta_{12}$ and $\Delta m^2 = \Delta m^2_{21}$.

While the solar neutrino experiments are able to put quite stringent limits on θ_{12}, KamLAND has narrowed down the allowed region for the mass squared difference Δm^2_{21} (to which the solar neutrino experiments are not very sensitive). As a

[3] Of the order of 1 km or less.

Figure removed from online version for copyright reasons. See printed version or reference for figure.

Figure 6.8. The impact of combining the KamLAND results with the results from solar neutrino experiments. The dashed regions correspond to the results from solar neutrino experiments only, while the shaded contours are the results after including the KamLAND results. As can be seen from the figure, the impact is mainly to drastically shrink the allowed region for Δm^2_{21}, while the effect on the allowed θ_{12} is only marginal. The contours correspond to 90 %, 95 %, 99 %, and 3σ confidence levels at two degrees of freedom. Reprinted figure with permission from Ref. [99].

Figure removed from online version for copyright reasons. See printed version or reference for figure.

Figure 6.9. The results of the KamLAND L/E analysis along with the best-fit predictions of neutrino oscillations, neutrino decay, and neutrino decoherence. Reprinted figure with permission from Ref. [61]. ©(2005) by the American Physical Society.

result, the measurements of the solar neutrino experiments and KamLAND complement each other as can be observed in Fig. 6.8. In addition, as the in the case of the Super-Kamiokande experiment, the L/E behavior in KamLAND has been studied and compared to the predictions of neutrino oscillations and other mechanisms of neutrino flavor transition [61]. Just as in the Super-Kamiokande analysis, neutrino oscillations was found to be the favored description, see Fig. 6.9.

6.5 Accelerator neutrinos

Yet another way of searching for neutrino oscillations is to study neutrinos which are artificially produced at particle accelerators [62–64, 129–131, 247–250], usually by having some particle with a significant branching ratio into neutrinos decay in a decay pipe. One of the great advantages of using accelerator neutrinos lies in the fact that the entire experiment can be completely designed and controlled by physicists. In the case of atmospheric and solar neutrinos, the resulting conclusions are unavoidably based on models of the neutrino source, while in the case of reactor neutrinos, the main task of the neutrino source is to produce electricity, not neutrinos. In addition, the range of energies and baselines available for accelerator neutrinos is broad, unlike in the case of solar and reactor neutrinos, which are restricted to relatively low energies.

6.5.1 K2K and MINOS

There are currently two experiments with accelerator neutrinos which have explored the same parameter space as the atmospheric neutrino experiments. These are the

Figure removed from online version for copyright reasons. See printed version or reference for figure.

Figure 6.10. The results from the K2K (left panel) and MINOS (right panel) experiments in the $\sin^2(2\theta_{23})$–Δm^2_{32} plane. Reprinted figures with permission from Ref. [63] and Ref. [64], respectively.

Figure removed from online version for copyright reasons. See printed version or reference for figure.

Figure 6.11. The results of the LSND experiment with the 90 % confidence level exclusion contours of other neutrino oscillation searches superimposed. Note the characteristic shape of both the LSND result and the exclusion contours. Reprinted figure with permission from Ref. [131].

KEK to Kamioka (K2K) [62,63] in Japan and the Main Injector Neutrino Oscillation Search (MINOS) [64] in the United States. Both of these experiments have an initial beam of muon neutrinos and study the disappearance of these muon neutrinos, while the MINOS experiment is also searching for appearance of electron neutrinos. The K2K experiment has a baseline of about 250 km and a typical neutrino energy of approximately 1 GeV and the baseline of the MINOS experiment is about 735 km with a typical neutrino energy of a few GeV. It should be noted that this means that the two experiments are working in the same L/E range (*i.e.*, the range important for oscillations driven by Δm^2_{31} that also happens to be the oscillations which are important for atmospheric neutrinos). It is important to test neutrino oscillations at different length scales as deviations from the L/E behavior could be a signal of non-standard physics.

The results of K2K and MINOS are in perfect agreement with the results of the atmospheric neutrino oscillation experiments, see Fig. 6.10. While the electron neutrino appearance channel in MINOS could also give some information on the lepton mixing angle θ_{13}, taking non-standard interactions into account in the analysis will ruin this possibility, see Paper [6].

6.5.2 The LSND anomaly

While most neutrino oscillation experiments point toward a coherent three-flavor neutrino oscillation framework with the neutrino oscillation parameters given in Tab. 5.1, there is one important exception. This exception is the Liquid Scintillator Neutrino Detector (LSND) experiment [129–131], which was an accelerator neutrino experiment with a baseline length of 30 m and neutrino energies in the range of 20-200 MeV, making it sensitive to mass squared differences of the order of of 1 eV^2. The LSND found evidence for oscillations of anti-muon neutrinos into anti-electron neutrinos, see Fig. 6.11. However, if the standard neutrino oscillation framework is a good description of Nature and if there is no CPT-violation, then the resulting

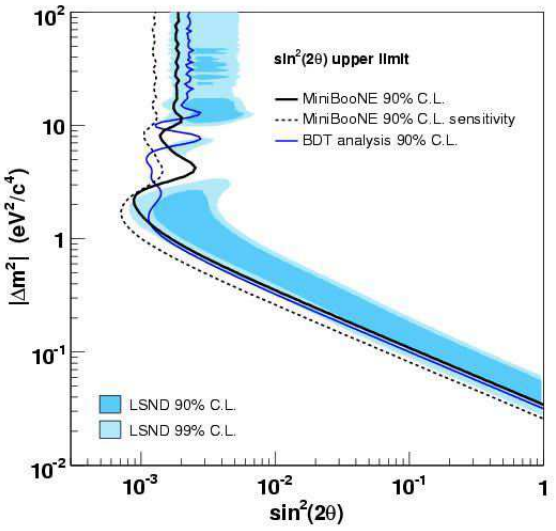

Figure 6.12. The exclusion contours of the MiniBooNE results compared to the LSND results. Courtesy of Fermilab [252].

mass squared difference of $\Delta m^2 \simeq 1$ eV^2 would be incompatible with the ones resulting from other neutrino oscillation experiments, since there can be only two independent mass squared differences in the case of three neutrino flavors.

The LSND result has recently been tested by the MiniBooNE (Mini Booster Neutrino Experiment) [251, 252], which is also an accelerator based experiment searching for the very same type of oscillations as that observed in the LSND and the same L/E, although with a different baseline and energy range. The results of MiniBooNE rejects the LSND result, assuming that it was caused by the effect of neutrino oscillations, see Fig. 6.12. Thus, this also rejects the description of the LSND results in terms of oscillations including sterile neutrinos [253–257], which had been one of the most popular descriptions. However, it is still possible that the LSND result could be correct, although caused by some non-standard effect with a different dependence on L and E (see Papers [4, 5]).

Chapter 7

Leptogenesis

We cannot conceive of matter being formed of nothing, since things require a seed to start from...
– William Shakespeare

7.1 An asymmetric Universe

One question that has had physicists puzzled for a long time is why we can exist, or in other terms, why there is an excess of matter as compared to anti-matter in the Universe. Without this excess of matter, there would be no protons, neutrons, and electrons from which our bodies could be built. If one assumes that the Universe was symmetric at some early time, then it follows that the asymmetry between matter and anti-matter must have been created during the evolution of the Universe.

Over the years, there have been many possible descriptions for the generation of this asymmetry. For example, one solution could be that the excess of matter over anti-matter is local, *i.e.*, matter has accreted in some regions of the Universe and anti-matter in some other regions. However, with such a setup, there would inevitably be collisions between chunks of matter and anti-matter in the border regions which would release radiation that would be detectable. Thus, it seems more promising to make an attempt to describe the creation of the matter–anti-matter asymmetry from physical models.

In 1967, Andrei Sakharov formulated the three necessary conditions that a model must fulfill in order to produce this asymmetry [258]. Simply put, these conditions (known as the Sakharov conditions) tell us that any model that describes the creation of the matter–anti-matter asymmetry must include processes which are matter–anti-matter asymmetric, these interactions must occur out of thermal equilibrium, and it must include violation of baryon number (since what we observe is really an asymmetry of baryons and anti-baryons).

One of the models that may be able to produce the asymmetry is based on the same heavy neutrinos that are present in the seesaw mechanism. In the early Universe, there is an abundance of these heavy neutrinos which are in thermal equilibrium with the rest of the Universe. As the temperature of the expanding Universe decreases, the heavy neutrinos will fall out of thermal equilibrium and decay into other particles or anti-particles. If the heavy neutrinos decay into particles more often than into anti-particles, then this may describe why there is an excess of particles in the present Universe. This model for creation of the matter–anti-matter asymmetry is known as leptogenesis.

7.2 The baryon asymmetry

It is a very well established fact that there is a larger abundance of matter than anti-matter in the Universe. However, a reasonable physical theory to describe the Universe should also be able to predict how large the over-abundance of matter is, this is quantified by defining the baryon asymmetry of the Universe (the BAU) as

$$\eta_B = \frac{n_B - n_{\bar{B}}}{n_\gamma}, \tag{7.1}$$

where n_B is the baryon number density, $n_{\bar{B}}$ is the anti-baryon number density, and n_γ is the photon number density. The observed value for the BAU is [259]

$$\eta_B = (6.1 \pm 0.2) \cdot 10^{-10}, \tag{7.2}$$

which, although very small, is far above what could be expected from the SM. Unless we assume that there was an initial baryon asymmetry in the beginning of the Universe, this baryon asymmetry has to be generated during its early evolution.

In 1967, Sakharov presented the three conditions that any physical model has to fulfill in order to be able to produce a baryon asymmetry [258]:

1. Baryon number violation.

2. C- and CP-violation.

3. Out of equilibrium processes.

In more detail, these conditions, known as the Sakharov conditions, tell us that in any model producing a non-zero BAU, there are processes in which the number of baryons before the process is different from the number of baryons after the process, processes which do not occur at the same probability when exchanging particles for anti-particles, and there has to be some period during the evolution of the Universe when these processes were out of thermal equilibrium.

7.3 The leptogenesis mechanism

One of the most intriguing features of the seesaw mechanism is that the heavy right-handed neutrinos also provide us with a possible model [260–274] for generating the BAU. In this model, the BAU is produced by first generating a lepton asymmetry from the out of thermal equilibrium decay of right-handed neutrinos, followed by a conversion of this lepton asymmetry into a baryon asymmetry by non-perturbative processes, which are already present in the SM. Thus, the first of the Sakharov conditions is fulfilled by SM physics [275–277], while the last two are fulfilled by physics related to the seesaw mechanism.

7.3.1 Decay of right-handed neutrinos

Let us assume that there is a mass hierarchy among the right-handed neutrinos and that the mass of the lightest right-handed neutrino N_1 is M_1. As we will show, the final lepton asymmetry generated in this scenario is mostly dependent on the lightest right-handed neutrino, and thus, we will ignore the effects of the heavier right-handed neutrinos.

When the Universe is very hot, *i.e.*, $T \gg M_1$, then the abundance of right-handed Majorana neutrinos will be held in thermal equilibrium by processes such as

$$N_1 \longleftrightarrow \Phi + L, \tag{7.3}$$

where Φ is the Higgs doublet and L is a lepton doublet. However, as the Universe cools down and the temperature drops below the right-handed neutrino mass, the N_1 equilibrium distribution becomes Boltzmann suppressed. If the life-time of the right-handed neutrino is long enough, then a significant fraction of them will remain and decay out of thermal equilibrium.

We define the decay asymmetry ε according to

$$\varepsilon = \frac{\Gamma(N_1 \to \Phi + L) - \Gamma(N_1 \to \Phi^\dagger + L^c)}{\Gamma(N_1 \to \Phi + L) + \Gamma(N_1 \to \Phi^\dagger + L^c)}, \tag{7.4}$$

i.e., it is the difference in the rate of decays into particles and the rate of decays into anti-particles normalized by the total decay rate. If the decay rates are only computed on tree-level, see Fig. 7.1, then the decay asymmetry will be zero, since the matrix element for the decay into particles is simply the complex conjugate of the matrix element for the decay into anti-particles. Thus, in order to find a non-zero decay asymmetry, the decay rates in the numerator must be computed to (at least) one-loop level, involving the diagrams shown in Fig. 7.2.

If one considers right-handed neutrinos which are degenerate in mass, then resonance effects can come into play [272] and we also need to compute the decay asymmetry of the next-to-lightest right-handed neutrino N_2. This computation is completely analogous to the one for computing the decay asymmetry for N_1.

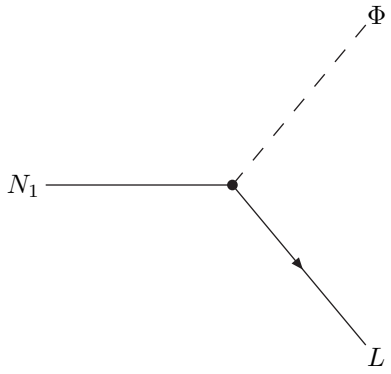

Figure 7.1. The tree-level contribution to the decay $N_1 \to \phi + L$. As the tree-level amplitude for the *CP*-conjugate decay $N_1 \to \phi^* + L^c$ is simply the complex conjugate of the amplitude of the above diagram, the decay asymmetry ε is equal to zero on tree-level.

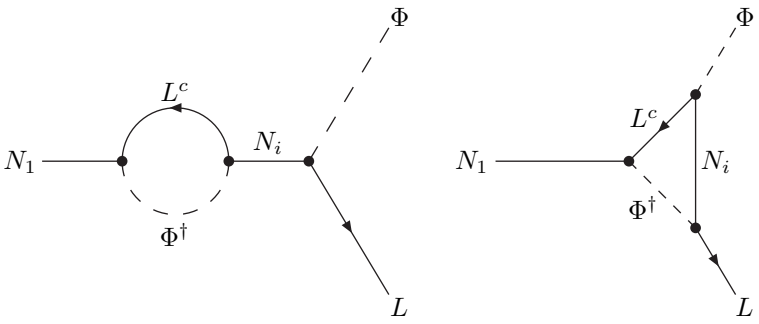

Figure 7.2. One-loop diagrams contributing to the decay asymmetry ε. It is necessary to include these diagrams in order to have a non-zero decay asymmetry, since the tree-level decay rate is *CP*-symmetric.

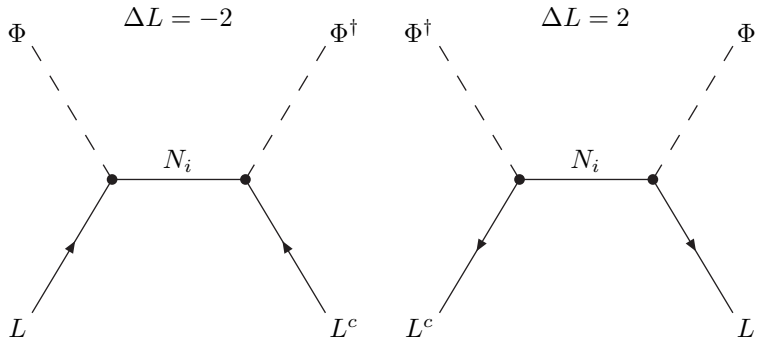

Figure 7.3. The $\Delta L = \pm 2$ scattering processes involving the lepton doublets and the Higgs with an intermediate right-handed neutrino. The amplitudes for these processes obviously have the same magnitude, and thus, they will drive the lepton number toward zero.

7.3.2 Transport equations and washout

If there was a number n_{N_1} of right-handed neutrinos which would simply decay and that was the end of the story, then the final number of leptons would be given by

$$n_L = \varepsilon n_{N_1}. \tag{7.5}$$

However, if we introduce the decays of the right-handed neutrinos, we should also include the real intermediate contributions from the $\Delta L = 2$ scattering shown in Fig. 7.3. The Boltzmann equations for the system which only takes decays and inverse decays into account are given by [273]

$$\frac{dN_{N_1}}{dz} = \frac{z}{H_1}\Gamma_D \left(N_{N_i}^{\rm eq} - N_{N_i}\right), \tag{7.6a}$$

$$\frac{d\eta_L}{dz} = -\varepsilon\frac{z}{H_1}\Gamma_D \left(N_{N_i}^{\rm eq} - N_{N_i}\right) - \frac{z}{H_1}\Gamma_W \eta_L, \tag{7.6b}$$

where $z = M_1/T$, N_p is the number of particles p normalized to the the comoving volume containing one photon at $z \ll 1$, $N_{N_1}^{\rm eq}$ is the equilibrium number of N_1 (*i.e.*, $N_{N_1}^{\rm eq} = 3/4$ for $z \ll 1$), H_1 is the Hubble expansion parameter at $z = 1$, Γ_D is the decay rate, and Γ_W is the washout rate. The formal solution for N_L in this system

of equations can be written as

$$\begin{aligned} N_L(z) &= N_L^i \exp\left[-\int_{z_i}^{z} dz' \frac{z'}{H_1}\Gamma_W(z')\right] \\ &\quad -\varepsilon \int_{z_i}^{z} dz' \frac{dN_{N_1}}{dz'} \exp\left[-\int_{z'}^{z} dz'' \frac{z''}{H_1}\Gamma_W(z'')\right] \\ &= N_L^i \exp\left[-\int_{z_i}^{z} dz' \frac{z'}{H_1}\Gamma_W(z')\right] + \varepsilon\kappa(z), \end{aligned} \tag{7.7}$$

where $\kappa(z)$ is the ε-independent efficiency factor defined by

$$\kappa(z) = -\int_{z_i}^{z} dz' \frac{dN_{N_1}}{dz'} \exp\left[-\int_{z'}^{z} dz'' \frac{z''}{H_1}\Gamma_W(z'')\right] \tag{7.8}$$

and N_L^i is the initial lepton number at $z = z_i \ll 1$, which could be due to some other lepton number generating process such as the decay of the other right-handed neutrinos. From Eq. (7.7), it is apparent that any initial abundance (*e.g.*, any abundance coming from the decay of heavier right-handed neutrinos) is suppressed by the inverse decays so that the remaining lepton asymmetry is simply the one originating from the decay of the lightest right-handed neutrinos, *i.e.*, the final lepton asymmetry is given by

$$N_L(\infty) = \varepsilon\kappa(\infty). \tag{7.9}$$

While this model is clearly over-simplified, it has many of the features of the full set of Boltzmann equations, which should also include different types of scatterings. An introduction to a more complete set of Boltzmann equations and its behavior and parameter dependence can be found in Ref. [273].

7.3.3 Sphaleron processes

When the lepton asymmetry has been generated, we need some description of how it is converted into a baryon asymmetry in order for our model to produce the observed baryon asymmetry. Such a feature is already embedded into the SM in the form of non-perturbative effects [275–277] known as sphaleron processes. With the structure of the gauge theory and the Higgs field, there will be several topologically distinct energy minima of the field configurations, *i.e.*, field configurations that are not related by continuous gauge transformations.

When introducing fermions into the theory according to the SM prescription, the accidental $B - L$ symmetry is still preserved and has the same value for all of the minima, while $B+L$ is no longer conserved and takes different values depending on the minima. Thus, the process of changing minima will imply a different value for $B + L$ which, since $B - L$ is conserved, will convert a part of the generated lepton asymmetry into a baryon asymmetry, see Fig. 7.4. Taking the details of the

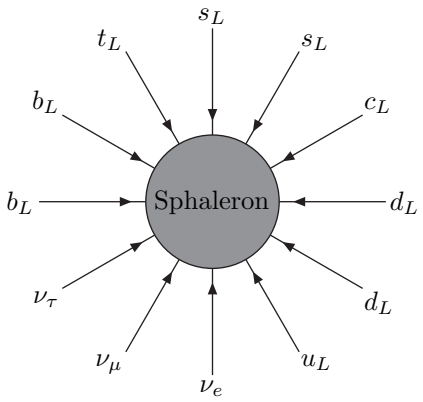

Figure 7.4. An example of a sphaleron process. While $B - L$ is conserved, $B + L$ changes by six. In general, the difference in $B + L$ between two different energy minima is $\Delta B + \Delta L = 2n_f$, where n_f is the number of fermion generations.

conversion into account, the final baryon number density is given by [276, 277]

$$N_B = -\frac{8n_f + 4m}{22n_f + 13m} N_L^{\text{lep}}, \tag{7.10a}$$

where $N_L^{\text{lep}} = -N_{B-L}$ is the lepton asymmetry generated during leptogenesis, m is the number of Higgs doublets, and n_f is the number of fermion generations. In the SM, we have only one Higgs doublet and three fermion generations, *i.e.*, $m = 1$ and $n_f = 3$, which results in

$$N_B = -\frac{28}{79} N_L^{\text{lep}}. \tag{7.10b}$$

Since $B - L$ is conserved, we find that the lepton asymmetry after the sphaleron processes have come into equilibrium is given by

$$N_L = \frac{51}{79} N_L^{\text{lep}}. \tag{7.10c}$$

In other words, if N_B is positive (signifying an abundance of baryons over anti-baryons), then N_L must be negative (signifying an abundance of anti-leptons over leptons). This holds true even if leptogenesis is not the progenitor of the $B - L$ asymmetry, in which case N_L^{lep} should be replaced by $-N_{B-L}$ for the mechanism considered. The final baryon number density should be compared to the photon number density $N_\gamma^{\text{rec}} \simeq 28$ [273] at recombination where the baryon asymmetry η_B is frozen out. Thus, the baryon asymmetry is given by

$$\eta_B = \frac{N_B}{N_\gamma^{\text{rec}}} \simeq -\frac{1}{79} N_L^{\text{lep}} \simeq -1.3 \cdot 10^{-2} \varepsilon \kappa(\infty). \tag{7.11}$$

In Paper [7], we have used the leptogenesis mechanism in order to discriminate among the eight different solutions for the right-handed mass matrix in the type I+II seesaw mechanism.

Chapter 8

Summary and conclusions

A matter that becomes clear ceases to concern us.
– Friedrich Nietzsche

In this introductory part of the thesis, we have introduced the background theory and experimental evidence necessary in order to put the papers of Part II into context. We have introduced the SM of particle physics and discussed how it fails to account for, amongst other things, neutrino oscillations, since it is unable to accommodate massive neutrinos. We also discussed possible ways of extending the SM in order to include neutrino masses. The theory and phenomenology of neutrino oscillations were introduced and the experimental status of neutrino oscillations were reviewed. Finally, we briefly discussed the leptogenesis mechanism for generating the BAU, which is a very nice feature of the seesaw mechanism for generating neutrino mass.

Throughout this part, we have also mentioned where the papers of Part II come into context. Below, we list the most important conclusions of the papers:

- The three-flavor effects on the day-night asymmetry have been computed. Essentially, the day-night difference in the survival probability scales as c_{13}^6, while the overall probability scales as c_{13}^4. Therefore, the day-night asymmetry scales as c_{13}^2.

- The day-night asymmetry could possibly be used as a complementary way of setting bounds for the lepton mixing angle θ_{13} due to its c_{13}^2 behavior. This was further elaborated on by Akhmedov *et al.* in Ref. [238].

- The two-flavor neutrino oscillation probability in matter has been exactly solved in terms of a series solution with a recursive relation for the coefficients. This has been done by rewriting the differential equations describing the Schrödinger equation for neutrino oscillations in matter as a second order non-linear differential equation for the neutrino oscillation probability.

- The effective two-flavor case which arises in matter with very large densities ($2VE \gg \Delta|m^2_{ij}|$) has been studied in detail. The accuracy of the approximation of infinitely dense matter ($2VE/\Delta m^2_{ij} \to \infty$) has also been examined both numerically and analytically.

- The concept of general incoherent effects (damping signatures) altering the neutrino oscillation probabilities has been introduced along with examples of scenarios where they occur. The incoherent effects have been divided into two main classes, probability conserving (decoherence-like) and probability violating (decay-like) effects.

- The alteration of the neutrino oscillation probabilities due to incoherent effects have been carefully examined in both the two- and three-flavor cases.

- The impact of incoherent effects on the determination of the fundamental neutrino oscillation parameters has been discussed. We have given an example where damping signatures may lead to an erroneous determination of the lepton mixing angle θ_{13} and examined how one can distinguish among different types of damping signatures.

- The general coherent effects have been studied. We have discussed the possibility to distinguish between different coherent effects on the basis of their explicit form in different bases.

- The degeneracy between neutrino oscillation parameters and general coherent effects has been analyzed. In particular, the degeneracy between the lepton mixing angle θ_{13} and coherent effects has been computed in a perturbation theory framework.

- We have analyzed the possibility to distinguish between different types of coherent and incoherent effects, as well as between coherent effects and subleading standard oscillation effects, such as non-zero θ_{13}. This analysis has been made for a numerical example of a fictive future neutrino factory.

- We have discriminated among the eight possible solutions for the right-handed neutrino masses in a left-right symmetric type I+II seesaw scenario. This has been done using criteria of stability and viability of leptogenesis for the different solutions.

- In particular, we have found that leptogenesis is viable in four out of the eight possible solutions. This is due to extra Majorana-type *CP*-violating phases, which can be present due to the left-right symmetry. For the four possible solutions, the ratio v_R/v_L is found to be in the range 10^{18}–10^{21} due to reasons of leptogenesis and stability as well as the gravitino bound.

- The impact of including non-standard neutrino interactions in the analysis of the MINOS experiment has been studied both numerically and analytically. The impact on the MINOS sensitivity regions have been computed.

- We have discussed the possibility to put constraints on the effective NSI parameter $\varepsilon_{e\tau}$ or the lepton mixing angle θ_{13} from the MINOS results. We found that MINOS will not be able to put further bounds on any of these two parameters unless the external bounds on the other parameter can be improved.

In addition, more detailed conclusions are listed separately at the end of each paper.

Bibliography

[1] M. Blennow, T. Ohlsson and H. Snellman, *Day-night effect in solar neutrino oscillations with three flavors*, Phys. Rev. **D69**, 073006 (2004), hep-ph/0311098.

[2] M. Blennow and T. Ohlsson, *Exact series solution to the two flavor neutrino oscillation problem in matter*, J. Math. Phys. **45**, 4053 (2004), hep-ph/0405033.

[3] M. Blennow and T. Ohlsson, *Effective neutrino mixing and oscillations in dense matter*, Phys. Lett. **B609**, 330 (2005), hep-ph/0409061.

[4] M. Blennow, T. Ohlsson and W. Winter, *Damping signatures in future neutrino oscillation experiments*, JHEP **06**, 049 (2005), hep-ph/0502147.

[5] M. Blennow, T. Ohlsson and W. Winter, *Non-standard Hamiltonian effects on neutrino oscillations*, Eur. Phys. J. **C49**, 1023 (2007), hep-ph/0508175.

[6] M. Blennow, T. Ohlsson and J. Skrotzki, *Effects of non-standard interactions in the MINOS experiment*, (2007), hep-ph/0702059.

[7] E. K. Akhmedov *et al.*, *Stability and leptogenesis in the left-right symmetric seesaw mechanism*, JHEP **04**, 022 (2007), hep-ph/0612194.

[8] I. Newton, *Philosophiae naturalis principia mathematica*, (1687).

[9] Super-Kamiokande collaboration, Y. Fukuda *et al.*, *Evidence for oscillation of atmospheric neutrinos*, Phys. Rev. Lett. **81**, 1562 (1998), hep-ex/9807003.

[10] J. J. Thompson, *Cathode rays*, Phil. Mag. **44**, 293 (1897).

[11] E. Rutherford, *Collisions of alpha particles with light atoms. IV. An anomalous effect in nitrogen*, Phil. Mag. **37**, 581 (1919).

[12] L. Meitner and O. Hahn, *Über die Verteilung der Beta-Strahlen auf die einzelnen Produkte des aktiven Niederschlags des Thoriums*, Phys. Z. **13**, 390 (1912).

[13] J. Chadwick, *Distribution in intensity in the magnetic spectrum of the β-rays of radium*, Verh. Deutsch Phys. Ges. **16**, 383 (1914).

[14] J. Chadwick, *Possible existence of a neutron*, Nature **129**, 312 (1932).

[15] E. Fermi, *Tentativo di una teoria dei raggi β*, Nuovo Cim. **11**, 1 (1934).

[16] E. Fermi, *An attempt of a theory of beta radiation. 1*, Z. Phys. **88**, 161 (1934).

[17] S. L. Glashow, *Partial symmetries of weak interactions*, Nucl. Phys. **22**, 579 (1961).

[18] S. Weinberg, *A model of leptons*, Phys. Rev. Lett. **19**, 1264 (1967).

[19] A. Salam, Proceedings of the Eighth Nobel Symposium, edited by N. Svartholm, p. 367, Almqvist och Wiksell, Stockholm, 1968.

[20] H. Bethe and R. Peierls, *The 'neutrino'*, Nature **133**, 532 (1934).

[21] B. Pontecorvo, *Inverse β process*, Chalk River Report PD-205, November 1946 (unpublished).

[22] F. Reines and C. L. Cowan, *Detection of the free neutrino*, Phys. Rev. **92**, 830 (1953).

[23] F. Reines and C. L. Cowan, *The neutrino*, Nature **178**, 446 (1956).

[24] F. Reines, Nobel prize lecture, 1995.

[25] G. Danby *et al.*, *Observation of high-energy neutrino reactions and the existence of two kinds of neutrinos*, Phys. Rev. Lett. **9**, 36 (1962).

[26] M. L. Perl *et al.*, *Evidence for anomalous lepton production in e^+e^- annihilation*, Phys. Rev. Lett. **35**, 1489 (1975).

[27] DONUT collaboration, K. Kodama *et al.*, *Observation of tau-neutrino interactions*, Phys. Lett. **B504**, 218 (2001), `hep-ex/0012035`.

[28] B. Pontecorvo, *Mesonium and antimesonium*, Sov. Phys. JETP **6**, 429 (1957).

[29] B. Pontecorvo, *Inverse beta processes and nonconservation of lepton charge*, Sov. Phys. JETP **7**, 172 (1958).

[30] M. Gell-Mann and A. Pais, *Behavior of neutral particles under charge conjugation*, Phys. Rev. **97**, 1387 (1955).

[31] Z. Maki, M. Nakagawa and S. Sakata, *Remarks on the unified model of elementary particles*, Prog. Theor. Phys. **28**, 870 (1962).

[32] M. Nakagawa *et al.*, *Possible existence of a neutrino with mass and partial conservation of muon charge*, Prog. Theor. Phys. **30**, 727 (1963).

[33] B. Pontecorvo, *Neutrino experiments and the question of leptonic-charge conservation*, Sov. Phys. JETP **26**, 984 (1968).

[34] V. N. Gribov and B. Pontecorvo, *Neutrino astronomy and lepton charge*, Phys. Lett. **B28**, 493 (1969).

[35] H. Fritzsch and P. Minkowski, *Vector-like weak currents, massive neutrinos, and neutrino beam oscillations*, Phys. Lett. **B62**, 72 (1976).

[36] S. M. Bilenky, *Neutrino oscillations and neutrino mixing*, Sov. J. Part. Nucl. **18**, 188 (1987).

[37] L. Wolfenstein, *Neutrino oscillations in matter*, Phys. Rev. **D17**, 2369 (1978).

[38] S. P. Mikheyev and A. Y. Smirnov, *Resonance enhancement of oscillations in matter and solar neutrino spectroscopy*, Sov. J. Nucl. Phys. **42**, 913 (1985).

[39] S. P. Mikheyev and A. Y. Smirnov, *Resonant amplification of neutrino oscillations in matter and solar neutrino spectroscopy*, Nuovo Cim. **C9**, 17 (1986).

[40] J. Davis, Raymond, D. S. Harmer and K. C. Hoffman, *Search for neutrinos from the Sun*, Phys. Rev. Lett. **20**, 1205 (1968).

[41] B. T. Cleveland *et al.*, *Update on the measurement of the solar neutrino flux with the Homestake chlorine detector*, Nucl. Phys. Proc. Suppl. **38**, 47 (1995).

[42] B. T. Cleveland *et al.*, *Measurement of the solar electron neutrino flux with the Homestake chlorine detector*, Astrophys. J. **496**, 505 (1998).

[43] GALLEX collaboration, P. Anselmann *et al.*, *GALLEX results from the first 30 solar neutrino runs*, Phys. Lett. **B327**, 377 (1994).

[44] GALLEX collaboration, W. Hampel *et al.*, *GALLEX solar neutrino observations: Results for GALLEX IV*, Phys. Lett. **B447**, 127 (1999).

[45] SAGE collaboration, J. N. Abdurashitov *et al.*, *Measurement of the solar neutrino capture rate with gallium metal*, Phys. Rev. **C60**, 055801 (1999), `astro-ph/9907113`.

[46] SAGE collaboration, J. N. Abdurashitov *et al.*, *Measurement of the solar neutrino capture rate by the Russian-American gallium solar neutrino experiment during one half of the 22-year cycle of solar activity*, J. Exp. Theor. Phys. **95**, 181 (2002), `astro-ph/0204245`.

[47] Kamiokande-II collaboration, K. S. Hirata *et al.*, *Observation of ^8B solar neutrinos in the Kamiokande-II detector*, Phys. Rev. Lett. **63**, 16 (1989).

[48] Kamiokande-II collaboration, K. S. Hirata *et al.*, *Results from one thousand days of real-time, directional solar-neutrino data*, Phys. Rev. Lett. **65**, 1297 (1990).

[49] Kamiokande-II collaboration, K. S. Hirata *et al.*, *Real time, directional measurement of ^8B solar neutrinos in the Kamiokande-II detector*, Phys. Rev. **D44**, 2241 (1991).

[50] J. N. Bahcall and R. K. Ulrich, *Solar models, neutrino experiments and helioseismology*, Rev. Mod. Phys. **60**, 297 (1988).

[51] J. N. Bahcall and M. H. Pinsonneault, *Standard solar models, with and without helium diffusion and the solar neutrino problem*, Rev. Mod. Phys. **64**, 885 (1992).

[52] Super-Kamiokande collaboration, S. Fukuda *et al.*, *Solar ^8B and hep neutrino measurements from 1258 days of Super-Kamiokande data*, Phys. Rev. Lett. **86**, 5651 (2001), `hep-ex/0103032`.

[53] Super-Kamiokande collaboration, S. Fukuda *et al.*, *Constraints on neutrino oscillations using 1258 days of Super-Kamiokande solar neutrino data*, Phys. Rev. Lett. **86**, 5656 (2001), `hep-ex/0103033`.

[54] Super-Kamiokande collaboration, S. Fukuda *et al.*, *Determination of solar neutrino oscillation parameters using 1496 days of Super-Kamiokande-I data*, Phys. Lett. **B539**, 179 (2002), `hep-ex/0205075`.

[55] SNO collaboration, Q. R. Ahmad *et al.*, *Measurement of the charged current interactions produced by ^8B solar neutrinos at the Sudbury Neutrino Observatory*, Phys. Rev. Lett. **87**, 071301 (2001), `nucl-ex/0106015`.

[56] SNO collaboration, Q. R. Ahmad *et al.*, *Direct evidence for neutrino flavor transformation from neutral-current interactions in the Sudbury Neutrino Observatory*, Phys. Rev. Lett. **89**, 011301 (2002), `nucl-ex/0204008`.

[57] SNO collaboration, S. N. Ahmed *et al.*, *Measurement of the total active ^8B solar neutrino flux at the Sudbury Neutrino Observatory with enhanced neutral current sensitivity*, Phys. Rev. Lett. **92**, 181301 (2004), `nucl-ex/0309004`.

[58] Super-Kamiokande collaboration, Y. Ashie *et al.*, *Evidence for an oscillatory signature in atmospheric neutrino oscillation*, Phys. Rev. Lett. **93**, 101801 (2004), `hep-ex/0404034`.

[59] Super-Kamiokande collaboration, Y. Ashie *et al.*, *A measurement of atmospheric neutrino oscillation parameters by Super-Kamiokande I*, Phys. Rev. **D71**, 112005 (2005), `hep-ex/0501064`.

[60] KamLAND collaboration, K. Eguchi *et al.*, *First results from KamLAND: Evidence for reactor anti-neutrino disappearance*, Phys. Rev. Lett. **90**, 021802 (2003), `hep-ex/0212021`.

[61] KamLAND collaboration, T. Araki *et al.*, *Measurement of neutrino oscillation with KamLAND: Evidence of spectral distortion*, Phys. Rev. Lett. **94**, 081801 (2005), `hep-ex/0406035`.

[62] K2K collaboration, M. H. Ahn *et al.*, *Indications of neutrino oscillation in a 250-km long- baseline experiment*, Phys. Rev. Lett. **90**, 041801 (2003), `hep-ex/0212007`.

[63] K2K collaboration, E. Aliu *et al.*, *Evidence for muon neutrino oscillation in an accelerator-based experiment*, Phys. Rev. Lett. **94**, 081802 (2005), `hep-ex/0411038`.

[64] MINOS collaboration, D. G. Michael *et al.*, *Observation of muon neutrino disappearance with the MINOS detectors and the NuMI neutrino beam*, Phys. Rev. Lett. **97**, 191801 (2006), `hep-ex/0607088`.

[65] C. N. Yang and R. L. Mills, *Conservation of isotopic spin and isotopic gauge invariance*, Phys. Rev. **96**, 191 (1954).

[66] W. M. Yao *et al.*, *Review of Particle Physics*, Journal of Physics G **33**, 1 (2006).

[67] F. Englert and R. Brout, *Broken symmetry and the mass of gauge vector mesons*, Phys. Rev. Lett. **13**, 321 (1964).

[68] P. W. Higgs, *Broken symmetries, massless particles and gauge fields*, Phys. Lett. **12**, 132 (1964).

[69] G. S. Guralnik, C. R. Hagen and T. W. B. Kibble, *Global conservation laws and massless particles*, Phys. Rev. Lett. **13**, 585 (1964).

[70] P. W. Higgs, *Spontaneous symmetry breakdown without massless bosons*, Phys. Rev. **145**, 1156 (1966).

[71] K. Nishijima, *Charge independence theory of V particles*, Prog. Theor. Phys. **13**, 285 (1955).

[72] M. Gell-Mann, *The interpretation of the new particles as displaced charged multiplets*, Nuovo Cim. Suppl. **4**, 848 (1956).

[73] N. Cabibbo, *Unitary Symmetry and Leptonic Decays*, Phys. Rev. Lett. **10**, 531 (1963).

[74] M. Kobayashi and T. Maskawa, *CP Violation in the Renormalizable Theory of Weak Interaction*, Prog. Theor. Phys. **49**, 652 (1973).

[75] E. Majorana, *Theory of the symmetry of electrons and positrons*, Nuovo Cim. **14**, 171 (1937).

[76] H. V. Klapdor-Kleingrothaus *et al.*, *Evidence for neutrinoless double beta decay*, Mod. Phys. Lett. **A16**, 2409 (2001), `hep-ph/0201231`.

[77] C. E. Aalseth *et al.*, *Comment on 'Evidence for neutrinoless double beta decay'*, Mod. Phys. Lett. **A17**, 1475 (2002), `hep-ex/0202018`.

[78] H. L. Harney, *Reply to the comment on 'Evidence for neutrinoless double beta decay'. (Mod. Phys. Lett. A16(2001) 2409)*, (2001), `hep-ph/0205293`.

[79] H. V. Klapdor-Kleingrothaus, *Reply to a comment of article 'Evidence for neutrinoless double beta decay'*, (2002), `hep-ph/0205228`.

[80] M. Doi *et al.*, *CP violation in Majorana neutrinos*, Phys. Lett. **B102**, 323 (1981).

[81] S. M. Bilenky, J. Hosek and S. T. Petcov, *On oscillations of neutrinos with Dirac and Majorana masses*, Phys. Lett. **B94**, 495 (1980).

[82] M. Doi, T. Kotani and E. Takasugi, *Double beta decay and Majorana neutrino*, Prog. Theor. Phys. Suppl. **83**, 1 (1985).

[83] H. Fritzsch, M. Gell-Mann and P. Minkowski, *Vector-like weak currents and new elementary fermions*, Phys. Lett. **B59**, 256 (1975).

[84] P. Minkowski, $\mu \to e\gamma$ *at a rate of one out of 1-billion muon decays?*, Phys. Lett. **B67**, 421 (1977).

[85] M. Gell-Mann, P. Ramond and R. Slansky, *Complex spinors and unified theories* in *Supergravity, Proceedings of the Workshop, Stony Brook, New York, 1979*, edited by P. van Nieuwenhuizen and D. Freedman, North-Holland, Amsterdam, 1979.

[86] T. Yanagida, *Horizontal gauge symmetry and masses of neutrinos*, In Proceedings of the Workshop on the Baryon Number of the Universe and Unified Theories, Tsukuba, Japan, 13-14 Feb 1979.

[87] S. L. Glashow, *The future of elementary particle physics*, NATO Adv. Study Inst. Ser. B Phys. **59**, 687 (1979).

[88] R. N. Mohapatra and G. Senjanović, *Neutrino mass and spontaneous parity nonconservation*, Phys. Rev. Lett. **44**, 912 (1980).

[89] M. Magg and C. Wetterich, *Neutrino mass problem and gauge hierarchy*, Phys. Lett. **B94**, 61 (1980).

[90] J. Schechter and J. W. F. Valle, *Neutrino masses in* $SU(2) \times U(1)$ *theories*, Phys. Rev. **D22**, 2227 (1980).

[91] R. N. Mohapatra and G. Senjanović, *Neutrino masses and mixings in gauge models with spontaneous parity violation*, Phys. Rev. **D23**, 165 (1981).

[92] G. Senjanović and R. N. Mohapatra, *Exact left-right symmetry and spontaneous violation of parity*, Phys. Rev. **D12**, 1502 (1975).

[93] R. N. Mohapatra, F. E. Paige and D. P. Sidhu, *Symmetry breaking and naturalness of parity conservation in weak neutral currents in left-right symmetric gauge theories*, Phys. Rev. **D17**, 2462 (1978).

[94] N. G. Deshpande *et al.*, *Left-right symmetric electroweak models with triplet Higgs*, Phys. Rev. **D44**, 837 (1991).

[95] E. K. Akhmedov and M. Frigerio, *Seesaw duality*, Phys. Rev. Lett. **96**, 061802 (2006), `hep-ph/0509299`.

[96] E. K. Akhmedov and M. Frigerio, *Interplay of type I and type II seesaw contributions to neutrino mass*, JHEP **01**, 043 (2007), `hep-ph/0609046`.

[97] P. Hosteins, S. Lavignac and C. A. Savoy, *Quark-lepton unification and eightfold ambiguity in the left-right symmetric seesaw mechanism*, Nucl. Phys. **B755**, 137 (2006), `hep-ph/0606078`.

[98] S. M. Bilenky and B. Pontecorvo, *Lepton mixing and neutrino oscillations*, Phys. Rept. **41**, 225 (1978).

[99] M. Maltoni *et al.*, *Status of global fits to neutrino oscillations*, New J. Phys. **6**, 122 (2004), `hep-ph/0405172`.

[100] A. Strumia and F. Vissani, *Implications of neutrino data circa 2005*, Nucl. Phys. **B726**, 294 (2005), `hep-ph/0503246`.

[101] G. L. Fogli *et al.*, *Global analysis of three-flavor neutrino masses and mixings*, Prog. Part. Nucl. Phys. **57**, 742 (2006), `hep-ph/0506083`.

[102] V. D. Barger, K. Whisnant and R. J. N. Phillips, *CP violation in three neutrino oscillations*, Phys. Rev. Lett. **45**, 2084 (1980).

[103] C. Jarlskog, *Commutator of the quark mass matrices in the standard electroweak model and a measure of maximal CP violation*, Phys. Rev. Lett. **55**, 1039 (1985).

[104] N. Cabibbo, *Time reversal violation in neutrino oscillation*, Phys. Lett. **B72**, 333 (1978).

[105] D. Nötzold and G. Raffelt, *Neutrino dispersion at finite temperature and density*, Nucl. Phys. **B307**, 924 (1988).

[106] S. J. Parke, *Nonadiabatic level crossing in resonant neutrino oscillations*, Phys. Rev. Lett. **57**, 1275 (1986).

[107] A. B. Balantekin, S. H. Fricke and P. J. Hatchell, *Analytical and semiclassical aspects of matter enhanced neutrino oscillations*, Phys. Rev. **D38**, 935 (1988).

[108] A. Nicolaidis, *WKB calculation of neutrino matter oscillations*, Phys. Lett. **B242**, 480 (1990).

[109] H. Lehmann, P. Osland and T. T. Wu, *Mikheyev–Smirnov–Wolfenstein effect for linear electron density*, Commun. Math. Phys. **219**, 77 (2001), `hep-ph/0006213`.

[110] S. T. Petcov, *Exact analytic description of two neutrino oscillations in matter with exponentially varying density*, Phys. Lett. **B200**, 373 (1988).

[111] P. Osland and T. T. Wu, *Solar Mikheyev–Smirnov–Wolfenstein effect with three generations of neutrinos*, Phys. Rev. **D62**, 013008 (2000), `hep-ph/9912540`.

[112] P. M. Fishbane and S. G. Gasiorowicz, *On equations for neutrino propagation in matter*, Phys. Rev. **D64**, 113017 (2001), `hep-ph/0012230`.

[113] M. Freund, *Analytic approximations for three neutrino oscillation parameters and probabilities in matter*, Phys. Rev. **D64**, 053003 (2001), `hep-ph/0103300`.

[114] C. S. Lim, *Resonant solar neutrino oscillation versus laboratory neutrino oscillation experiments*, Presented at BNL Neutrino Workshop, Upton, N.Y., Feb 5-7, 1987.

[115] E. Akhmedov, *Three-flavour effects and CP- and T-violation in neutrino oscillations*, Phys. Scripta **T121**, 65 (2005), `hep-ph/0412029`.

[116] A. Cervera *et al.*, *Golden measurements at a neutrino factory*, Nucl. Phys. **B579**, 17 (2000), `hep-ph/0002108`.

[117] M. Freund, P. Huber and M. Lindner, *Systematic exploration of the neutrino factory parameter space including errors and correlations*, Nucl. Phys. **B615**, 331 (2001), `hep-ph/0105071`.

[118] V. Barger, D. Marfatia and K. Whisnant, *Breaking eight-fold degeneracies in neutrino CP violation, mixing, and mass hierarchy*, Phys. Rev. **D65**, 073023 (2002), `hep-ph/0112119`.

[119] E. K. Akhmedov *et al.*, *Series expansions for three-flavor neutrino oscillation probabilities in matter*, JHEP **04**, 078 (2004), `hep-ph/0402175`.

[120] T. K. Kuo and J. T. Pantaleone, *The solar neutrino problem and three neutrino oscillations*, Phys. Rev. Lett. **57**, 1805 (1986).

[121] A. Y. Smirnov, *Three neutrino oscillations in matter.*, Yad. Fiz. **46**, 1152 (1987).

[122] T. Ohlsson and H. Snellman, *Three flavor neutrino oscillations in matter*, J. Math. Phys. **41**, 2768 (2000), `hep-ph/9910546`.

[123] J. Arafune and J. Sato, *CP and T violation test in neutrino oscillation*, Phys. Rev. **D55**, 1653 (1997), `hep-ph/9607437`.

[124] J. Arafune, M. Koike and J. Sato, *CP violation and matter effect in long baseline neutrino oscillation experiments*, Phys. Rev. **D56**, 3093 (1997), `hep-ph/9703351`.

[125] H. Minakata and H. Nunokawa, *CP violation vs. matter effect in long-baseline neutrino oscillation experiments*, Phys. Rev. **D57**, 4403 (1998), `hep-ph/9705208`.

[126] H. Minakata and H. Nunokawa, *How to measure CP violation in neutrino oscillation experiments?*, Phys. Lett. **B413**, 369 (1997), `hep-ph/9706281`.

[127] S. M. Bilenky, C. Giunti and W. Grimus, *Long-baseline neutrino oscillation experiments and CP violation in the lepton sector*, Phys. Rev. **D58**, 033001 (1998), `hep-ph/9712537`.

[128] K. Dick *et al.*, *CP-violation in neutrino oscillations*, Nucl. Phys. **B562**, 29 (1999), `hep-ph/9903308`.

[129] LSND collaboration, C. Athanassopoulos *et al.*, *Evidence for $\bar{\nu}_\mu \to \bar{\nu}_e$ oscillation from the LSND experiment at the Los Alamos Meson Physics Facility*, Phys. Rev. Lett. **77**, 3082 (1996), `nucl-ex/9605003`.

[130] LSND collaboration, C. Athanassopoulos *et al.*, *Evidence for $\nu_\mu \to \nu_e$ neutrino oscillations from LSND*, Phys. Rev. Lett. **81**, 1774 (1998), `nucl-ex/9709006`.

[131] LSND collaboration, A. Aguilar *et al.*, *Evidence for neutrino oscillations from the observation of $\bar{\nu}_e$ appearance in a $\bar{\nu}_\mu$ beam*, Phys. Rev. **D64**, 112007 (2001), `hep-ex/0104049`.

[132] J. N. Bahcall, N. Cabibbo and A. Yahil, *Are neutrinos stable particles?*, Phys. Rev. Lett. **28**, 316 (1972).

[133] V. D. Barger, W. Y. Keung and S. Pakvasa, *Majoron emission by neutrinos*, Phys. Rev. **D25**, 907 (1982).

[134] P. B. Pal and L. Wolfenstein, *Radiative decays of massive neutrinos*, Phys. Rev. **D25**, 766 (1982).

[135] J. W. F. Valle, *Fast neutrino decay in horizontal Majoron models*, Phys. Lett. **B131**, 87 (1983).

[136] V. D. Barger *et al.*, *Neutrino decay as an explanation of atmospheric neutrino observations*, Phys. Rev. Lett. **82**, 2640 (1999), `astro-ph/9810121`.

[137] V. D. Barger *et al.*, *Neutrino decay and atmospheric neutrinos*, Phys. Lett. **B462**, 109 (1999), `hep-ph/9907421`.

[138] S. Pakvasa, *Do neutrinos decay?*, AIP Conf. Proc. **542**, 99 (2000), `hep-ph/0004077`.

[139] M. Lindner, T. Ohlsson and W. Winter, *A combined treatment of neutrino decay and neutrino oscillations*, Nucl. Phys. **B607**, 326 (2001), `hep-ph/0103170`.

[140] M. Lindner, T. Ohlsson and W. Winter, *Decays of supernova neutrinos*, Nucl. Phys. **B622**, 429 (2002), `astro-ph/0105309`.

[141] J. F. Beacom and N. F. Bell, *Do solar neutrinos decay?*, Phys. Rev. **D65**, 113009 (2002), `hep-ph/0204111`.

[142] J. F. Beacom *et al.*, *Decay of high-energy astrophysical neutrinos*, Phys. Rev. Lett. **90**, 181301 (2003), `hep-ph/0211305`.

[143] C. Giunti, C. W. Kim and U. W. Lee, *Coherence of neutrino oscillations in vacuum and matter in the wave packet treatment*, Phys. Lett. **B274**, 87 (1992).

[144] C. Giunti and C. W. Kim, *Coherence of neutrino oscillations in the wave packet approach*, Phys. Rev. **D58**, 017301 (1998), `hep-ph/9711363`.

[145] W. Grimus, P. Stockinger and S. Mohanty, *The field-theoretical approach to coherence in neutrino oscillations*, Phys. Rev. **D59**, 013011 (1999), `hep-ph/9807442`.

[146] C. Y. Cardall, *Coherence of neutrino flavor mixing in quantum field theory*, Phys. Rev. **D61**, 073006 (2000), `hep-ph/9909332`.

[147] C. Giunti, *Coherence and wave packets in neutrino oscillations*, Found. Phys. Lett. **17**, 103 (2004), `hep-ph/0302026`.

[148] J. W. F. Valle, *Resonant oscillations of massless neutrinos in matter*, Phys. Lett. **B199**, 432 (1987).

[149] M. M. Guzzo, A. Masiero and S. T. Petcov, *On the MSW effect with massless neutrinos and no mixing in the vacuum*, Phys. Lett. **B260**, 154 (1991).

[150] E. Roulet, *Mikheyev-Smirnov-Wolfenstein effect with flavor-changing neutrino nteractions*, Phys. Rev. **D44**, 935 (1991).

[151] S. Bergmann, *The solar neutrino problem in the presence of flavor-changing neutrino interactions*, Nucl. Phys. **B515**, 363 (1998), hep-ph/9707398.

[152] P. I. Krastev and J. N. Bahcall, FCNC solutions to the solar neutrino problem in Santa Monica 1997, Flavor-changing neutral currents, pp. 259–263, 1997, hep-ph/9703267.

[153] S. Bergmann and A. Kagan, *Z-induced FCNCs and their effects on neutrino oscillations*, Nucl. Phys. **B538**, 368 (1999), hep-ph/9803305.

[154] S. Bergmann and Y. Grossman, *Can lepton flavor violating interactions explain the LSND results?*, Phys. Rev. **D59**, 093005 (1999), hep-ph/9809524.

[155] S. Bergmann, Y. Grossman and E. Nardi, *Neutrino propagation in matter with general interactions*, Phys. Rev. **D60**, 093008 (1999), hep-ph/9903517.

[156] S. Bergmann, Y. Grossman and D. M. Pierce, *Can lepton flavor violating interactions explain the atmospheric neutrino problem?*, Phys. Rev. **D61**, 053005 (2000), hep-ph/9909390.

[157] S. Bergmann *et al.*, *Status of the solution to the solar neutrino problem based on non-standard neutrino interactions*, Phys. Rev. **D62**, 073001 (2000), hep-ph/0004049.

[158] M. Guzzo *et al.*, *Status of a hybrid three-neutrino interpretation of neutrino data*, Nucl. Phys. **B629**, 479 (2002), hep-ph/0112310.

[159] G. L. Fogli *et al.*, *Evidence for Mikheyev-Smirnov-Wolfenstein effects in solar neutrino flavor transitions*, Phys. Lett. **B583**, 149 (2004), hep-ph/0309100.

[160] N. Fornengo *et al.*, *Probing neutrino non-standard interactions with atmospheric neutrino data*, Phys. Rev. **D65**, 013010 (2002), hep-ph/0108043.

[161] M. C. Gonzalez-Garcia *et al.*, *New CP violation in neutrino oscillations*, Phys. Rev. **D64**, 096006 (2001), hep-ph/0105159.

[162] P. Huber and J. W. F. Valle, *Non-standard interactions: Atmospheric versus neutrino factory experiments*, Phys. Lett. **B523**, 151 (2001), hep-ph/0108193.

[163] P. Huber, T. Schwetz and J. W. F. Valle, *How sensitive is a neutrino factory to the angle θ_{13}?*, Phys. Rev. Lett. **88**, 101804 (2002), hep-ph/0111224.

[164] T. Ota, J. Sato and N. a. Yamashita, *Oscillation enhanced search for new interaction with neutrinos*, Phys. Rev. **D65**, 093015 (2002), hep-ph/0112329.

[165] G. L. Fogli *et al.*, *Revisiting nonstandard interaction effects on supernova neutrino flavor oscillations*, Phys. Rev. **D66**, 013009 (2002), hep-ph/0202269.

[166] P. Huber, T. Schwetz and J. W. F. Valle, *Confusing non-standard neutrino interactions with oscillations at a neutrino factory*, Phys. Rev. **D66**, 013006 (2002), hep-ph/0202048.

[167] B. Bekman *et al.*, *Matter effects and CP violating neutrino oscillations with non-decoupling heavy neutrinos*, Phys. Rev. **D66**, 093004 (2002), hep-ph/0207015.

[168] M. Campanelli and A. Romanino, *Effects of new physics in neutrino oscillations in matter*, Phys. Rev. **D66**, 113001 (2002), hep-ph/0207350.

[169] T. Ota and J. Sato, *Can ICARUS and OPERA give information on a new physics?*, Phys. Lett. **B545**, 367 (2002), hep-ph/0202145.

[170] J. W. F. Valle, *Standard and nonstandard neutrino oscillations*, J. Phys. **G29**, 1819 (2003).

[171] A. Friedland, C. Lunardini and C. Peña-Garay, *Solar neutrinos as probes of neutrino-matter interactions*, Phys. Lett. **B594**, 347 (2004), hep-ph/0402266.

[172] O. G. Miranda, M. A. Tórtola and J. W. F. Valle, *Are solar neutrino oscillations robust?*, JHEP **10**, 008 (2006), hep-ph/0406280.

[173] M. C. Gonzalez-Garcia and M. Maltoni, *Atmospheric neutrino oscillations and new physics*, Phys. Rev. **D70**, 033010 (2004), hep-ph/0404085.

[174] A. Friedland, C. Lunardini and M. Maltoni, *Atmospheric neutrinos as probes of neutrino matter interactions*, Phys. Rev. **D70**, 111301 (2004), hep-ph/0408264.

[175] A. Friedland and C. Lunardini, *A test of tau neutrino interactions with atmospheric neutrinos and K2K*, Phys. Rev. **D72**, 053009 (2005), hep-ph/0506143.

[176] E. Lisi, A. Marrone and D. Montanino, *Probing possible decoherence effects in atmospheric neutrino oscillations*, Phys. Rev. Lett. **85**, 1166 (2000), hep-ph/0002053.

[177] F. Benatti and R. Floreanini, *Open system approach to neutrino oscillations*, JHEP **02**, 032 (2000), hep-ph/0002221.

[178] S. L. Adler, *Comment on a proposed Super-Kamiokande test for quantum gravity induced decoherence effects*, Phys. Rev. **D62**, 117901 (2000), hep-ph/0005220.

[179] T. Ohlsson, *Equivalence between neutrino oscillations and neutrino decoherence*, Phys. Lett. **B502**, 159 (2001), hep-ph/0012272.

[180] F. Benatti and R. Floreanini, *Massless neutrino oscillations*, Phys. Rev. **D64**, 085015 (2001), hep-ph/0105303.

[181] A. M. Gago *et al.*, *A study on quantum decoherence phenomena with three generations of neutrinos*, hep-ph/0208166.

[182] G. L. Fogli *et al.*, *Status of atmospheric $\nu_\mu \to \nu_\tau$ oscillations and decoherence after the first K2K spectral data*, Phys. Rev. **D67**, 093006 (2003), hep-ph/0303064.

[183] G. Barenboim and N. E. Mavromatos, *CPT violating decoherence and LSND: A possible window to Planck scale physics*, JHEP **01**, 034 (2005), hep-ph/0404014.

[184] G. Barenboim and N. E. Mavromatos, *Decoherent neutrino mixing, dark energy and matter-antimatter asymmetry*, Phys. Rev. **D70**, 093015 (2004), hep-ph/0406035.

[185] D. Morgan *et al.*, *Probing quantum decoherence in atmospheric neutrino oscillations with a neutrino telescope*, Astropart. Phys. **25**, 311 (2006), astro-ph/0412618.

[186] G. L. Fogli *et al.*, *Probing non-standard decoherence effects with solar and KamLAND neutrinos*, (2007), arXiv:0704.2568 [hep-ph].

[187] P. Gu, X. Wang and X. Zhang, *Dark energy and neutrino mass limits from baryogenesis*, Phys. Rev. **D68**, 087301 (2003), hep-ph/0307148.

[188] R. Fardon, A. E. Nelson and N. Weiner, *Dark energy from mass varying neutrinos*, JCAP **0410**, 005 (2004), astro-ph/0309800.

[189] X. J. Bi *et al.*, *Thermal leptogenesis in a model with mass varying neutrinos*, Phys. Rev. **D69**, 113007 (2004), hep-ph/0311022.

[190] P. Q. Hung and H. Päs, *Cosmo MSW effect for mass varying neutrinos*, Mod. Phys. Lett. **A20**, 1209 (2005), astro-ph/0311131.

[191] D. B. Kaplan, A. E. Nelson and N. Weiner, *Neutrino oscillations as a probe of dark energy*, Phys. Rev. Lett. **93**, 091801 (2004), hep-ph/0401099.

[192] P. Gu and X. Bi, *Leptogenesis with triplet Higgs boson*, Phys. Rev. **D70**, 063511 (2004), hep-ph/0405092.

[193] K. M. Zurek, *New matter effects in neutrino oscillation experiments*, JHEP **10**, 058 (2004), hep-ph/0405141.

[194] R. D. Peccei, *Neutrino models of dark energy*, Phys. Rev. **D71**, 023527 (2005), hep-ph/0411137.

[195] H. Li, Z. Dai and X. Zhang, *Testing mass varying neutrino with short gamma ray burst*, Phys. Rev. **D71**, 113003 (2005), hep-ph/0411228.

[196] X. J. Bi *et al.*, *Cosmological evolution of interacting dark energy models with mass varying neutrinos*, (2004), hep-ph/0412002.

[197] V. Barger, P. Huber and D. Marfatia, *Solar mass-varying neutrino oscillations*, Phys. Rev. Lett. **95**, 211802 (2005), hep-ph/0502196.

[198] M. Cirelli, M. C. Gonzalez-Garcia and C. Peña-Garay, *Mass varying neutrinos in the Sun*, Nucl. Phys. **B719**, 219 (2005), hep-ph/0503028.

[199] A. W. Brookfield *et al.*, *Cosmology with massive neutrinos coupled to dark energy*, Phys. Rev. Lett. **96**, 061301 (2006), astro-ph/0503349.

[200] R. Horvat, *Mass-varying neutrinos from a variable cosmological constant*, (2005), astro-ph/0505507.

[201] N. Afshordi, M. Zaldarriaga and K. Kohri, *On the stability of dark energy with mass-varying neutrinos*, (2005), astro-ph/0506663.

[202] R. Takahashi and M. Tanimoto, *Model of mass varying neutrinos in SUSY*, (2005), hep-ph/0507142.

[203] R. Fardon, A. E. Nelson and N. Weiner, *Supersymmetric theories of neutrino dark energy*, JHEP **03**, 042 (2006), hep-ph/0507235.

[204] G. Barr, T. K. Gaisser and T. Stanev, *Flux of atmospheric neutrinos*, Phys. Rev. **D39**, 3532 (1989).

[205] M. Honda *et al.*, *Calculation of the flux of atmospheric neutrinos*, Phys. Rev. **D52**, 4985 (1995), hep-ph/9503439.

[206] T. K. Gaisser and M. Honda, *Flux of atmospheric neutrinos*, Ann. Rev. Nucl. Part. Sci. **52**, 153 (2002), hep-ph/0203272.

[207] M. Honda *et al.*, *A new calculation of the atmospheric neutrino flux in a 3-dimensional scheme*, Phys. Rev. **D70**, 043008 (2004), astro-ph/0404457.

[208] D. Casper *et al.*, *Measurement of atmospheric neutrino composition with IMB-3*, Phys. Rev. Lett. **66**, 2561 (1991).

[209] R. Becker-Szendy *et al.*, *The Electron-neutrino and muon-neutrino content of the atmospheric flux*, Phys. Rev. **D46**, 3720 (1992).

[210] Kamiokande-II collaboration, K. S. Hirata *et al.*, *Observation of a small atmospheric ν_μ/ν_e ratio in Kamiokande*, Phys. Lett. **B280**, 146 (1992).

[211] Kamiokande collaboration, Y. Fukuda *et al.*, *Atmospheric ν_μ/ν_e ratio in the multi-GeV energy range*, Phys. Lett. **B335**, 237 (1994).

[212] Fréjus collaboration, K. Daum *et al.*, *Determination of the atmospheric neutrino spectra with the Fréjus detector*, Z. Phys. **C66**, 417 (1995).

[213] W. W. M. Allison *et al.*, *Measurement of the atmospheric neutrino flavour composition in Soudan-2*, Phys. Lett. **B391**, 491 (1997), `hep-ex/9611007`.

[214] Soudan 2 collaboration, M. C. Sanchez *et al.*, *Observation of atmospheric neutrino oscillations in Soudan 2*, Phys. Rev. **D68**, 113004 (2003), `hep-ex/0307069`.

[215] J. N. Bahcall, M. H. Pinsonneault and S. Basu, *Solar models: Current epoch and time dependences, neutrinos, and helioseismological properties*, Astrophys. J. **555**, 990 (2001), `astro-ph/0010346`.

[216] J. N. Bahcall and M. H. Pinsonneault, *What do we (not) know theoretically about solar neutrino fluxes?*, Phys. Rev. Lett. **92**, 121301 (2004), `astro-ph/0402114`.

[217] J. N. Bahcall, A. M. Serenelli and S. Basu, *New solar opacities, abundances, helioseismology, and neutrino fluxes*, Astrophys. J. **621**, L85 (2005), `astro-ph/0412440`.

[218] Homepage of J.N. Bahcall, `http://www.sns.ias.edu/~jnb/`.

[219] S. L. Glashow and L. M. Krauss, *'Just so' neutrino oscillations*, Phys. Lett. **B190**, 199 (1987).

[220] G. L. Fogli *et al.*, *Three-flavor MSW solutions of the solar neutrino problem*, Phys. Rev. **D62**, 013002 (2000), `hep-ph/9912231`.

[221] J. N. Bahcall, P. I. Krastev and A. Y. Smirnov, *Solar neutrinos: Global analysis and implications for SNO*, JHEP **05**, 015 (2001), `hep-ph/0103179`.

[222] J. N. Bahcall, M. C. Gonzalez-Garcia and C. Peña-Garay, *Robust signatures of solar neutrino oscillation solutions*, JHEP **04**, 007 (2002), `hep-ph/0111150`.

[223] A. Cisneros, *Effect of neutrino magnetic moment on solar neutrino observations*, Astrophys. Space Sci. **10**, 87 (1971).

[224] J. Schechter and J. W. F. Valle, *Majorana neutrinos and magnetic fields*, Phys. Rev. **D24**, 1883 (1981).

[225] L. B. Okun, M. B. Voloshin and M. I. Vysotsky, *Electromagnetic properties of neutrino and possible semiannual variation cycle of the solar neutrino flux*, Sov. J. Nucl. Phys. **44**, 440 (1986).

[226] L. B. Okun, M. B. Voloshin and M. I. Vysotsky, *Neutrino electrodynamics and possible consequences for solar neutrinos*, Sov. Phys. JETP **64**, 446 (1986).

[227] C. S. Lim and W. J. Marciano, *Resonant spin-flavor precession of solar and supernova neutrinos*, Phys. Rev. **D37**, 1368 (1988).

[228] E. K. Akhmedov, *Resonant amplification of neutrino spin rotation in matter and the solar-neutrino problem*, Phys. Lett. **B213**, 64 (1988).

[229] E. K. Akhmedov and J. Pulido, *Solar neutrino oscillations and bounds on neutrino magnetic moment and solar magnetic field*, Phys. Lett. **B553**, 7 (2003), `hep-ph/0209192`.

[230] A. J. Baltz and J. Weneser, *Effect of transmission through the earth on neutrino oscillations*, Phys. Rev. **D35**, 528 (1987).

[231] A. J. Baltz and J. Weneser, *Matter oscillations: Neutrino transformation in the Sun and regeneration in the Earth*, Phys. Rev. **D37**, 3364 (1988).

[232] E. Lisi and D. Montanino, *Earth regeneration effect in solar neutrino oscillations: An analytic approach*, Phys. Rev. **D56**, 1792 (1997), `hep-ph/9702343`.

[233] A. H. Guth, L. Randall and M. Serna, *Day-night and energy variations for maximal neutrino mixing angles*, JHEP **08**, 018 (1999), `hep-ph/9903464`.

[234] A. S. Dighe, Q. Y. Liu and A. Y. Smirnov, *Coherence and the day-night asymmetry in the solar neutrino flux*, (1999), `hep-ph/9903329`.

[235] M. C. Gonzalez-Garcia, C. Peña-Garay and A. Y. Smirnov, *Zenith angle distributions at Super-Kamiokande and SNO and the solution of the solar neutrino problem*, Phys. Rev. **D63**, 113004 (2001), `hep-ph/0012313`.

[236] A. Bandyopadhyay *et al.*, *Constraints on neutrino oscillation parameters from the SNO salt phase data*, Phys. Lett. **B583**, 134 (2004), `hep-ph/0309174`.

[237] P. C. de Holanda and A. Y. Smirnov, *Solar neutrinos: The SNO salt phase results and physics of conversion*, Astropart. Phys. **21**, 287 (2004), `hep-ph/0309299`.

[238] E. K. Akhmedov, M. A. Tórtola and J. W. F. Valle, *A simple analytic three-flavour description of the day-night effect in the solar neutrino flux*, JHEP **05**, 057 (2004), `hep-ph/0404083`.

[239] A. N. Ioannisian *et al.*, *A precise analytical description of the Earth matter effect on oscillations of low energy neutrinos*, Phys. Rev. **D71**, 033006 (2005), `hep-ph/0407138`.

[240] Super-Kamiokande collaboration, M. B. Smy *et al.*, *Precise measurement of the solar neutrino day/night and seasonal variation in Super-Kamiokande-I*, Phys. Rev. **D69**, 011104 (2004), `hep-ex/0309011`.

[241] SNO collaboration, Q. R. Ahmad *et al.*, *Measurement of day and night neutrino energy spectra at SNO and constraints on neutrino mixing parameters*, Phys. Rev. Lett. **89**, 011302 (2002), `nucl-ex/0204009`.

[242] SNO collaboration, B. Aharmim *et al.*, *Electron energy spectra, fluxes, and day-night asymmetries of ^{8}B solar neutrinos from the 391-day salt phase SNO data set*, Phys. Rev. **C72**, 055502 (2005), `nucl-ex/0502021`.

[243] Y. Declais *et al.*, *Search for neutrino oscillations at 15-meters, 40-meters, and 95-meters from a nuclear power reactor at Bugey*, Nucl. Phys. **B434**, 503 (1995).

[244] CHOOZ collaboration, M. Apollonio *et al.*, *Limits on neutrino oscillations from the CHOOZ experiment*, Phys. Lett. **B466**, 415 (1999), `hep-ex/9907037`.

[245] CHOOZ collaboration, M. Apollonio *et al.*, *Search for neutrino oscillations on a long base-line at the CHOOZ nuclear power station*, Eur. Phys. J. **C27**, 331 (2003), `hep-ex/0301017`.

[246] F. Boehm *et al.*, *Final results from the Palo Verde neutrino oscillation experiment*, Phys. Rev. **D64**, 112001 (2001), `hep-ex/0107009`.

[247] CHORUS collaboration, E. Eskut *et al.*, *The CHORUS experiment to search for $\nu_\mu \to \nu_\tau$ oscillation*, Nucl. Instrum. Meth. **A401**, 7 (1997).

[248] NOMAD collaboration, J. Altegoer *et al.*, *The NOMAD experiment at the CERN SPS*, Nucl. Instrum. Meth. **A404**, 96 (1998).

[249] NOMAD collaboration, P. Astier *et al.*, *Final NOMAD results on $\nu_\mu \to \nu_\tau$ and $\nu_e \to \nu_\tau$ oscillations including a new search for nu/tau appearance using hadronic tau decays*, Nucl. Phys. **B611**, 3 (2001), `hep-ex/0106102`.

[250] KARMEN collaboration, B. Armbruster *et al.*, *Upper limits for neutrino oscillations $\bar{\nu}_\mu \to \bar{\nu}_e$ from muon decay at rest*, Phys. Rev. **D65**, 112001 (2002), `hep-ex/0203021`.

[251] BooNE collaboration, A. O. Bazarko, *MiniBooNE: The booster neutrino experiment*, (1999), `hep-ex/9906003`.

[252]

[253] P. Langacker, *A mechanism for ordinary-sterile neutrino mixing*, Phys. Rev. **D58**, 093017 (1998), `hep-ph/9805281`.

[254] V. D. Barger *et al.*, *Fate of the sterile neutrino*, Phys. Lett. **B489**, 345 (2000), hep-ph/0008019.

[255] O. L. G. Peres and A. Y. Smirnov, *(3+1) spectrum of neutrino masses: A chance for LSND?*, Nucl. Phys. **B599**, 3 (2001), hep-ph/0011054.

[256] A. Strumia, *Interpreting the LSND anomaly: Sterile neutrinos or CPT-violation or...?*, Phys. Lett. **B539**, 91 (2002), hep-ph/0201134.

[257] M. Sorel, J. M. Conrad and M. Shaevitz, *A combined analysis of short-baseline neutrino experiments in the (3+1) and (3+2) sterile neutrino oscillation hypotheses*, Phys. Rev. **D70**, 073004 (2004), hep-ph/0305255.

[258] A. D. Sakharov, *Violation of CP invariance, C asymmetry, and baryon asymmetry of the Universe*, Pisma Zh. Eksp. Teor. Fiz. **5**, 32 (1967).

[259] WMAP collaboration, D. N. Spergel *et al.*, *First year Wilkinson Microwave Anisotropy Probe (WMAP) observations: Determination of cosmological parameters*, Astrophys. J. Suppl. **148**, 175 (2003), astro-ph/0302209.

[260] M. Fukugita and T. Yanagida, *Baryogenesis without grand unification*, Phys. Lett. **B174**, 45 (1986).

[261] M. A. Luty, *Baryogenesis via leptogenesis*, Phys. Rev. **D45**, 455 (1992).

[262] W. Buchmüller and M. Plümacher, *Baryon asymmetry and neutrino mixing*, Phys. Lett. **B389**, 73 (1996), hep-ph/9608308.

[263] A. Pilaftsis, *CP violation and baryogenesis due to heavy Majorana neutrinos*, Phys. Rev. **D56**, 5431 (1997), hep-ph/9707235.

[264] E. Ma and U. Sarkar, *Neutrino masses and leptogenesis with heavy Higgs triplets*, Phys. Rev. Lett. **80**, 5716 (1998), hep-ph/9802445.

[265] W. Buchmüller and M. Plümacher, *Neutrino masses and the baryon asymmetry*, Int. J. Mod. Phys. **A15**, 5047 (2000), hep-ph/0007176.

[266] G. C. Branco *et al.*, *A bridge between CP violation at low energies and leptogenesis*, Nucl. Phys. **B617**, 475 (2001), hep-ph/0107164.

[267] G. C. Branco *et al.*, *Leptogenesis, CP violation and neutrino data: What can we learn?*, Nucl. Phys. **B640**, 202 (2002), hep-ph/0202030.

[268] S. Davidson and A. Ibarra, *A lower bound on the right-handed neutrino mass from leptogenesis*, Phys. Lett. **B535**, 25 (2002), hep-ph/0202239.

[269] E. K. Akhmedov, M. Frigerio and A. Y. Smirnov, *Probing the seesaw mechanism with neutrino data and leptogenesis*, JHEP **09**, 021 (2003), hep-ph/0305322.

[270] G. F. Giudice *et al.*, *Towards a complete theory of thermal leptogenesis in the SM and MSSM*, Nucl. Phys. **B685**, 89 (2004), `hep-ph/0310123`.

[271] T. Hambye *et al.*, *Constraints on neutrino masses from leptogenesis models*, Nucl. Phys. **B695**, 169 (2004), `hep-ph/0312203`.

[272] A. Pilaftsis and T. E. J. Underwood, *Resonant leptogenesis*, Nucl. Phys. **B692**, 303 (2004), `hep-ph/0309342`.

[273] W. Buchmüller, P. Di Bari and M. Plümacher, *Leptogenesis for pedestrians*, Ann. Phys. **315**, 305 (2005), `hep-ph/0401240`.

[274] S. Antusch and S. F. King, *Type II leptogenesis and the neutrino mass scale*, Phys. Lett. **B597**, 199 (2004), `hep-ph/0405093`.

[275] V. A. Kuzmin, V. A. Rubakov and M. E. Shaposhnikov, *On the anomalous electroweak baryon number nonconservation in the early Universe*, Phys. Lett. **B155**, 36 (1985).

[276] S. Y. Khlebnikov and M. E. Shaposhnikov, *The statistical theory of anomalous fermion number nonconservation*, Nucl. Phys. **B308**, 885 (1988).

[277] J. A. Harvey and M. S. Turner, *Cosmological baryon and lepton number in the presence of electroweak fermion number violation*, Phys. Rev. **D42**, 3344 (1990).

Part II

Scientific papers

1

Paper 1

Mattias Blennow, Tommy Ohlsson, and Håkan Snellman
Day-night effect in solar neutrino oscillations with three flavors
Physical Review D **69**, 073006 (2004).

2

Paper 2

Mattias Blennow and Tommy Ohlsson
Exact series solution to the two flavor neutrino oscillation problem in matter
Journal of Mathematical Physics **45**, 4053 (2004).

Paper 3

Mattias Blennow and Tommy Ohlsson
Effective neutrino mixing and oscillations in dense matter
Physics Letters B **609**, 330 (2005).

3

Paper 4

Mattias Blennow, Tommy Ohlsson, and Walter Winter
Damping signatures in future neutrino oscillation experiments
Journal of High Energy Physics **06**, 049 (2005).

4

Paper 5

Mattias Blennow, Tommy Ohlsson, and Walter Winter
Non-standard Hamiltonian effects on neutrino oscillations
The European Physical Journal C **49**, 1023 (2007).

5

Paper 6

Mattias Blennow, Tommy Ohlsson, and Julian Skrotzki
Effects of non-standard interactions in the MINOS experiment
hep-ph/0702059

6

Paper 7

Evgeny Akhmedov, *Mattias Blennow*, Thomas Konstandin, Tomas Hällgren, and Tommy Ohlsson

Stability and leptogenesis in the left-right symmetric seesaw mechanism

Journal of High Energy Physics **04**, 022 (2007).

7